

WOODS TIRE MODEL

by

PRIYANK VASANT NANDU

Presented to the Faculty of the Graduate School of

The University of Texas at Arlington in Partial Fulfillment

of the Requirements for the Degree of

MASTER OF SCIENCE IN MECHANICAL ENGINEERING.

THE UNIVERSITY OF TEXAS AT ARLINGTON

August 2018

Copyright © by Priyank Nandu

2018

All Rights Reserved



Acknowledgements

This thesis was made possible by the help of several individuals to whom I owe a great deal. I would like to acknowledge Professor Dr. Robert L. Woods for supervising my work and giving me an opportunity to work on a project of these scale. You encouraged me to do my best, while giving me guidance along the way. At the same time, you gave me the freedom necessary for this work to truly be my own.

I would like to Acknowledge Milliken Research Associates Inc. for providing all the resources in terms of numerous papers and insights on TTC forums. I would like to acknowledge all the volunteers and contributors of the FSAE TTC program, including Calspan Tire Research Facility. Your work has created many opportunities and helped hundreds of university students like me in expanding our knowledge and allowing us to grow as vehicle dynamic engineers. I would like to recognize all the volunteers of the many FSAE and FS competitions around the world.

Second, I would like to give a special thanks to University of Texas Arlington MAE department for your continued support of the FSAE program. Thanks also to all the current and past members of the UTA Racing team. Our current level of success would not have been possible without all the work you put in. Finally, I would like to thank my family for putting up with 5 years of my involvement in the FSAE program. My parents, you have always encouraged me to follow my dreams and have given me never ending support throughout my many years of school. You pushed me to do my best while giving me the space I needed.

August 8, 2018.

Abstract

SEMI-EMPERICAL (WOODS) TIRE MODEL

Priyank Vasant Nandu, MS

The University of Texas at Arlington, 2018

Supervising Professor: Robert L. Woods

The performance of a racecar in a maneuver is almost totally determined by the characteristics of the tires and the suspension setup. If the suspension is properly tuned for the maneuver, then the limiting factor is the tire. Therefore, any racecar design and performance analysis must start with a full description of the performance of the tire [1].

Mathematical models for tire performance such as the Pacejka model have been in use for a long time and have become the standard for expressing how a tire will perform dynamically. It comprises of curve fit to experimental data and requires about 17 coefficients to describe the sensitivity of tire adhesion as a function of several variables. These coefficients are not easy to interpret or to estimate. Presented in this paper is the Woods model for tire performance that will provide a physical interpretation to each coefficient and allows an estimate of the coefficient of a

new tire based on knowledge of tested tires. Using Woods tire model, based on Pacejka model with different mathematic curve fits we were able represent the data with same accuracy.

The main objective of this project is to verify the assumptions and mathematical curve fits used in Woods tire model for tires with different compound, sizes and manufacturers and also to express degradation in the coefficient of friction and the value of slip that results in peak force as a function of normal load and camber.

Contents

Acknowledgements.....	iii
Abstract.....	iv
Contents	vi
List of Illustrations	viii
Abbreviations	viii
Chapter 1: Introduction	1
Motivation	1
Chapter 2: Tire forces and moments	2
2.1 Definition.....	3
2.2 Fundamental Tire force and moment characteristics.	5
Chapter 3: Tire modeling	8
3.1 The Pacejka Tire Model.....	8
Chapter 4: Tire test data	11
4.1 Tire testing	11
Chapter 5: Woods Tire Model.....	13
5.1 Pajecka Tire models	13
5.1.1 Pacejka Lateral Model	14
5.1.2 Pacejka Longitudinal Model.....	15
5.2 Woods Tire Models.....	17
5.2.1 Woods tire Model	18
5.2.2 Normalized Longitudinal Pacejka Model.....	23
Performance Interpretation of Woods tire model.....	26
Chapter 6: Verification	28
6.1 Data Parsing	28
6.2 Curve fitting to TTC raw data.....	30
6.3 Curve fitting of scaling factors.	32
6.4 Woods model vs TTC raw data.	34

Chapter 7: Results and conclusion.....	36
Appendix.....	38
Appendix A-1	38
Appendix A-2- graphs.....	42
Hoosier R10 LCO	42
Avon R10*16.....	61
Goodyear 20x7-13 D2509	72
Hoosier R13 20.5*7 R25B	90
References	112

List of Illustrations

Figure 1: SAE Standard tire axis system. 2

Figure 2: Fundamental lateral force versus slip angle curve[1]. 6

Figure 3: Typical lateral force behavior across three different normal loads. [1] 7

Figure 4: Comparison of Magic Formula computed results with measured data [3]. 10

Figure 5: Main testing machine Calspan, TIRF..... 12

Figure 6: Force and slip angle characteristics of a typical race tire. 13

Figure 7: Data channels at TTC. 29

Figure 8: Normalized Lateral Load vs Slip angle from TTC raw data. 30

Figure 9: Curve Fit Template. 31

Figure 10: Curve fitting over TTC raw data. 32

Figure 11: Curve fit for obtaining scaling factors..... 33

Figure 12: Woods model vs TTC raw data..... 35

Figure 13: Maximizing slip for various loads vs camber. 36

Figure 14: μ for various loads vs Camber. 37

Abbreviations

SAE: Society of Automotive Engineers

FSAE: Formula SAE

TTC: Tire test consortium

F_z = normal load on tire

F_y = lateral force generated by the tire in a turn

F_x = longitudinal force generated by the tire in acceleration or braking

α = slip angle in a turn

σ = slip ratio in acceleration or braking

γ = camber angle of tire

D_y, D_x = peak factor

C_y, C_x = shape factor

B_y, B_x = stiffness factor

E_y, E_x = curvature factor

S_{yh}, S_{xh} = horizontal shift

S_{yv}, S_{xv} = vertical shift

a_i, b_i = curve fit coefficients

Chapter 1: Introduction

The objective in motor racing is to win races, whether one views racing as a sport, promotional entertainment, or corporate R& D activity. It is the dynamic behavior of the combination of high tech machines and infinitely complex human beings that makes the sport so intriguing for participants and spectators alike.

Vehicle performance is the function of how well the vehicle interacts with the road surface. Tires are the primary source of forces and torques which provide control and stability (handling) to the vehicle. The forces and torques developed by the pneumatic tire affect the vehicle in a variety of ways. Obviously, the tires support the vehicle weight and any other vertical loads but also take lateral forces and torques. The interactions between the tire and road surfaces generates tractive, braking and cornering forces for maneuvering the vehicle [1].

Motivation

As mentioned previously, it is critical to understand the interactions between the tire and road surfaces, the forces and moments generated by the tire and how to take advantage of these effects on vehicle stability, control and performance. This creates two specific needs. First, there is a need for data on the force and moment characteristics of tire. Second, a direct expression on the maximum adhesion and maximizing slip which allows an engineer to determine car setup parameters and quantify adjustments[2].

Chapter 2: Tire forces and moments

The tire is the principal means for creating tire forces and moments to produce vehicle motion. In this section, definitions of the various forces and moments, along with associated operating variables, are introduced. The fundamental tire force and moment axis system is shown in Figure 1. This appears in two Society of Automotive (SAE) standards documents, Surface Vehicle Recommended Practice [SAE J670E, 1976] and Tire Performance Technology [SAE J2047, 1998]. The definitions that follow are also based on these two sources.

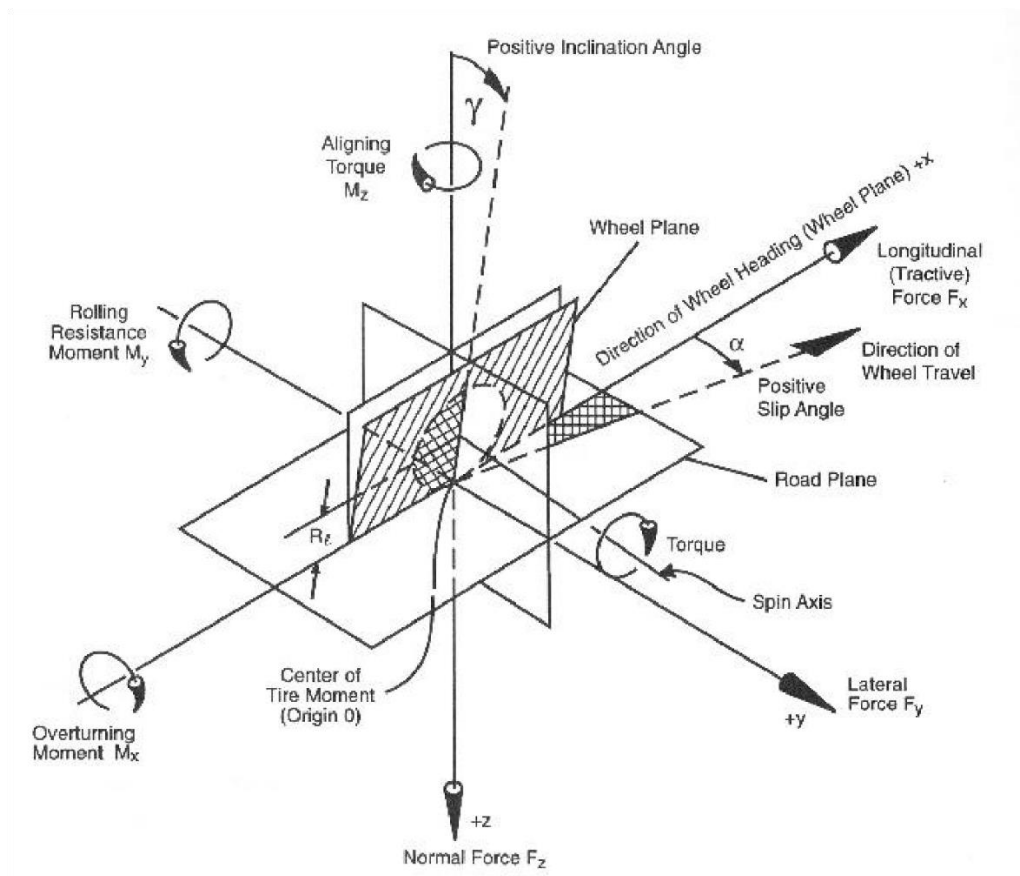


Figure 1: SAE Standard tire axis system.

2.1 Definition

There are four tire forces and moments of interest. They are described in a tire-relative axis system with origin located in the wheel plane below the wheel center on the ground. The x-axis points in the direction of the wheel plane in the ground plane. The y-axis points perpendicular to the wheel plane in the ground plane. The z-axis is normal to the ground plane and is positive downward [1]. The forces and moment produced by the tire are:

- Longitudinal force, F_x : Tire force produced in the X-axis direction principally as a function of slip ratio. Informally, this is the tractive/braking force.
- Lateral force, F_y : Tire force produced in the Y-axis direction principally as a function of slip angle, but also a weak but notable function of inclination angle. Informally, this is the cornering force.
- Aligning Torque, M_z : Tire moment about the Z-axis which usually acts as a restoring torque. Tires generally resist the introduction of slip angle through this mechanism. This is one source of the self-centering exhibited by automobile steering wheels.
- Overturning Moment, M_x : Tire moment about the X-axis resulting from the fact that the resultant normal load vector can experience a lateral offset from the origin of the SAE tire axis system. It is important for load transfer and suspension compliance calculations.

These four forces and moments are considered tire outputs. There is a fifth component, the rolling resistance moment, but this is often treated separately by vehicle dynamicists. There are five principal operating variables the tire experiences:

- Normal Load, F_z : Tire force in the Z-axis direction indicating the amount of weight being carried by a tire at a given instant in time. In the SAE system, tire loads are described as being

applied by the road to the vehicle. This is an upward direction so, strictly speaking, tire loads have a negative sign. It is commonplace however, to omit the negative sign whenever it doesn't affect the mathematics, such as during discussions or in written material.

- Slip angle, α : The difference between the tire's velocity and heading vectors as projected onto the ground plane. This angle is produced not only by steering the front wheels, but also by vehicle motions including yaw rate, sideslip and suspension kinematics/compliances. Positive slip angles produce negative lateral forces for turning left.
- Inclination angle, γ : The angle at which the top of the tire is tilted left or right from the vertical. Inclination angle results from suspension design and body roll during cornering. It has important, but not primary, effects on all four force and moment outputs. Inclination angle is sometimes incorrectly referred to as "camber angle". Both describe the tilt of the tire, but camber angle is relative to the vehicle such that when the top of the tire tilts toward the vehicle centerline it is referred to as "negative camber". Inclination angle is negative when the top of the tire tilts to the left of its velocity vector.
- Slip ratio, σ : While not shown in Figure, slip ratio is a measure of how fast the tire is rotating relative to how fast the roadway is passing by. There are a variety of expressions in use as summarized by [Milliken, 1995]. For the SAE definition used a slip ratio of zero means the tire is "free rolling" and not trying to develop any drive or brake forces. Positive slip ratios represent a faster rotation than needed for the free rolling condition, leading to tractive forces. Negative ratios indicate a slower rotation than needed for free rolling, which produces braking forces.
- Roadway Friction Coefficient, μ : Also, not shown the roadway friction coefficient is a metric to indicate the interaction between the roadway and the tire. Common asphalt or concrete has a value near 1.0, while packed snow is around 0.3-0.4 and wet ice can be as low as 0.1 or less [Wallingford, 1990].

It should be noted that the system presented above is the SAE standard and is in use across North America and, to a lesser extent, across the rest of the world.

2.2 Fundamental Tire force and moment characteristics.

One of the earliest publications on tire behavior was by Broulhiet [Broulheit, 1925] in which he established the concept of the slip angle. Until that time, the tire was largely seen as a suspension component (vertical response was studied) and as a source of power loss (rolling resistance). These were the major benefit and concern associated with the introduction of the pneumatic tire to bicycles in the 1880s. While tires had become more reliable, more complex and more effective in the decades since then, the overriding perception of the tire's role had changed little. The tire force & moment characteristics of significant interest to modern vehicle dynamicists were only beginning to be explored in the 1920s [3].

In 1931 Becker, Fromm and Maruhn [Becker, 1931] produced lateral force data on a rotating drum, a side-effect of their investigation into the problem of tire shimmy. Drum testing of tire forces and moments grew throughout the 1930s, with significant contributions being made by Olley and Evans [Evans, 1935]. By the end of the decade Bull was able to envision a full six component drum-type test machine [Bull, 1939]. The information obtained from these early testing machines, while crude by today's standards, was sufficient to establish fundamental relationships between operating variables and tire outputs. Figure 2.3 [Milliken, 1995] shows the generic shape of a lateral force versus slip angle curve. The same shape is also representative of longitudinal force vs. slip ratio curves. For small slip angle values the tire behaves linearly, producing a lateral force proportional slip angle in an amount defined as the "cornering stiffness". Nearly all normal passenger car driving occurs in this "linear range" of the tire performance curve [4].

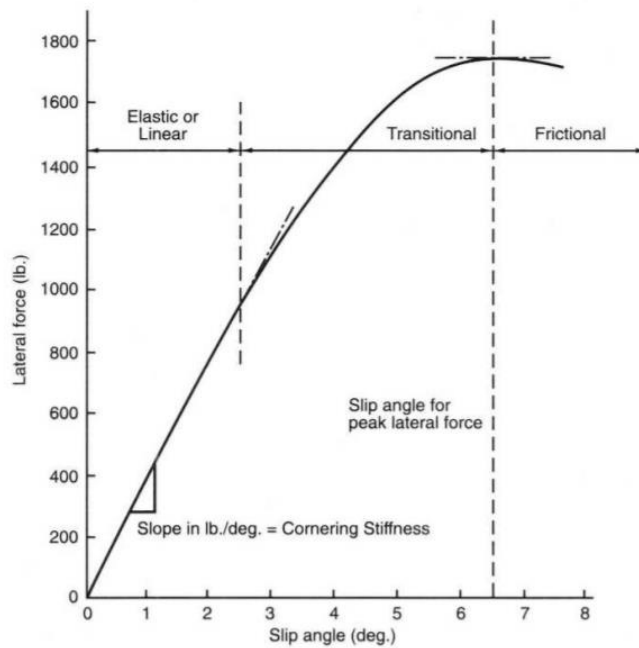


Figure 2: Fundamental lateral force versus slip angle curve[1].

There exists a certain slip angle value at which the lateral force is maximized. This is referred to as the peak of the curve. It is the area near the peak of the curve that race cars attempt to operate. Both the initial slope and the peak of the curve play a critical role throughout this dissertation. The curve in Figure 2.3 is drawn for a single normal load. As normal load is increased the height of the peak, location of the peak and initial slope of the curve all change, as shown in Figure 2.4 [Milliken, 1995]. Awareness of these trends is also essential to the work presented in later chapters [1].

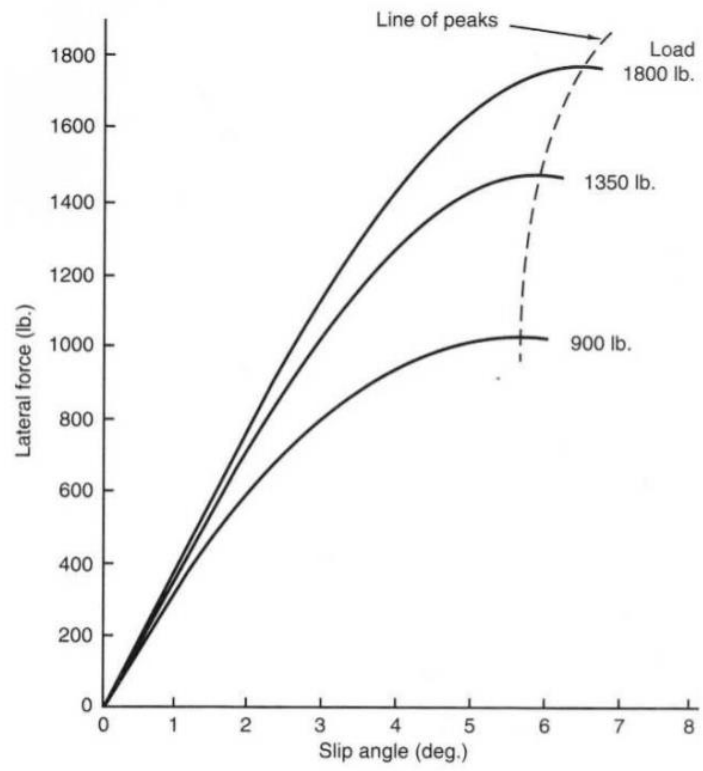


Figure 3: Typical lateral force behavior across three different normal loads. [1]

Chapter 3: Tire modeling

A tire model is a way to describe real world phenomena as a series of mathematical equations. Engineers use numerous models to describe the world in a minimalist form, draw insights into how various properties interact and predict the outcome of future events. To make a model simple and easy to understand, we have to make certain assumptions. The key is to develop a model that supplies the desired accuracy and detail for a specific problem, while remaining solvable given the time and resources available. Hence, there is no surprise that there are several ways to develop a tire model.

The focus of this thesis is the WOODS tire model based on the normalization of Pacejka model. This model has been developed to accurately predict and correlate physical(tunable) parameters as a function of peak slip angle and adhesion.

Tire model can be divided into several categories based upon the purpose the model serves. For example, Ride model focuses on the tire vertical behavior like spring rate and damping treating the tire as a suspension component while the handling model focuses on the forces and moments that produce the vehicle motion. WOODS tire model comes under the handling model.

3.1 The Pacejka Tire Model

Of the many different tire models that are available today, the magic formula tire model proposed in 1, 2 and 3 is one of the most advanced and has proven to be very accurate when compared to experimental data. The approach of the model is semi empirical, meaning that the formulas aren't derived from a physical background that models the tire structure but rather are Mathematical approximations of curves that were recorded and experiments. For this purpose, scaling factors must be obtained from measurements.

The general form of the Magic Formula is [3]:

$$y = D \sin[C \arctan\{Bx - (Bx - \arctan(bx))\}]$$

Where y represents a tire force or torque and x is the slip quantity this force or torque depends on (i.e. longitudinal or lateral slip). B , C , D , E are factors to define the curve's shape in order to get an appearance similar to the recorded. Specifically,

B is a stiffness factor

C is a shape factor

D is the peak value

E is a curvature factor

BCD is the slope of curve at origin.

Each of these factors must be approximated from measured data from experiments for the respective tire and environment. It is also possible to apply an offset in x and y direction with respect to origin to this general formula. An offset can arise due to ply sheer and conicity effects as well as wheel camber [3]. The shift in x and y can be performed by using the modified coordinates

$Y(X) = y(x) + S_V$ with S_V being the vertical shift and

$x = X + S_H$ with S_H being the horizontal shift.

As input variable X we can use $\tan \alpha$ (lateral slip angle) or σ (Longitudinal slip) – which depend on vertical load F_Z and camber angle γ . The output variable Y described by the formula might be F_X (longitudinal force), F_Y (lateral force) or M_Z (self-aligning torque), depending on the problem.

As an example, the lateral force F_{Y0} can be described as [3]:

$$F_{Y0} = D_Y \sin[C_Y \arctan\{B_Y \alpha_Y - E_Y(B_Y \alpha_Y - \arctan(B_Y \alpha_Y))\}] + S_{Yy}$$

Where α_y is the slip angle.

To display the agreement of the Magic Formula approach and experimental data figure 7 shows curves obtained from measurements compared to magic formula computed results.

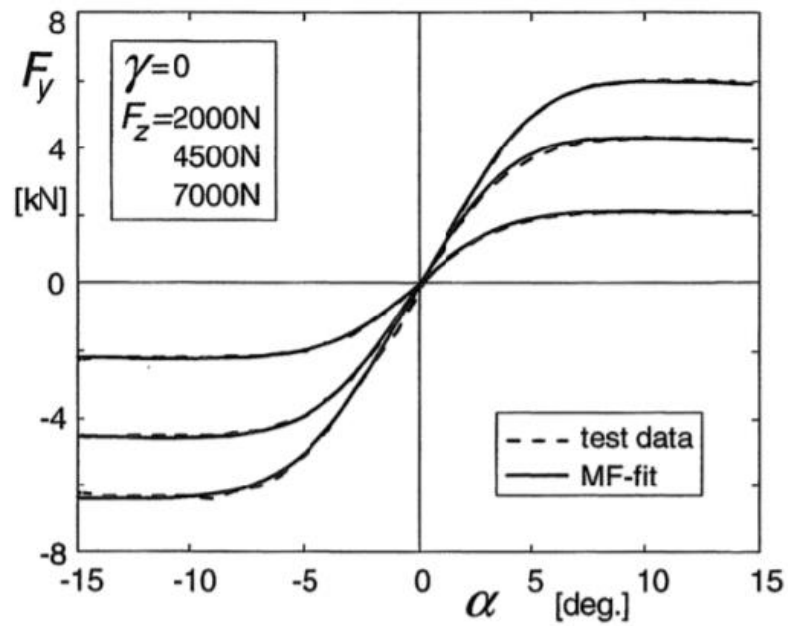


Figure 4: Comparison of Magic Formula computed results with measured data [3].

Chapter 4: Tire test data

4.1 Tire testing

Formula SAE (FSAE) is a highly competitive series organized annually at 5 different continents. University teams from around the world contest in this unique competition where students virtually have complete freedom to design, develop and manufacture a racecar. UTA racing has a great legacy starting back in 1982, where the team has won various championships and accolades. UTA racing has been one of the top most competitive teams in the world.

The need for greater access to tire data and engineers familiar with tire data is addressed through the establishment of the Formula SAE Tire Test Consortium. This organization collects a modest fee from registered members, all of whom are colleges and universities participating in the international Formula SAE competitions. The consortium organizes tire force and moment tests and then distributes the raw data to all registered members. It is the first time that low-cost, high quality tire force and moment data has been available to academia. Cornering tests begin with a “cold to hot” series of twelve slip angle sweeps at one load [5].



Figure 5: Main testing machine Calspan, TIRF.

The cornering test is run with a free-rolling (no slip ratio) tire, while the drive/brake tests hold constant slip angle while varying slip ratio. Five loads, five inclination angles and four inflation pressures are tested. The first slip angle sweep block is longer than the rest because it contains a few “conditioning sweeps”. A lot of care is taken to exercise the tire and stabilize its performance before taking the main block of force and moment data.

Chapter 5: Woods Tire Model

5.1 Pajecka Tire models

The Pacejka model has evolved slightly over the years and uses different signs for the coefficients in different coordinate systems used by various organizations, but the basic form is the sine of an inverse tangent function of the slip with various degradations and offsets as presented below [2].

Pacejka Model

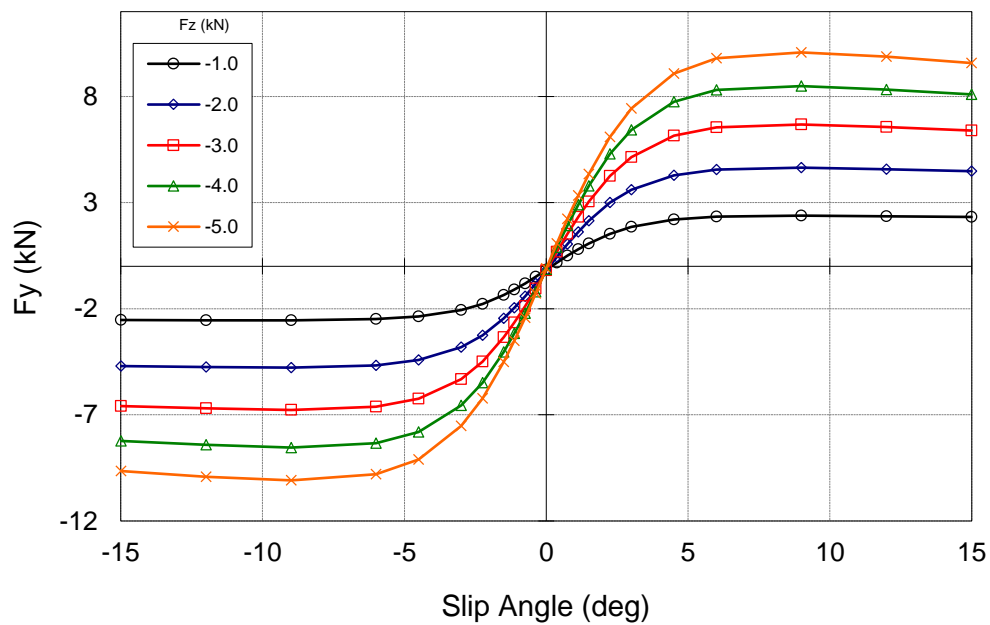


Figure 6: Force and slip angle characteristics of a typical race tire.

Figure 9 illustrates the force versus slip angle of a typical race tire as a function of normal load. In this graph, we are interested in two parameters, the slip angle that results in the maximum lateral force, and that lateral force relative to the normal load [2].

5.1.1 Pacejka Lateral Model

In lateral model 'slip' is the slip angle. The Pacejka formulation is given by the following equations. See the nomenclature in appendix A-1 for explanations of the variables and coefficients.

$$F_y = D_y \sin(C_y \theta_y) + S_{yv} \quad (1)$$

$$\begin{aligned} \theta_y &= \tan^{-1} \left\{ B_y (\alpha + S_{yh}) - E_y \left[B_y (\alpha + S_{yh}) - \tan^{-1} (B_y (\alpha + S_{yh})) \right] \right\} \\ &= \tan^{-1} \left\{ B_y (\alpha + S_{yh}) \left(1 - E_y \left[1 - \frac{\tan^{-1} (B_y (\alpha + S_{yh}))}{B_y (\alpha + S_{yh})} \right] \right) \right\} \end{aligned} \quad (2)$$

The coefficients D_y , C_y , B_y , E_y , S_{yh} , and S_{yv} are curve fit parameters and are stated in terms of 18 constants, a_i , that are determined for each tire.

$$C_y = a_0 \quad (3)$$

$$D_y = \left[(a_1 F_z + a_2) (1 - a_{15} \gamma^2) \right] F_z \quad (4)$$

$$B_y = \frac{a_3 \sin\left(2 \tan^{-1}\left(\frac{F_z}{a_4}\right)\right) (1 - a_5 |\gamma|)}{C_y D_y} \quad (5)$$

$$E_y = (a_6 F_z + a_7) [1 - (a_{16} \gamma + a_{17}) \text{sign}(\alpha + S_{yh})] \quad (6)$$

$$S_{yh} = a_8 F_z + a_9 + a_{10} \gamma \quad (7)$$

$$S_{yv} = a_{11} F_z + a_{12} + (a_{13} F_z + a_{14}) F_z \gamma \quad (8)$$

The a coefficients and the constants are explained at the end in appendix A-1.

5.1.2 Pacejka Longitudinal Model

In the longitudinal model, the “slip” is the slip ratio. The slip ratio is related to the normalized difference in the tangential speed of the tire, $R_t \omega$ and the longitudinal speed of the vehicle, v , (measured at the wheel axle). Various authors use differing conventions, but in this paper, the radius of the tire, R_t , is the loaded radius (considering speed) and ω is the rotational speed of the tire [2].

For acceleration, the slip ratio is the speed difference relative to the rotational speed.

$$\sigma = \frac{R_t \omega - v}{R_t \omega} = 1 - \frac{v}{R_t \omega} \quad (9a)$$

In acceleration, the tangential speed is greater than the vehicle speed, so the slip ratio is positive.

For deceleration, the slip ratio is the speed difference relative to the vehicle speed.

$$\sigma = \frac{R_t \omega - v}{v} = \frac{R_t \omega}{v} - 1 \quad (9b)$$

In deceleration, the vehicle speed is greater than the tangential speed, so the slip ratio is negative.

The longitudinal model is very similar to the lateral model, except camber effects are not considered.

$$F_x = D_x \sin(C_x \theta_x) + S_{xv} \quad (10)$$

$$\begin{aligned} \theta_x &= \tan^{-1} \left\{ B_x (\sigma + S_{sh}) - E_x \left[B_x (\sigma + S_{sh}) - \tan^{-1} (B_x (\sigma + S_{sh})) \right] \right\} \\ &= \tan^{-1} \left\{ B_x (\sigma + S_{sh}) \left(1 - E_x \left[1 - \frac{\tan^{-1} (B_x (\sigma + S_{sh}))}{B_x (\sigma + S_{sh})} \right] \right) \right\} \end{aligned} \quad (11)$$

For calculation of the longitudinal force, the B_x , C_x , D_x , E_x , S_{sh} , and S_{xv} coefficients are given in terms of 14 constants, b_i , derived from the measured data.

$$C_x = b_0 \quad (12)$$

$$D_x = (b_1 F_z + b_2) F_z \quad (13)$$

$$B_x = \frac{(b_3 F_z + b_4) F_z e^{-b_5 F_z}}{C_x D_x} \quad (14)$$

$$E_x = (b_6 F_z^2 + b_7 F_z + b_8) [1 - b_{13} \text{sign}(\sigma + S_{yh})] \quad (15)$$

$$S_{xh} = b_9 F_z + b_{10} \quad (16)$$

$$S_{xv} = b_{11} F_z + b_{12} \quad (17)$$

The b coefficients and the constants are explained at the end in appendix.

5.2 Woods Tire Models

The Pacejka models do an acceptable job of representing tire data, they fall short on three aspects that are of interest to analysis and simulation. First, the equations are not presented in a normalized form so it is not clear at what value of slip the tire force reaches a peak. For racing applications, one would want to know the slip angle at peak adhesion, so a peak slip angle should be presented explicitly. Second, one should be able to isolate this peak slip function as an independent equation so it can be shown how the slip varies with normal load and camber. Third, the a and b coefficients do not have any physical interpretation to which one can relate. In most cases, the coefficients are even presented without any units. When units are presented, measurements of force are often not consistent (vertical load measured in kN and adhesion forces measured in N).[2]

The normalization is both in the adhesion force relative to the normal load, and the slip relative to the peak slip (slip at which the adhesion force reaches a peak). In this normalized form, the equation for the peak slip function is clear and can be written independently.[2]

First the Pacejka model is normalized with respect to the normal load, F_z , and second, the slip terms are normalized and scaled so that the maximizing slip can be observed directly. This normalizing approach makes use of some recognizable physical parameters such as the coefficient of friction. When the parameters are not obvious, they are expressed as the value that would cause a 10% change in performance. This will give a physical feel for the coefficients and for their units.[2]

5.2.1 Woods tire Model

My normalization of the Pacejka model for lateral acceleration can be stated in the following form (similar to equation 1).

$$\frac{F_y}{F_z} = \mu_y \sin(C_y \theta_y) + \frac{F_{yoff}}{F_z} \quad (18)$$

where C_y = droop factor that adjusts the slope after peak adhesion.

The lateral coefficient of friction is μ_y and can be expressed as follows (similar to equation 4).

$$\mu_y = \frac{D_y}{F_z} = \mu_{y0} \left(1 - 0.1 \frac{F_z}{F_{y\mu}} \right) \left[1 - 0.1 \left(\frac{\gamma}{\gamma_{y\mu}} \right)^2 \right] \quad (19)$$

where μ_{y0} = the coefficient of friction that would occur with zero load and zero camber

$F_{y\mu}$ = the load that will result in a 10% degradation in μ

$\gamma_{y\mu}$ = the camber that will result in a 10% degradation in μ

The vertical offset of the forces is expressed as a function of normal load and camber (similar to equation 8).

$$F_{yoff} = F_{yoff0} + S_{yoff} \left[1 + \left(1 + 0.1 \frac{F_z}{F_{yoffz}} \right) \left(0.1 \frac{\gamma}{\gamma_{yoff}} \right) \right] F_z \quad (20)$$

where F_{yoff0} = the offset (or force intercept) that would occur with zero load

F_{yoffz} = the load that will result in a 10% change in offset related to camber

S_{yoff} = the sensitivity of lateral force to normal force

γ_{yoff} = a 10% normalizing factor for γ

The variable θ_y is a modified slip variable that is limited by an inverse tangent function (similar to equation 2).

$$\theta_y = \tan^{-1} \left\{ \frac{G_y (\alpha + \alpha_{off})}{\alpha_{peak}} \left[1 - E_y \left[1 - \frac{\tan^{-1} \left(\frac{G_y (\alpha + \alpha_{off})}{\alpha_{peak}} \right)}{\frac{G_y (\alpha + \alpha_{off})}{\alpha_{peak}}} \right] \right] \right\} \quad (21)$$

The term G_y is introduced to make the sine function reach its maximum value when the slip is at its approximate peak value.

$$G_y = \tan \left(\frac{\pi/2}{C_y} \right) \quad (22)$$

Notice that if α is at its peak value, then $\theta_y \approx \tan^{-1}(G_y)$, and therefore $C_y \theta_y = \pi/2$.

Using the above equation, we can clearly observe the slip angle at which maximum lateral force occurs as an independent function [2].

The horizontal offset is an offset in slip angle, α_{off} (similar to equation 7).

$$\alpha_{off} = S_{yh} = \alpha_{off0} \left[1 - 0.1 \frac{F_z}{F_{\alpha off}} + 0.1 \frac{\gamma}{\gamma_{\alpha off}} \right] \quad (23)$$

where α_{off0} = the offset that would occur with zero load and zero camber

$F_{\alpha off}$ = the load that will result in a 10% decrease in offset

$\gamma_{\alpha off}$ = the camber that will result in a 10% increase in offset

The E_y is a variable that modifies the slip function (similar to equation 6).

$$E_y = E_{y0} \left(1 + 0.1 \frac{F_z}{F_{ye}} \right) \left[1 - E_{yy} \left(1 + 0.1 \frac{\gamma}{\gamma_{ye}} \right) \text{sign}(\alpha + \alpha_{off}) \right] \quad (24)$$

where E_{y0} = the slip modifier that would occur with zero load and zero camber

F_{ye} = the load that will result in a 10% change in E

E_{yy} = another slip modifier constant

γ_{ye} = the camber that will result in a 10% change of the modifier constant.

The original B_y coefficient in the Pacejka model can be used (with some algebra) to find the slip angle at which the maximum adhesion occurs, α_{peak} (derived from equation 5 and others).[1]

$$\alpha_{peak} = \frac{G_y}{B_y} = \frac{\alpha_{peak0} \frac{\mu_y}{\mu_{y0}} \frac{2 \frac{F_z}{\alpha_4}}{\sin \left(2 \tan^{-1} \left(\frac{F_z}{\alpha_4} \right) \right)}}{\left(1 - 0.1 \frac{|\gamma|}{\gamma_{apeak}} \right)} \quad (25)$$

where α_{peak0} = the slip angle that would occur with zero load and zero camber

α_4 = Pacejka coefficient

γ_{apeak} = the camber that will result in a 10% change in α_{peak}

$$\alpha_{peak0} = \frac{C_y G_y \mu_{y0} F_{z\alpha}}{2 S_{apeak}} \quad (26)$$

where S_{apeak} = a load sensitivity = a_3

In the form expressed above, it is clear that the peaking slip angle is directly proportional to the coefficient of friction. In other words, as the μ increases, the slip angle will increase. [2]

The last term in the α_{peak} equation is mathematically equal to a parabolic function (which is much more simple than the trig functions). The Pacejka models do not make this simplification, but it will be used in all of the following equations even though it is not strictly a Pacejka model, it produces identical results and is easier to visualize than the original.[2]

$$\frac{2 \frac{F_z}{\alpha_4}}{\sin \left(2 \tan^{-1} \left(\frac{F_z}{\alpha_4} \right) \right)} = \left[1 + \left(\frac{F_z}{\alpha_4} \right)^2 \right] \quad (27)$$

Therefore, the α_{peak} equation can be simplified as follows.

$$\alpha_{peak} = \frac{\alpha_{peak0} \left(1 + 0.1 \left(\frac{F_z}{F_{z\alpha}} \right)^2 \right) \frac{\mu_y}{\mu_{y0}}}{\left(1 - 0.1 \frac{|\gamma|}{\gamma_{apeak}} \right)} \quad (28)$$

or

$$\alpha_{peak} = \frac{\alpha_{peak0} \left(1 + 0.1 \left(\frac{F_z}{F_{z\alpha}} \right)^2 \right) \left(1 - 0.1 \frac{F_z}{F_{y\mu}} \right) \left[1 - 0.1 \left(\frac{\gamma}{\gamma_{y\mu}} \right)^2 \right]}{\left(1 - 0.1 \frac{|\gamma|}{\gamma_{apeak}} \right)} \quad (29)$$

where

$F_{z\alpha}$ = the load that will result in a 10% increase in α_{peak}

For the conversions between the normalizing factors and the original Pacejka coefficients refer to appendix.

5.2.2 Normalized Longitudinal Pacejka Model

Normalization of the Pacejka model for acceleration and deceleration can be stated in the following form.

$$\frac{F_x}{F_z} = \mu_x \sin(C_x \theta_x) + \frac{F_{xoff}}{F_z} \quad (30)$$

$$\theta_x = \tan^{-1} \left\{ \frac{G_x (\sigma + \sigma_{off})}{\sigma_{peak}} \left[1 - E_x \left[1 - \frac{\tan^{-1} \left(\frac{G_x (\sigma + \sigma_{off})}{\sigma_{peak}} \right)}{\frac{G_x (\sigma + \sigma_{off})}{\sigma_{peak}}} \right] \right] \right\} \quad (31)$$

Again, the parameter G_x is introduced to make the longitudinal force curve saturate at σ_{peak} .

$$G_x = \tan \left(\frac{\pi/2}{C_x} \right) \quad (32)$$

The longitudinal coefficient of friction is μ_x and can be expressed as follows.

$$\mu_x = \frac{D_x}{F_z} = \mu_{x0} \left(1 - 0.1 \frac{F_z}{F_{x\mu}} \right) \quad (33)$$

where μ_{x0} = the coefficient of friction that would occur with zero load

$F_{x\mu}$ = the value of load that will result in a 10% degradation in μ

The vertical offset is F_{xoff} .

$$F_{xoff} = F_{xoff0} \left(1 + 0.1 \frac{F_z}{F_{xoffz}} \right) \quad (34)$$

where F_{xoff0} = the offset that would occur with zero load

F_{xoffz} = the load that will result in a 10% change in offset

The horizontal shift is given as follows.

$$\sigma_{off} = S_{sh} = \sigma_{off0} \left[1 - 0.1 \frac{F_z}{F_{\sigma off}} \right] \quad (35)$$

where σ_{off0} = the offset that would occur with zero load

$F_{\sigma off}$ = the value of load that will result in a 10% decrease in offset

The E_x is a variable that modifies the slip function.

$$E_x = E_{x0} \left[1 + 0.1 \frac{F_z}{F_{xe1}} + 0.1 \left(\frac{F_z}{F_{xe2}} \right)^2 \right] \left[1 - E_{x\sigma} \text{sign}(\sigma + \sigma_{off}) \right] \quad (36)$$

where E_{x0} = the slip modifier that would occur with zero load and zero camber

F_{xe1} = the value of load that will result in a 10% change in E_x

F_{xe2} = the value of load that will result in a 10% change in E_x

$E_{x\sigma}$ = another slip modifier constant

By noting that $B_x = G_x / \sigma_{peak}$, we can solve for the slip ratio at which the maximum adhesion occurs, σ_{peak} .

$$\sigma_{peak} = \frac{G_x}{B_x} = \frac{\sigma_{peak0} \frac{\mu_x}{\mu_{x0}}}{\left(1 - 0.1 \frac{F_z}{F_{\sigma z}}\right) e^{-\frac{F_z}{F_{\sigma e}}}} \quad (37)$$

where σ_{peak0} = the slip ratio that would occur with zero load

$F_{\sigma z}$ = the value of load that will result in about a 10% change in σ_{peak}

$F_{\sigma e}$ = a normalizing load factor

$$\sigma_{peak0} = \frac{C_x G_x \mu_{x0}}{\mu_{\sigma peak0}} \quad (38)$$

where $\mu_{\sigma peak0}$ = a normalizing friction factor

we can also solve for μ_{peak} at which maximum adhesion occurs

$$\mu_{peak} = \mu_{0peak} * \left[1 - 0.1 \frac{F_z}{F_{\mu peak}}\right] * \left[1 - 0.1 \frac{\gamma}{\gamma_{\mu peak}}\right]^2 \quad (39)$$

Where, μ_{0peak} = the μ that would occur with zero load

$F_{\mu peak}$ = the value of load that will result in about a 10% change in μ_{0peak}

$\gamma_{\mu peak}$ = normalising factor.

For the conversions between the normalizing factors and the original Pacejka coefficients refer to appendix.

5.3 Performance Interpretation of Woods tire model

Analytic tire models have several useful applications. One is the interpretation of the tire performance as the normal load and camber change. In driving applications of a vehicle of fixed weight, the normal load on a tire can change due to weight transfer in a driving maneuver. In particular, we are interested in how the coefficient of friction changes, and how the slip angle that results in peak adhesion changes with load and camber.[2]

This can be observed from the expressions for μ_y and α_{peak} derived in a previous section and presented below.[2]

$$\frac{\mu_y}{\mu_{y0}} = \left[1 - 0.1 \frac{F_z}{F_{y\mu}} \right] \left[1 - 0.1 \left(\frac{\gamma}{\gamma_{y\mu}} \right)^2 \right] \quad (40)$$

$$\frac{\alpha_{peak}}{\alpha_{peak0}} = \frac{\left[1 + 0.1 \left(\frac{F_z}{F_{z\alpha}} \right)^2 \right] \mu_y}{\left[1 - 0.1 \frac{|\gamma|}{\gamma_{cpeak}} \right] \mu_{y0}} \quad (41)$$

or by substitution of μ_y :

$$\frac{\alpha_{peak}}{\alpha_{peak0}} = \frac{\left[1 - 0.1 \frac{F_z}{F_{y\mu}}\right] \left[1 - 0.1 \left(\frac{\gamma}{\gamma_{y\mu}}\right)^2\right]}{\left[1 - 0.1 \frac{|\gamma|}{\gamma_{cpeak}}\right]} \left[1 + 0.1 \left(\frac{F_z}{F_{z\alpha}}\right)^2\right] \quad (42)$$

By using the above equations we can determine how μ and maximizing slip vary with load and camber.

Chapter 6: Verification

Using the equations in chapter 5, we can determine how μ and maximizing slip vary with load and camber. To verify our theory 4 different tire compounds from different manufacturers were selected:

- Hoosier R13 R25B.
- Hoosier R10 LCO.
- Goodyear R13 D2509.
- Avon R10 7*16.

These compounds were chosen because of the availability of testing data through Tire test consortium (TTC). Every tire is different in construction, material and geometry; hence a wide variety of manufacturers and compounds were selected to validate our tire model.

6.1 Data Parsing

The TTC records data over 16 channels at the frequency of 10-100Hz. All this raw data is dumped into a data file and is distributed to all the registered members. Due to the large number of input variables it's very important to understand the test procedure. The test accounts for tire break in and warm up to bring the tires up to temperature before every run. Hence it is important to parse the data and use the data that best simulates your purpose [5].

Channel	Units	Description
AMBTMP	degC or degF	Ambient room temperature
ET	sec	Elapsed time for the test
FX	N or lb	Longitudinal Force
FY	N or lb	Lateral Force
FZ	N or lb	Normal Load
IA	deg	Inclination Angle
MX	N-m or lb-ft	Overturning Moment
MZ	N-m or lb-ft	Aligning Torque
N	rpm	Wheel rotational speed
NFX	unitless	Normalized longitudinal force (FX/FZ)
NFY	unitless	Normalized lateral force (FY/FZ)
P	kPa or psi	Tire pressure
RE	cm or in	Effective Radius
RL	cm or in	Loaded Radius
RST	degC or degF	Road surface temperature
SA	deg	Slip Angle
SL	unitless	Slip Ratio based on RE (such that SL=0 gives FX=0)
SR	unitless	Slip Ratio based on RL (used for Calspan machine control, SR=0 does not give FX=0)
TSTC	degC or degF	Tire Surface Temperature--Center
TSTI	degC or degF	Tire Surface Temperature--Inboard
TSTO	degC or degF	Tire Surface Temperature--Outboard
V	kph or mph	Road Speed

Figure 7: Data channels at TTC.

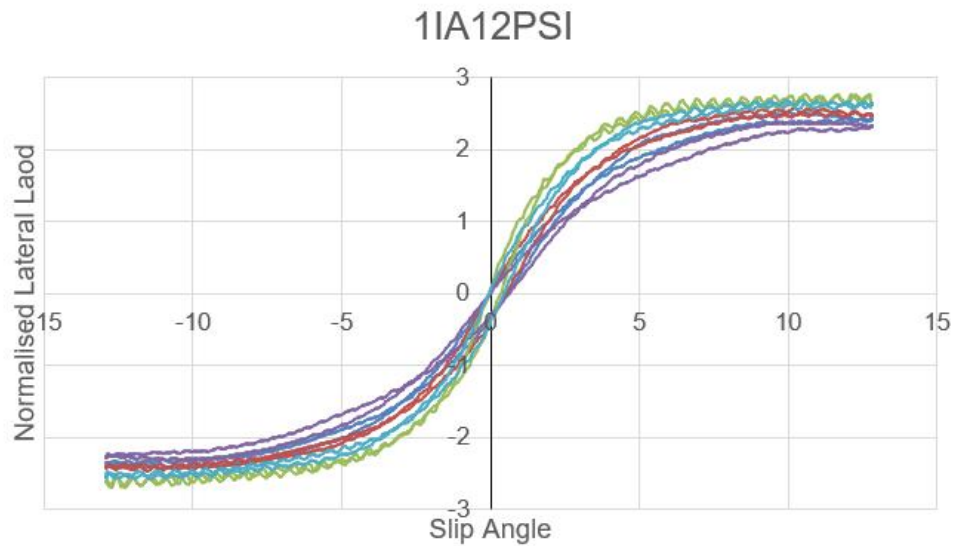


Figure 8: Normalized Lateral Load vs Slip angle from TTC raw data.

Once all the Data for a Tire has been parsed. We import the data into an excel spreadsheet where we proceed to start with manually curve fitting our mathematical model over the TTC raw data for each variable. The nomenclature followed here was:

X IA XXX FZ XX PSI

Where numbers preceding IA denote inclination angle,

FZ denote Normal Load,

And PSI denote inflation pressure.

6.2 Curve fitting to TTC raw data.

Figure 9 shows a curve fit template. On the left side of the template we paste the TTC raw data. The numbers in blue on the right-hand side of the template are scaling factors for our mathematical model. Changing various parameters modifies the curve fit seen in the figure 9. The following equations are used to generate the curve fit model.

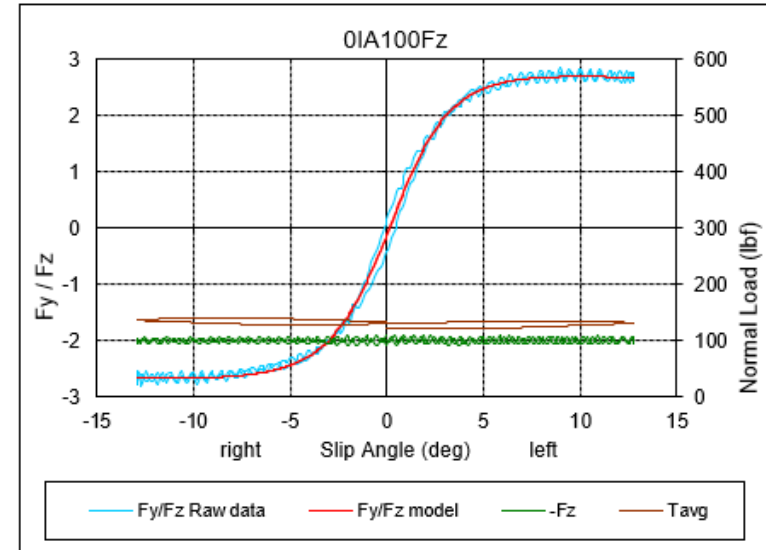
$$\frac{F_y}{F_z} = \mu_y \sin \theta_y$$

$$\theta_y = \frac{\pi}{2} \frac{\tan^{-1}\left(\frac{\alpha - \alpha_{off}}{g_y}\right)}{\tan^{-1}\left(\frac{\alpha_{peak} - \alpha_{off}}{g_y}\right)}$$

$\mu y0 =$	2.7
$F_{\mu y} =$	160
$\gamma_{\mu y} =$	40.0
$T_{peak} =$	190
$\Delta T_{\mu y} =$	80
$\alpha_{peak0} =$	9.5
$F_{\alpha peak} =$	150
$\gamma_{\alpha peak} =$	12
$\gamma_{y0} =$	2.1
$F_{\gamma y} =$	11
$\gamma_{\gamma y} =$	2
$\alpha_{off0} =$	-0.2
$S_{bias} =$	-0.05
$S_{\gamma} =$	0.18
$F_{\alpha off} =$	55
$F_{\alpha max} =$	350
$T_{max} =$	148
$F_{z off} =$	210
$F_t =$	145
$\mu_{peak0} =$	2.6
$F_{\mu peak} =$	160
$\gamma_{\mu peak} =$	3.6

modified numbers		
$F_z@peak =$	100	$IA = 0$
$\alpha_+ =$	10	$avg F_z = 100$
$\mu_+ =$	2.7	
$T_+ =$	135	
$\alpha_- =$	-11.5	
$\mu_- =$	-2.67	
$T_- =$	140	
$g =$	4	
$\mu_{off} =$	0	$N_{fy off} = -0.179$
$\alpha_{off} =$	0.15	$F_{y0 off} = 19.123$

Curve Fitting



$$\frac{F_y}{F_z} = \mu_y \sin \theta_y$$

$$\theta_y = \frac{\pi}{2} \frac{\tan^{-1}\left(\frac{\alpha - \alpha_{off}}{g_y}\right)}{\tan^{-1}\left(\frac{\alpha_{peak} - \alpha_{off}}{g_y}\right)}$$

Figure 9: Curve Fit Template.

The above listed coefficients were varied by hand to get a good curve fit to match raw data.

Below is an example of a good curve fit over TTC raw data.

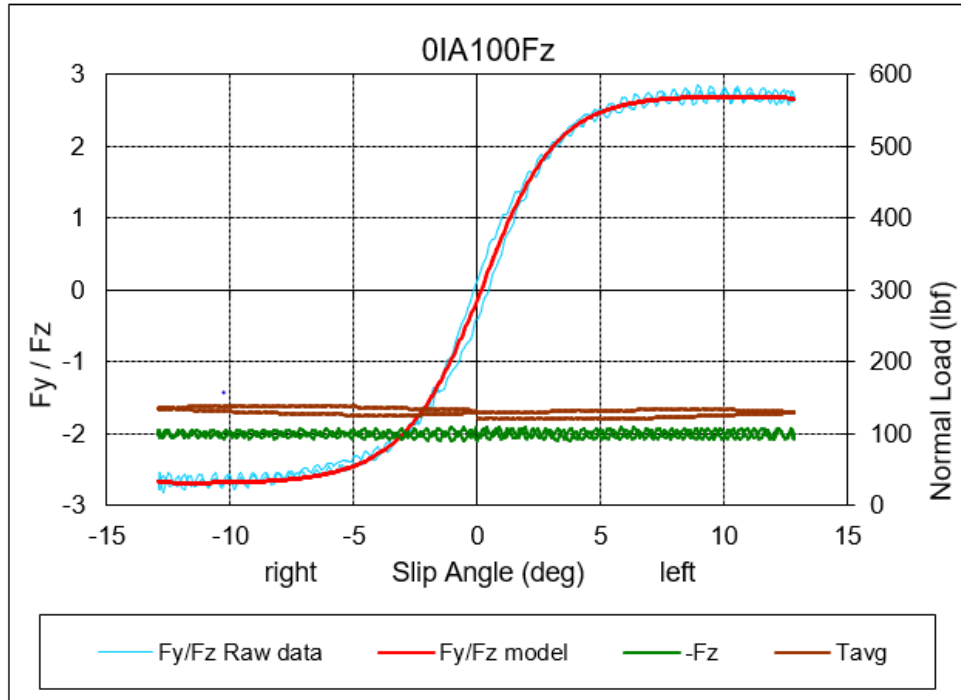


Figure 10: Curve fitting over TTC raw data.

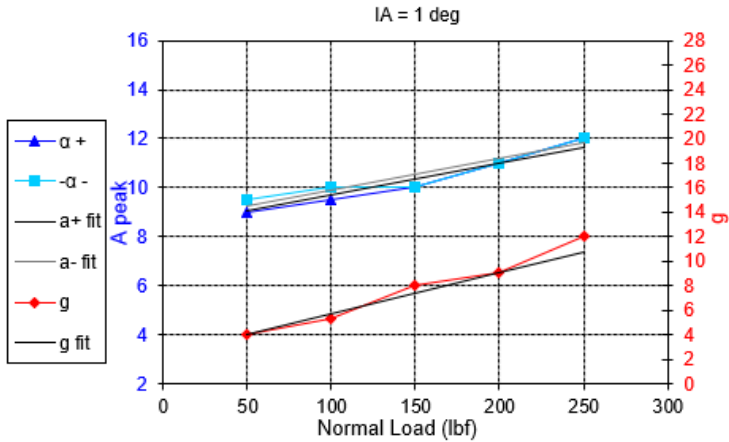
6.3 Curve fitting of scaling factors.

Trial and error method were used to achieve the best possible curve fit. For every inflation pressure 25 such curve fits were done per tire. Once you have achieved a satisfactory curve fit for all the parameters. The next step is to generate scaling coefficients for our mathematical model. Paying attention to every detail in the first step is key to getting accurate and quick results. Figure 11 shows a template to curve fit the scaling factors. After fine tuning every curve individually you can generate the scaling factors for our mathematical model.

Curve Fitting

μ_{y0}	3.3
$F_{\mu y}$	180
$\gamma_{\mu y}$	40.0
T_{peak}	205
$\Delta T_{\mu y}$	55
α_{peak0}	8.5
$F_{\alpha peak}$	65
$\gamma_{\alpha peak}$	12
g_{y0}	2.25
$F_{g y}$	7
$\gamma_{g y}$	2
α_{off0}	0.15
S_{bias}	-0.05
S_{γ}	0.15
$F_{\alpha off}$	60
$F_{\alpha max}$	300
T_{max}	140
$F_{z off}$	250
F_l	250

modified numbers		
	IA =	0
Fz@peak =	100	avg Fz = 100
$\alpha+$ =	10	
$\mu+$ =	2.7	
T+ =	135	
$\alpha-$ =	-11.5	
$\mu-$ =	-2.67	
T- =	140	
g =	4	
μ_{off} =	0	Nfy off = -0.179
α_{off} =	0.15	Fy0ff = 19.123



$$\mu_y = \mu_{y0} f_{\mu y} \left[1 - 0.1 \frac{F_z}{F_{\mu y}} \right] \left[1 + 0.1 \frac{\gamma}{\gamma_{\mu y}} \right] \left[1 - 0.1 \left(\frac{T - T_{peak}}{\Delta T_{\mu y}} \right)^2 \right]$$

$$\alpha_{peak} = f_{\alpha peak} \left[1 + 0.1 \frac{F_z}{F_{\alpha peak}} \right] \left[1 - 0.1 \left(\frac{\gamma}{\gamma_{\alpha peak}} \right) \right]$$

$$g_y = g_{y0} \left[1 + 0.1 \frac{F_z}{F_{g y}} \right] \left[1 + 0.1 \frac{LA}{LA_{g y}} \right]$$

$$\alpha_{off} = f_{\alpha off} \left[\alpha_{off0} + S_{bias} \left(\frac{F_z - F_{\alpha off}}{F_{\alpha max}} \right) + S_{\gamma} LA \sin \left(\frac{\pi}{2} \frac{F_z - F_{\alpha off}}{F_{\alpha max}} \right) \right]$$

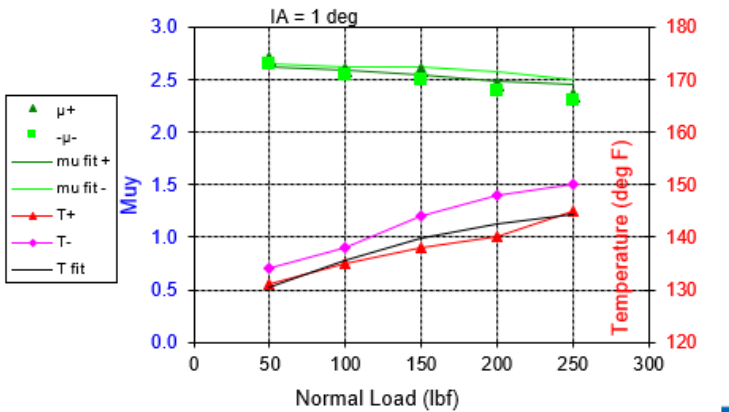


Figure 11: Curve fit for obtaining scaling factors.

	Hoosier R10*18 LCO	Avon R10*16	Hoosier R13*20 R25B	Goodyear R13*20 D2509
$\mu y_0 =$	3.3	2.7	3.25	3.25
$F_{\mu y} =$	160	160	170	160
$\gamma_{\mu y} =$	40.0	40.0	60	40.0
$T_{peak} =$	205	190	195	190
$\Delta T_{\mu y} =$	55	80	55	80
$\alpha_{peak0} =$	8.5	9.5	7.8	8.7
$F_{\alpha_{peak}} =$	65	150	100	75
$\gamma_{\alpha_{peak}} =$	12	12	9	12
$g_{y0} =$	2.5	2.1	1.7	0.27
$F_{g_y} =$	9	11	15.0	0.6
$\gamma_{g_y} =$	2	2	0.6	1.5
$\alpha_{off0} =$	0.15	-0.2	-0.020	-0.2
$S_{bias} =$	-0.05	-0.05	0.180	-0.05
$S_{\gamma} =$	0.15	0.18	0.155	0.18
$F_{\alpha_{off}} =$	60	55	45	55
$F_{\alpha_{max}} =$	300	350	330	350
$T_{max} =$	135	148	118	132
$F_{z_{off}} =$	300	210	260	320
$F_t =$	250	145	260	300
$\mu_{peak0} =$	2.8	2.6	3	3.1
$F_{\mu_{peak}} =$	160	160	160	160
$\gamma_{\mu_{peak}} =$	4.5	3.6	5	6

Figure 12: Woods coefficients for tested tires.

6.4 Woods model vs TTC raw data.

Once the scaling factors are obtained, we can verify our mathematical model by superimposing it over TTC raw data. The mathematical model accurately represents tire behavior as seen in figure

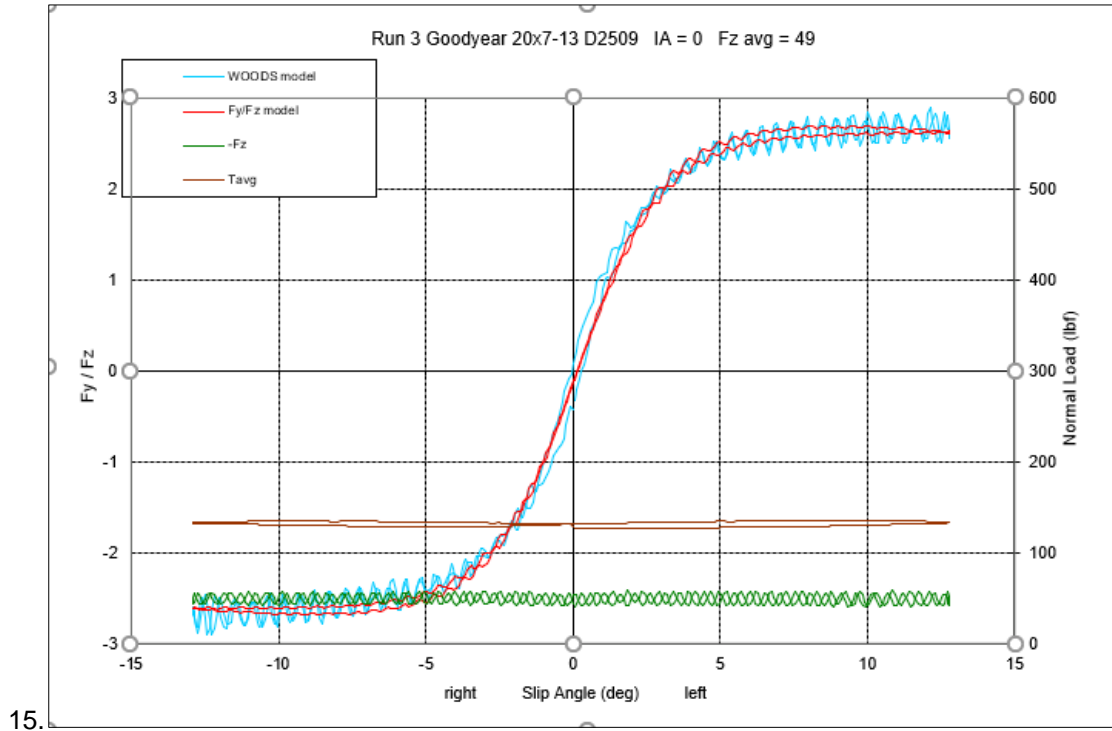


Figure 13: Woods model vs TTC raw data.

As seen in figure 13 all our assumptions and mathematical fits for obtaining scaling factors were accurate.

Chapter 7: Results and conclusion

The WOODS tire model for tire performance was verified in such a way that the value of slip that results in a maximum force can be clearly identified. Having these equations for maximizing slip, we could also determine how μ and the maximizing slip vary with load and camber. These characteristics help the racecar engineer to set optimum toe settings and handling properties.

$$\alpha_{peak} = \frac{\alpha_{peak0} \left(1 + 0.1 \left(\frac{F_z}{F_{z\alpha}} \right)^2 \right) \left(1 - 0.1 \frac{F_z}{F_{y\mu}} \right) \left[1 - 0.1 \left(\frac{\gamma}{\gamma_{y\mu}} \right)^2 \right]}{\left(1 - 0.1 \frac{|\gamma|}{\gamma_{apeak}} \right)}$$

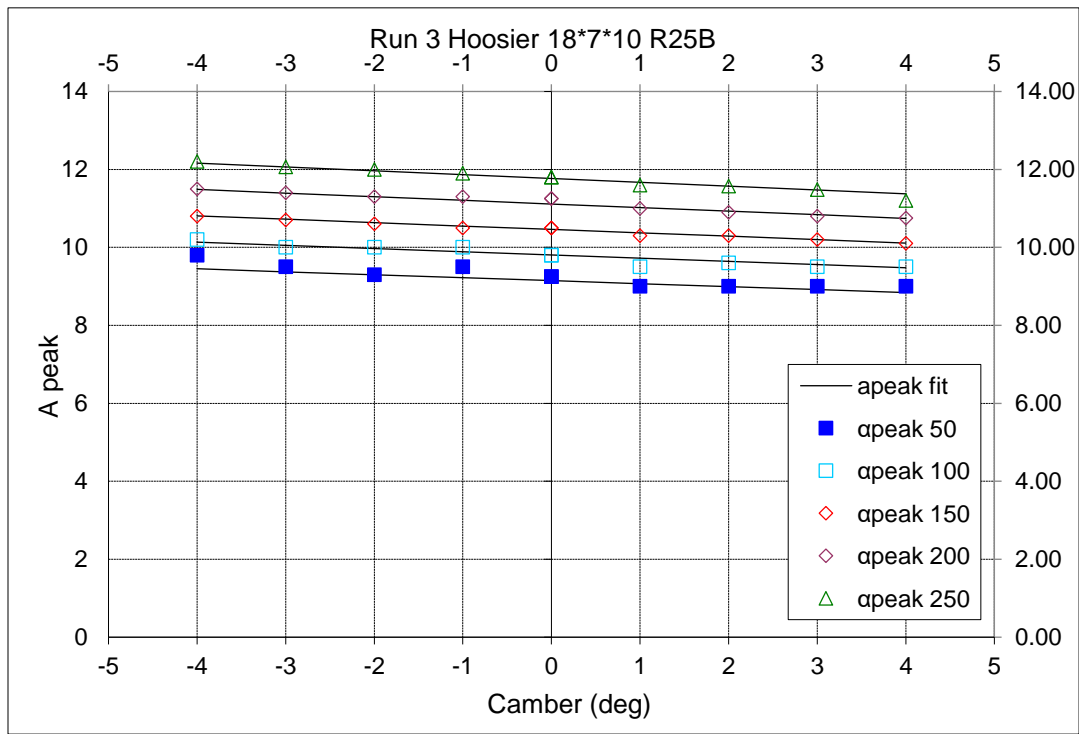


Figure 14: Maximizing slip for various loads vs camber.

Figure 14 shows us that we could successfully express maximizing slip as a function of normal loads and camber. As expected maximizing slip degrades with increase in normal load and inclination angle.

$$\mu_{peak} = \mu_{0peak} * \left[1 - 0.1 \frac{F_z}{F_{\mu peak}} \right] * \left[1 - 0.1 \frac{\gamma}{\gamma_{\mu peak}} \right]^2$$

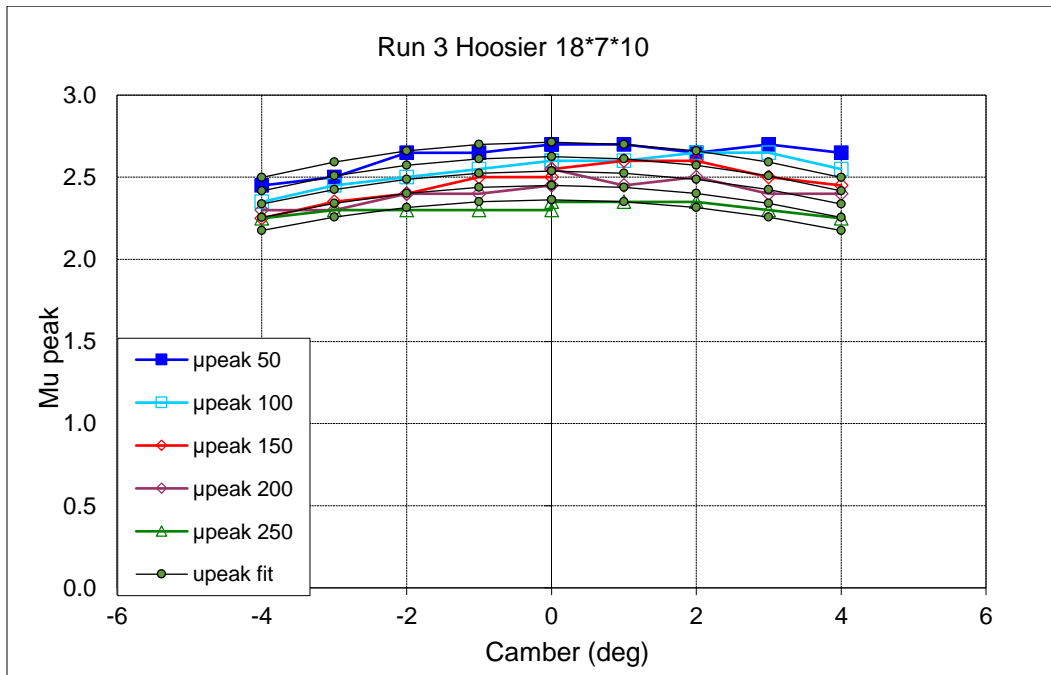


Figure 15: μ for various loads vs Camber.

Figure 15 shows us that we could successfully express μ as a function of normal loads and camber. As expected maximum adhesion degrades with increase in normal load.

For data on more tires please refer to appendix A-2.

Appendix

Appendix A-1

Conversions: The conversions between the original Pacejka coefficients and the physically relateable coefficients are given below. Note that in the SAE convention, some of the coefficients need to be divided by 1000 (to account for the conversion from kN to N) when they are used in the following conversion to normalized variables.

$$C_y = a_0$$

$$a_0 = C_y$$

$$G_y = \tan\left(\frac{\pi/2}{a_0}\right)$$

$$a_1 = \frac{-0.1 \mu_{y0} * 1000}{F_{\mu y}}$$

$$\mu_{y0} = a_2 / 1000$$

$$a_2 = \mu_{y0} * 1000$$

$$F_{y\mu} = \frac{-0.1 a_2}{a_1}$$

$$a_3 = S_{\alpha peak}$$

$$\gamma_{y\mu} = \sqrt{\frac{0.1}{a_{15}}}$$

$$a_4 = F_{z\alpha} \sqrt{10}$$

$$F_{yoff0} = a_{12}$$

$$a_5 = \frac{0.1}{\gamma_{\alpha peak}}$$

$$F_{yoffz} = \frac{0.1 a_{14}}{a_{13}}$$

$$a_6 = \frac{0.1 E_{y0}}{F_{ey1}}$$

$$S_{yoff} = \frac{a_{11}}{1000}$$

$$a_7 = E_{y0}$$

$$\gamma_{yoff} = \frac{0.1 a_{11}}{a_{14}}$$

$$a_8 = \frac{-0.1 \alpha_{off0}}{F_{aoff}}$$

$$\alpha_{off0} = a_9$$

$$a_9 = \alpha_{off0}$$

$$F_{aoff} = \frac{-0.1 a_9}{a_8}$$

$$a_{10} = \frac{0.1 \alpha_{off0}}{\gamma_{aoff}}$$

$$\gamma_{aoff} = \frac{0.1 a_9}{a_{10}}$$

$$a_{11} = S_{yoff} * 1000$$

$$E_{y0} = a_7$$

$$a_{12} = F_{yoff0}$$

$$E_{y\gamma} = a_{17}$$

$$a_{13} = \frac{(0.1)^2 S_{yoff} * 1000}{\gamma_{yoff} F_{yoffz}}$$

$$F_{ye} = \frac{0.1 a_7}{a_6}$$

$$a_{14} = \frac{0.1 S_{yoff} * 1000}{\gamma_{yoff}}$$

$$\gamma_{ye} = \frac{0.1 a_{17}}{a_{16}}$$

$$a_{15} = \frac{0.1}{\gamma_{\mu y}^2}$$

$$S_{apeak} = a_3$$

$$a_{16} = \frac{0.1 E_{y\gamma}}{\gamma_{ey}}$$

$$F_{z\alpha} = \frac{a_4}{\sqrt{10}}$$

$$a_{17} = E_{y\gamma}$$

$$\gamma_{apeak} = \frac{0.1}{a_5}$$

and

$$\alpha_{peak0} = \frac{a_0 \tan\left(\frac{\pi/2}{a_0}\right) \frac{a_2}{1000} a_4}{2 a_3}$$

Notice that I have defined two new coefficients, G_y and α_{peak0} , that are dependent on the original coefficients and does not increase the required information.

The normalizing factors can be related to the original Pacejka coefficients, b , as follows.

$$C_x = b_0$$

$$b_0 = C_x$$

$$G_x = \tan\left(\frac{\pi/2}{b_0}\right)$$

$$b_1 = \frac{-0.1 * 1000 \mu_{x0}}{F_{\mu x}}$$

$$\mu_{x0} = b_2 / 1000$$

$$b_2 = 1000 \mu_{x0}$$

$$F_{\mu x} = \frac{-0.1 b_2}{b_1}$$

$$b_3 = \frac{0.1 \mu_{\sigma peak0}}{F_{\sigma z}}$$

$$F_{xoff0} = b_{12}$$

$$b_4 = \mu_{\sigma peak0}$$

$$F_{xoffz} = 0.1 \frac{b_{12}}{b_{11}} * 1000$$

$$b_5 = \frac{1}{F_{\sigma e}}$$

$$\sigma_{off0} = b_{10}$$

$$b_6 = \frac{0.1 E_{x0}}{F_{xe2}^2}$$

$$F_{\sigma off} = \frac{-0.1 b_{10}}{b_9}$$

$$b_7 = \frac{0.1 E_{x0}}{F_{xe1}}$$

$$E_{x0} = b_8$$

$$b_8 = E_{x0}$$

$$F_{xe1} = \frac{0.1 b_8}{b_7}$$

$$b_9 = \frac{-0.1 \sigma_{off0}}{F_{\sigma off}}$$

$$F_{xe2} = \sqrt{\frac{0.1 b_8}{b_6}}$$

$$b_{10} = \sigma_{off0}$$

$$E_{x\sigma} = b_{13}$$

$$b_{11} = 0.1 \frac{F_{xoff0}}{F_{xoffz}} * 1000$$

$$F_{\sigma z} = \frac{-0.1 b_4}{b_3}$$

$$b_{12} = F_{xoff0}$$

$$F_{\sigma e} = \frac{1}{b_5}$$

$$b_{13} = E_{x\sigma}$$

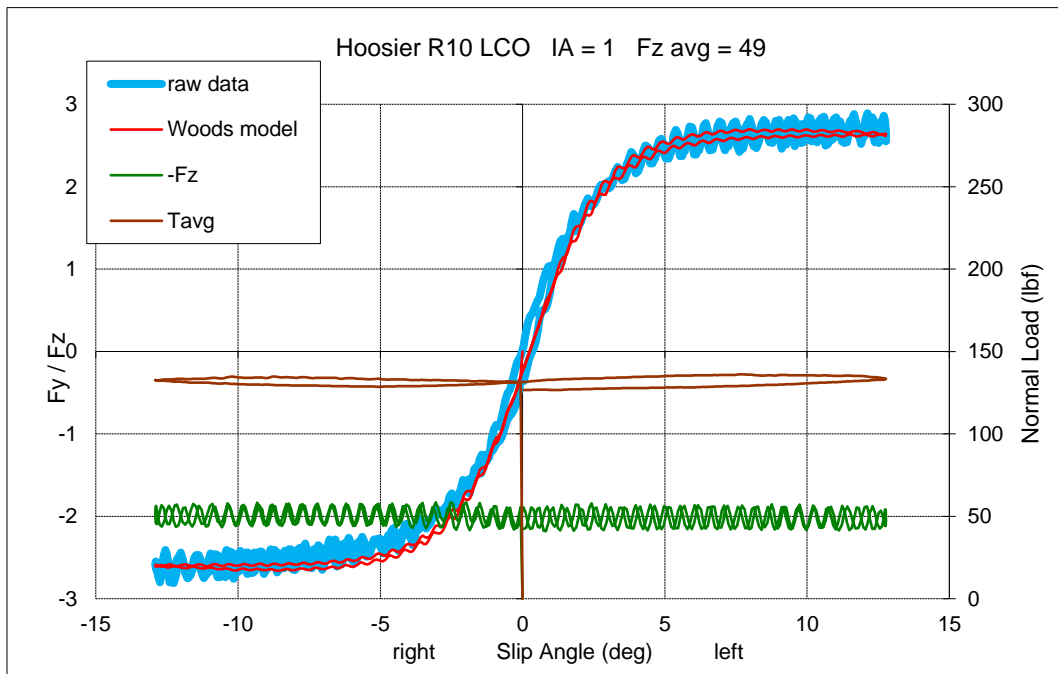
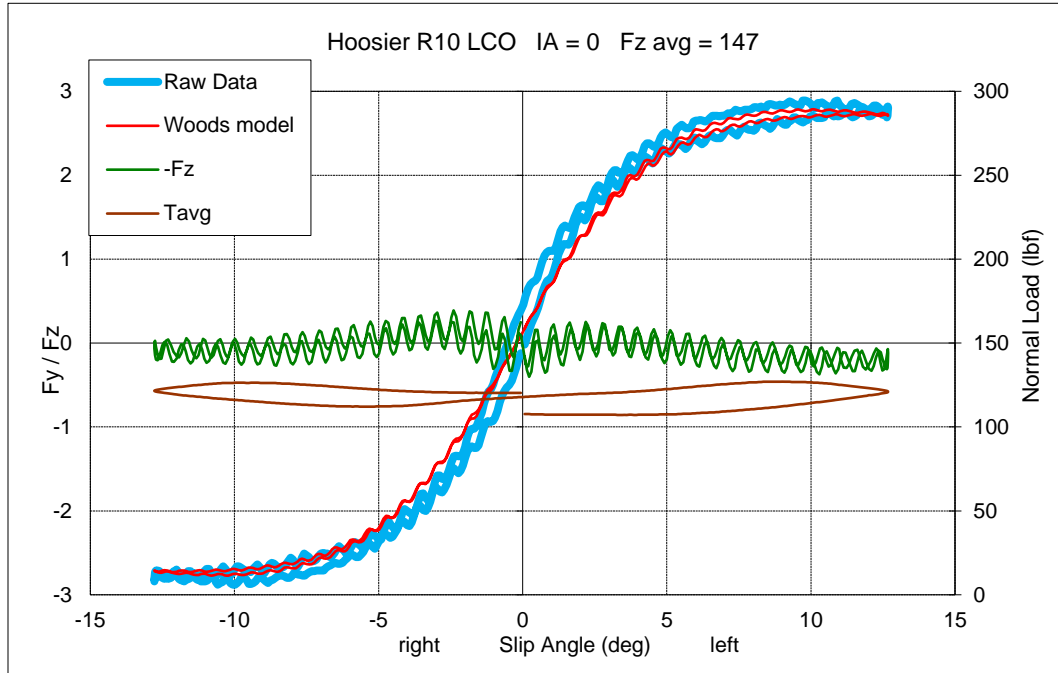
$$\mu_{\sigma peak0} = b_4$$

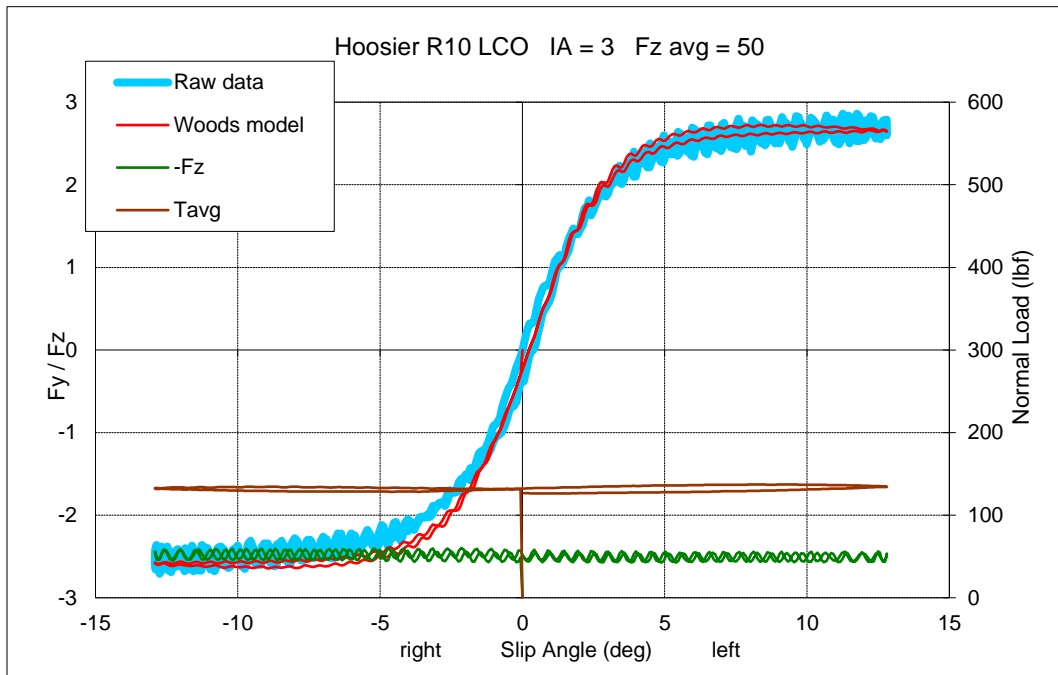
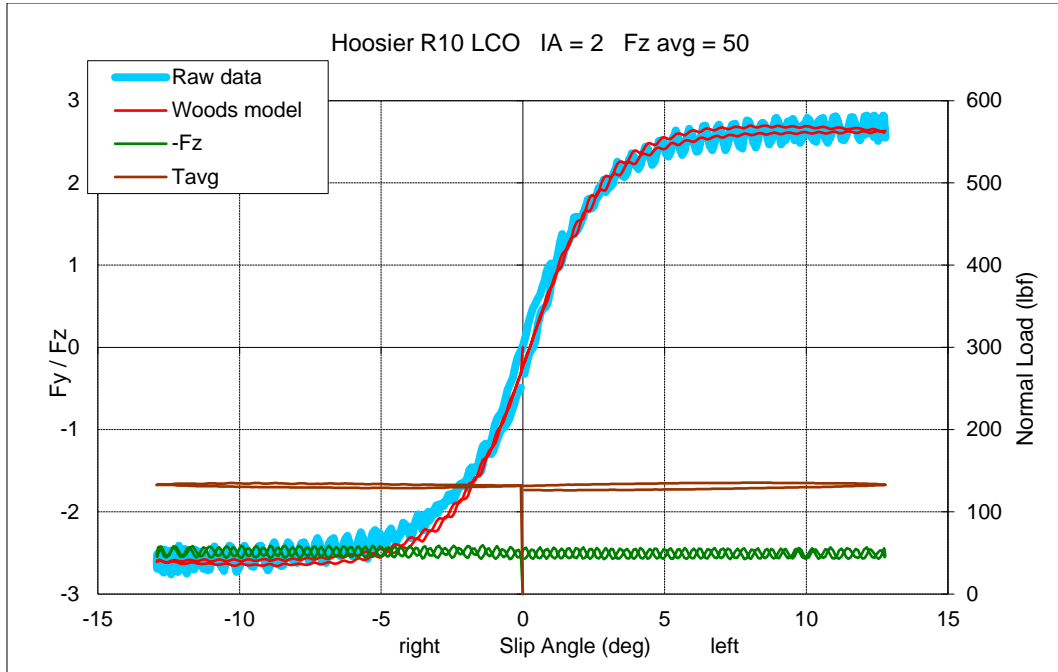
$$\sigma_{peak0} = \frac{b_0 \tan\left(\frac{\pi/2}{b_0}\right) \frac{b_2}{1000}}{b_4}$$

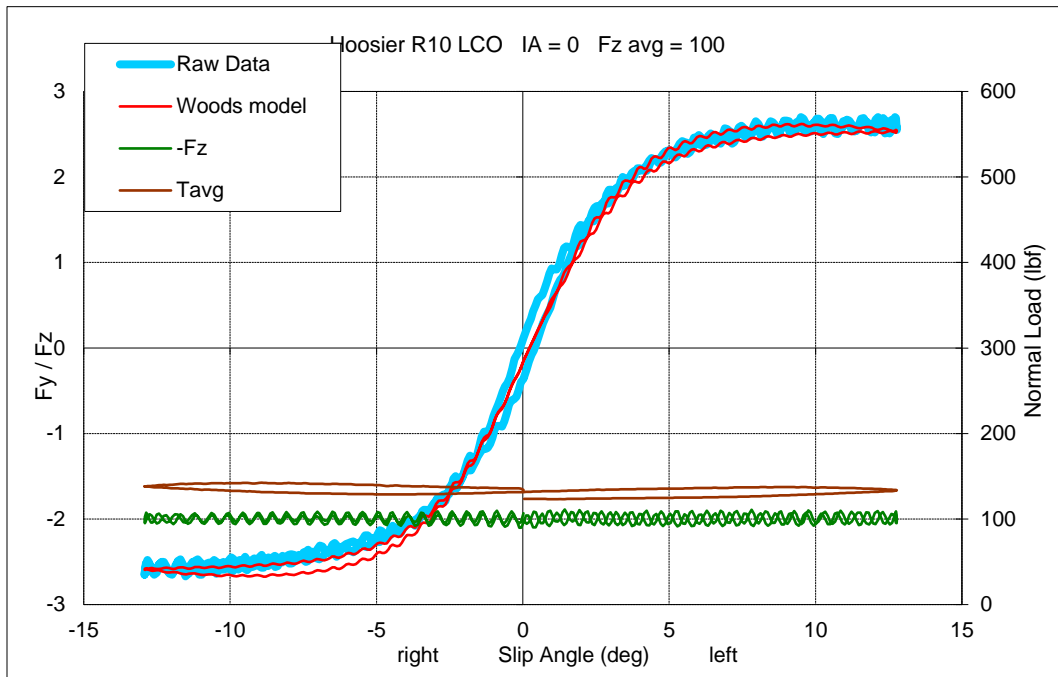
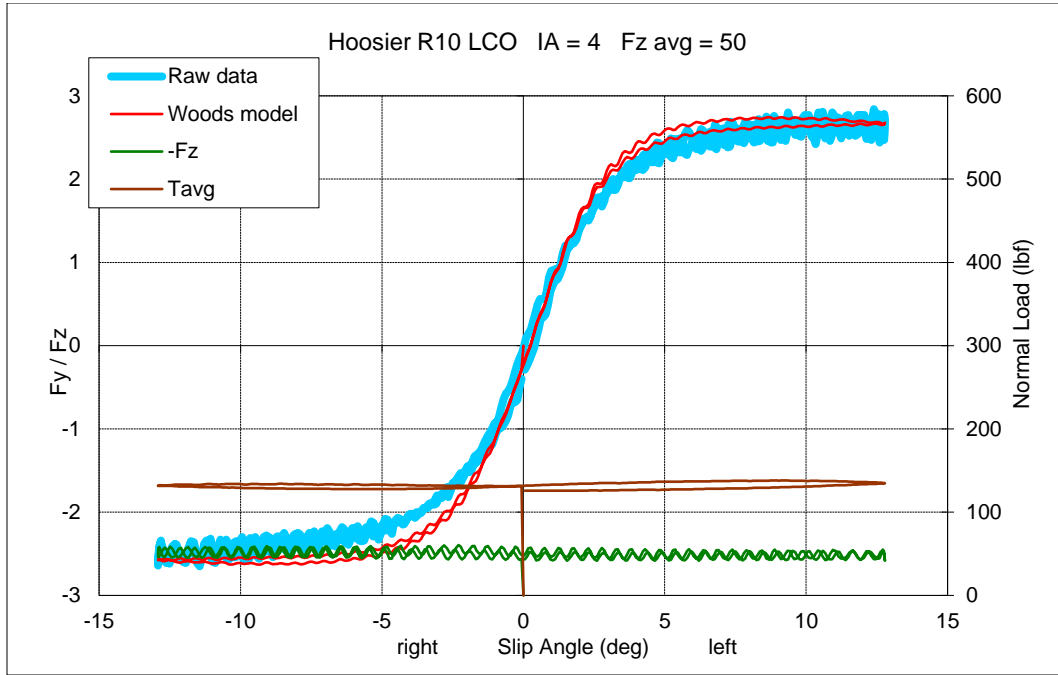
two more dependent variables are introduced G_x and σ_{peak0} .

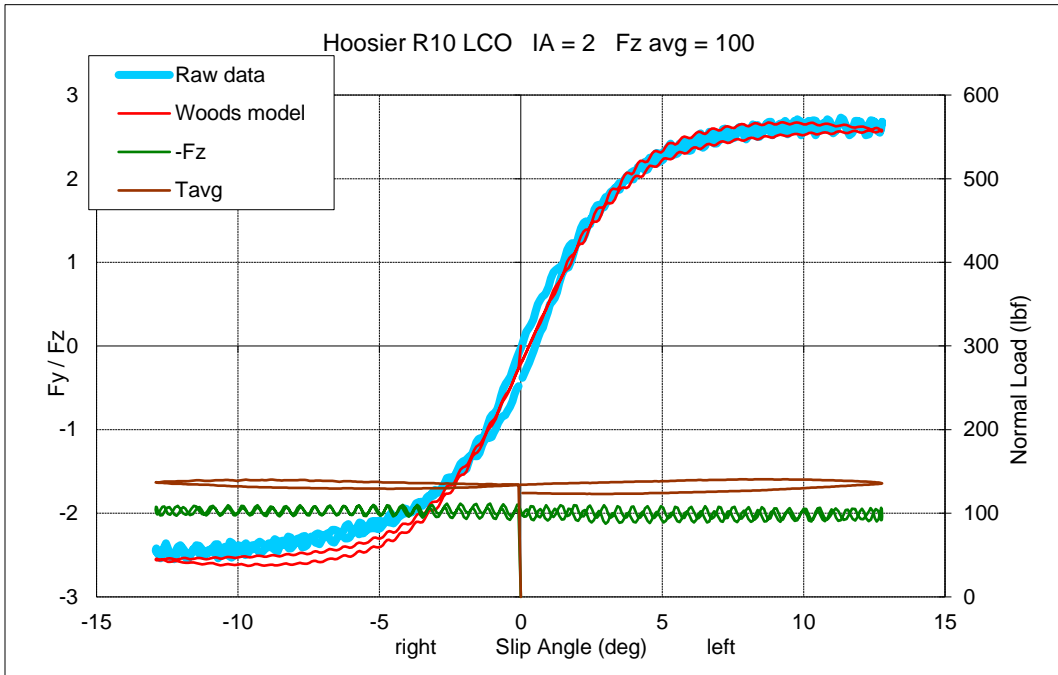
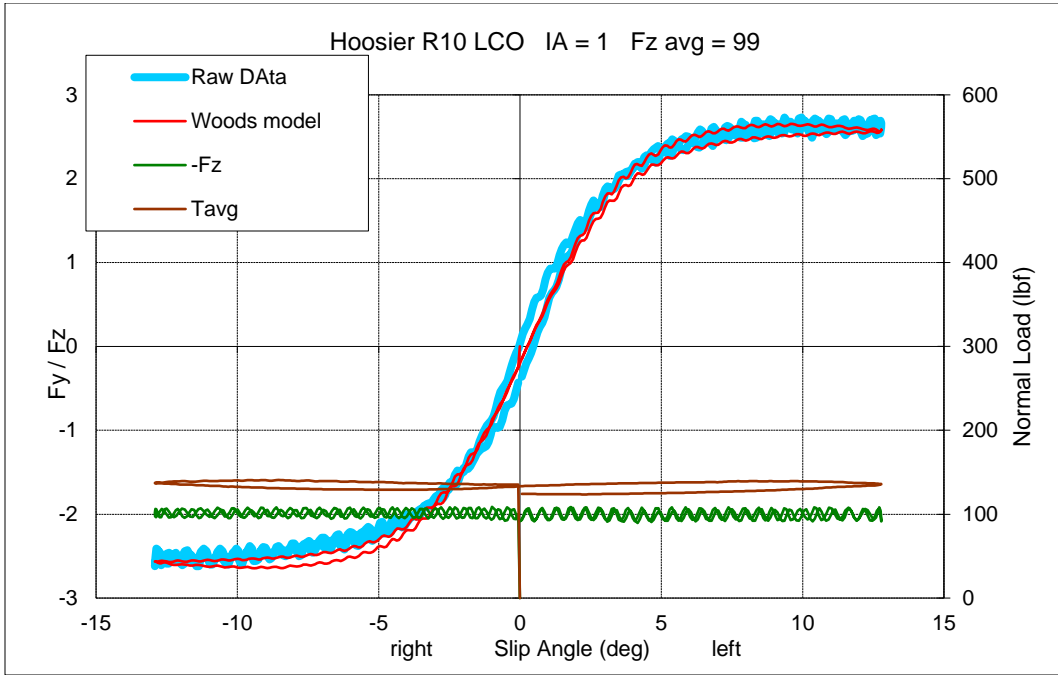
Appendix A-2- graphs

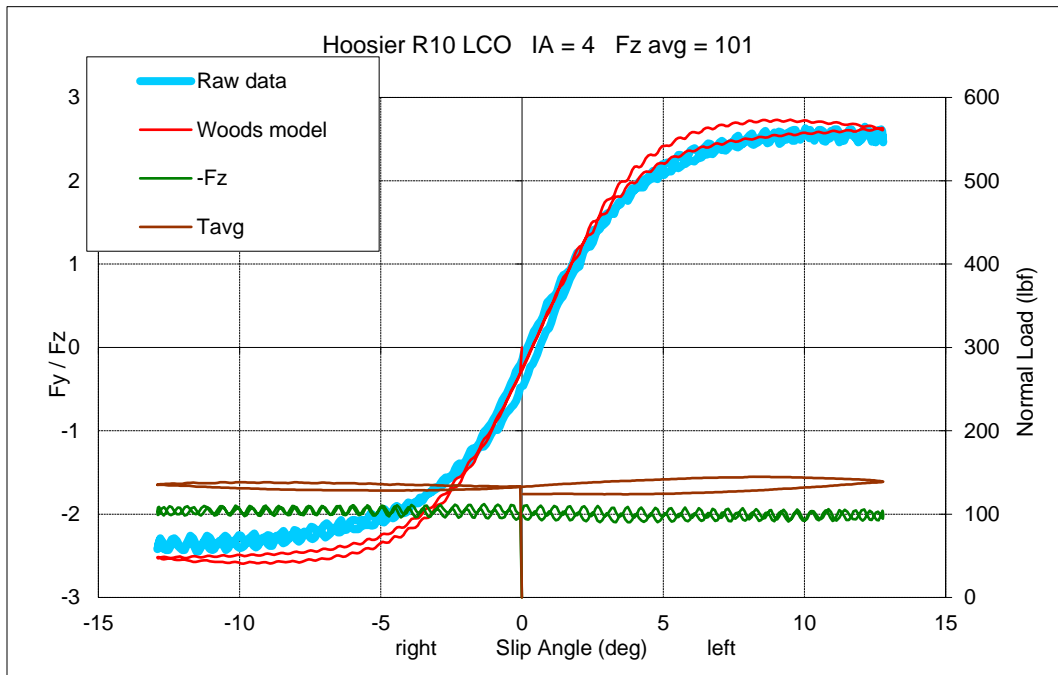
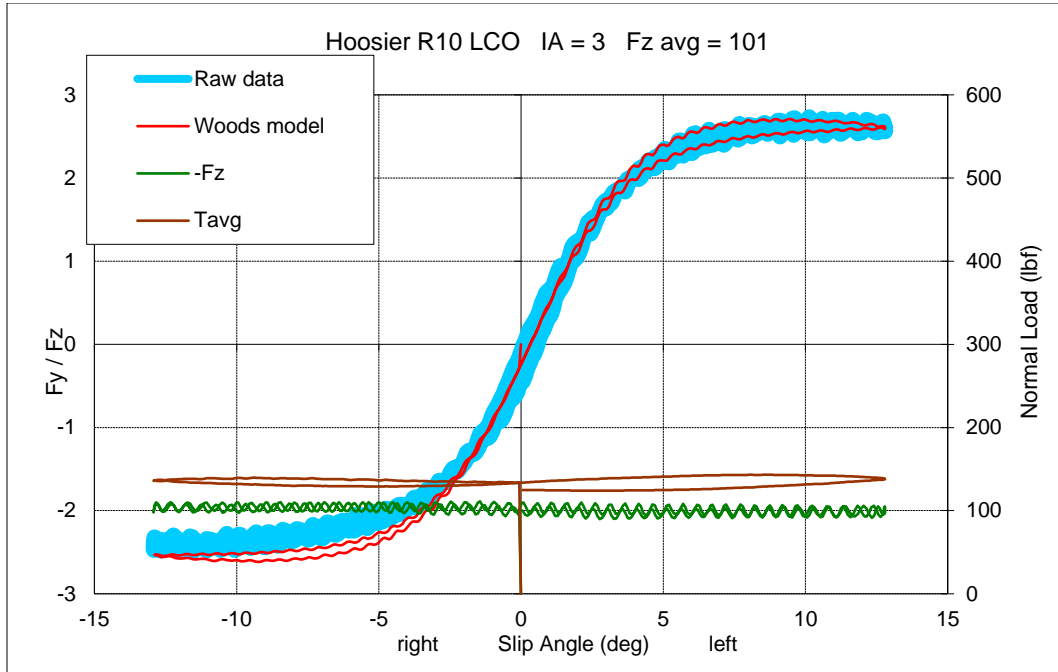
Hoosier R10 LCO

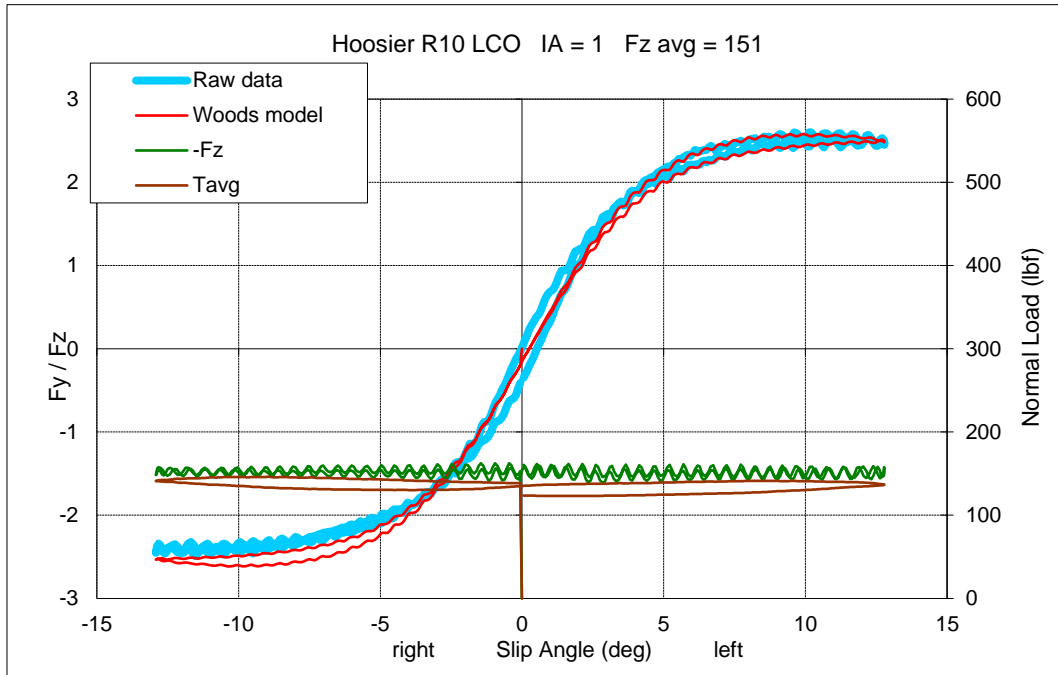
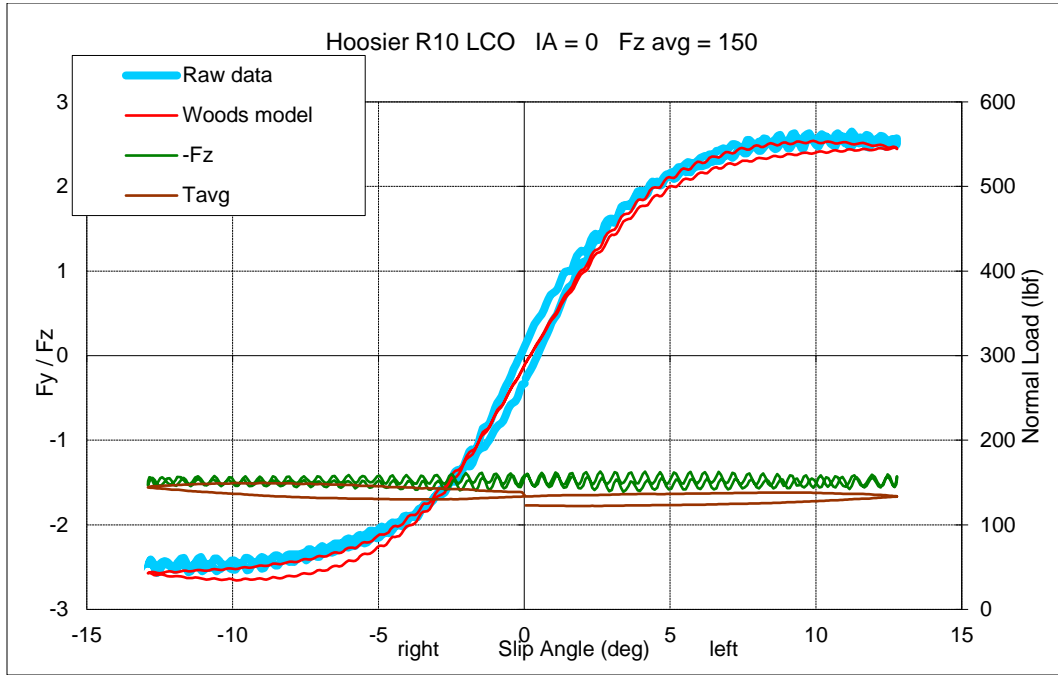


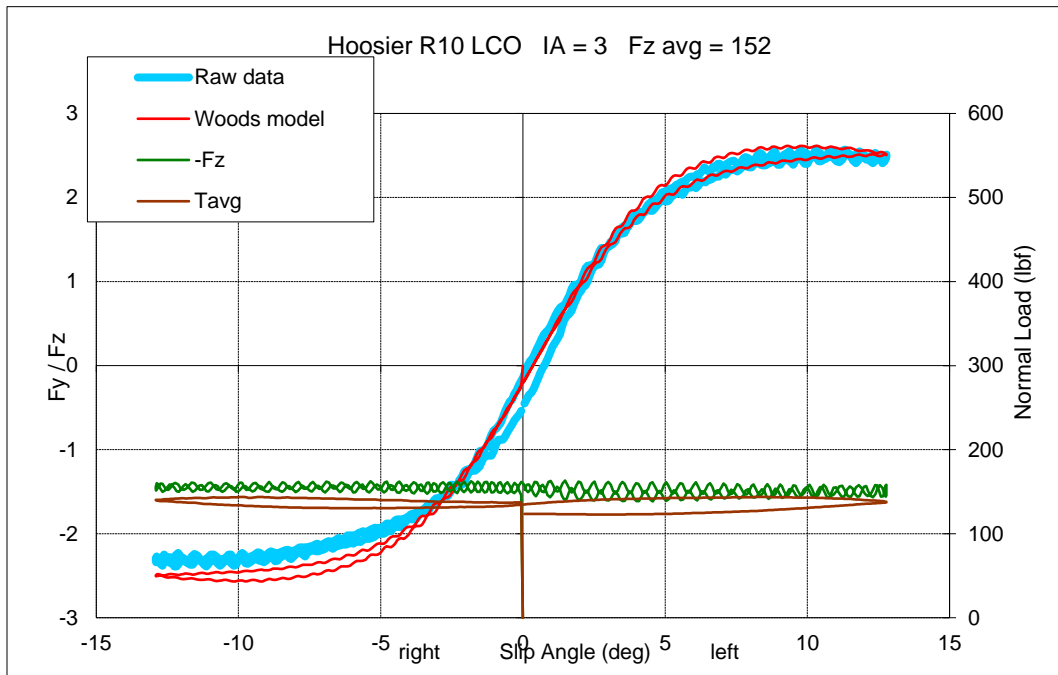
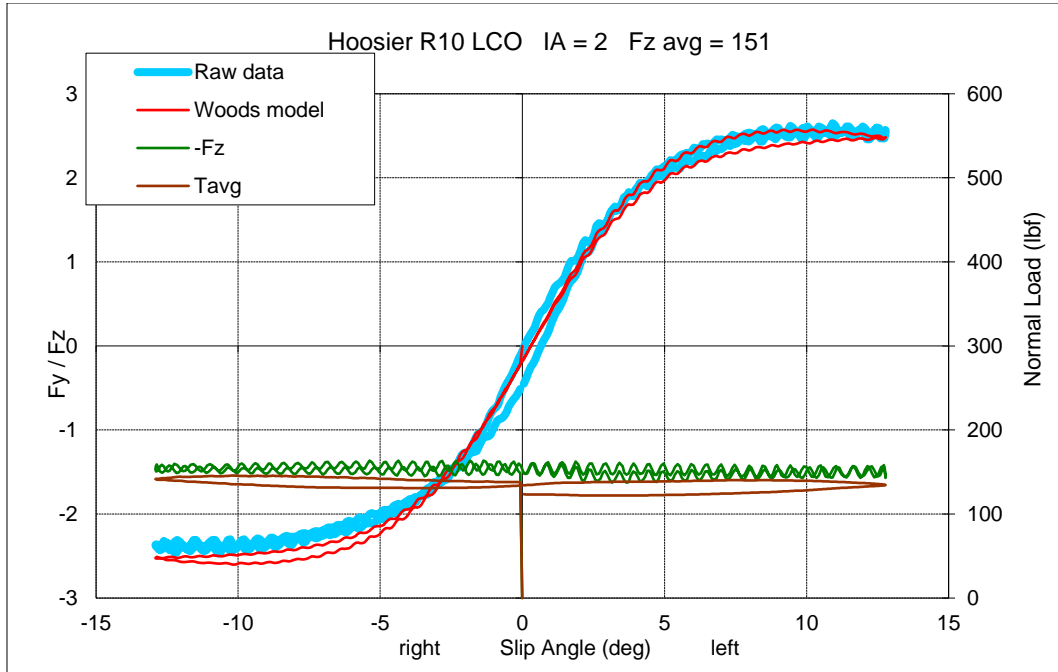


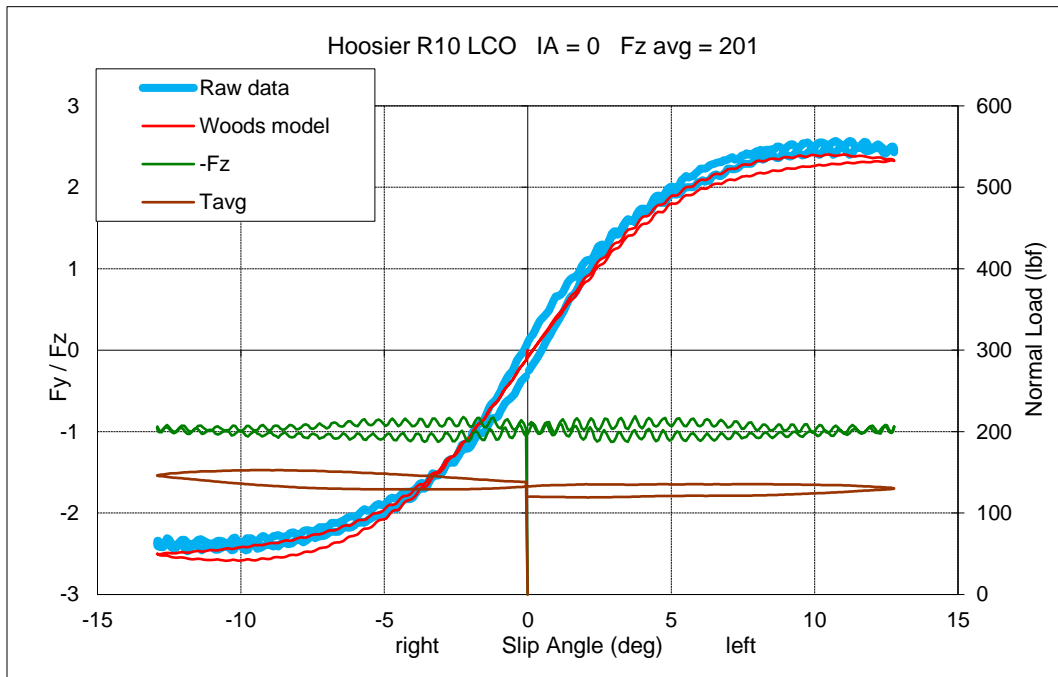
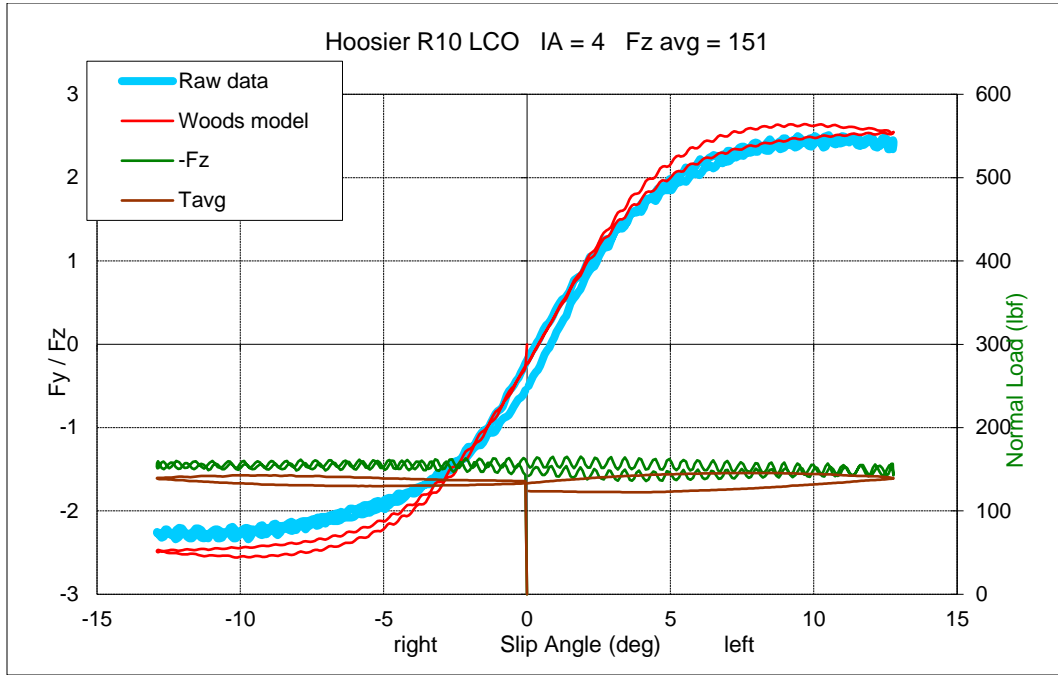


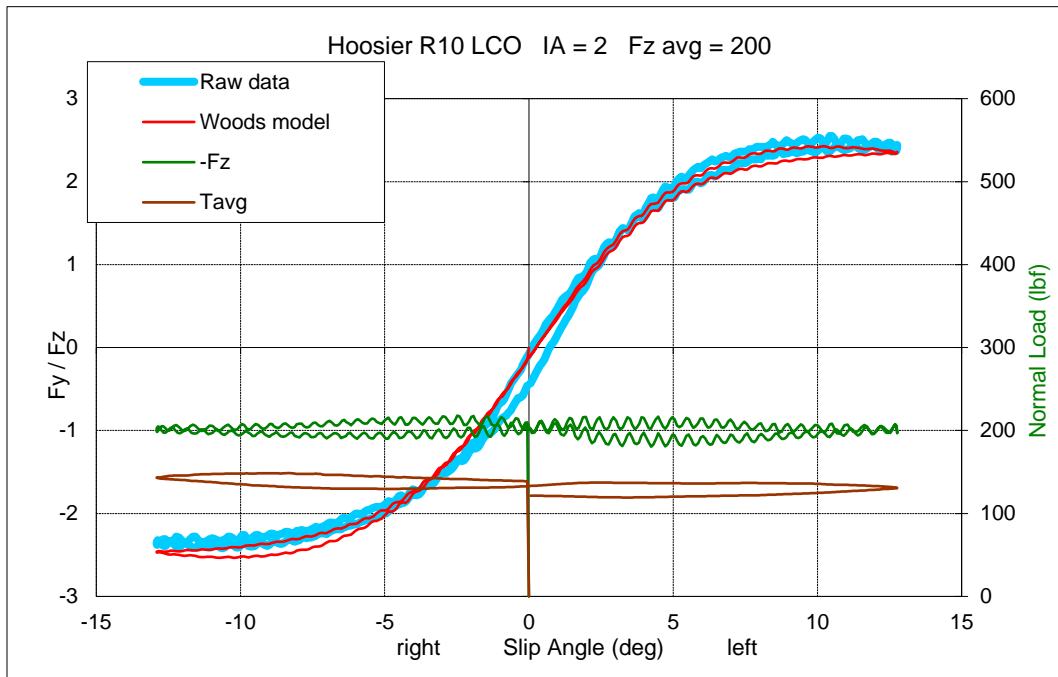
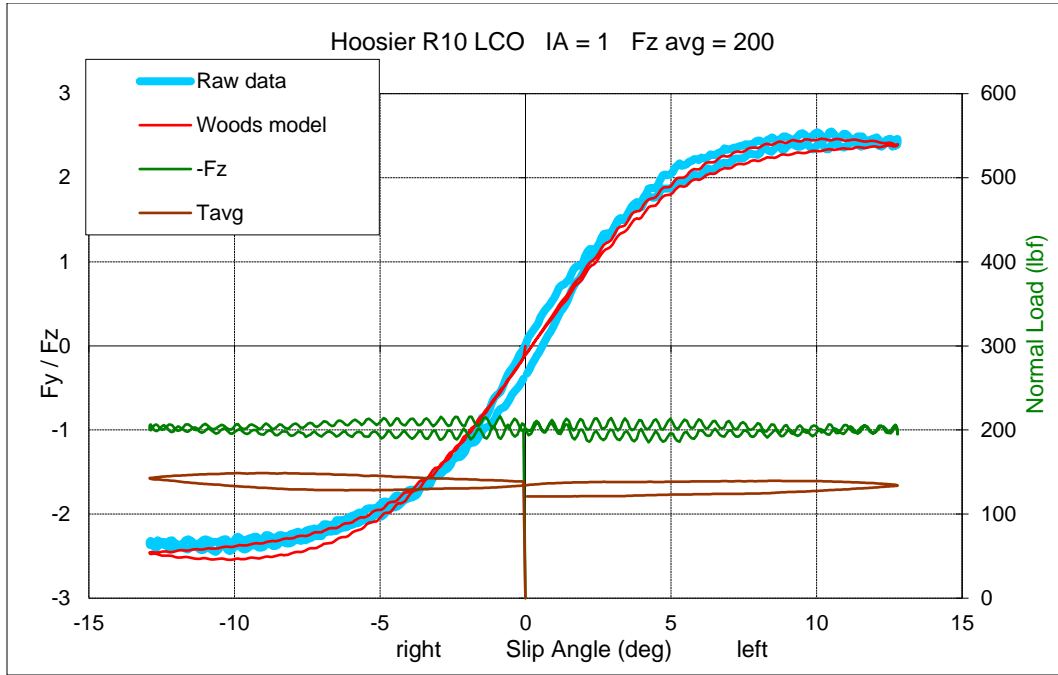


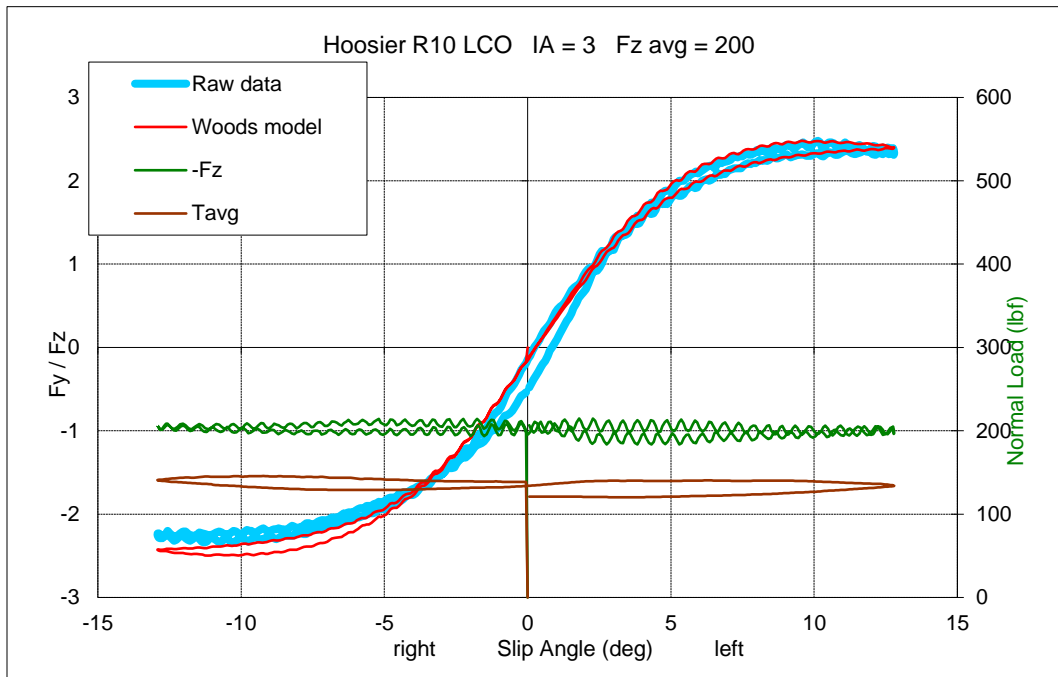
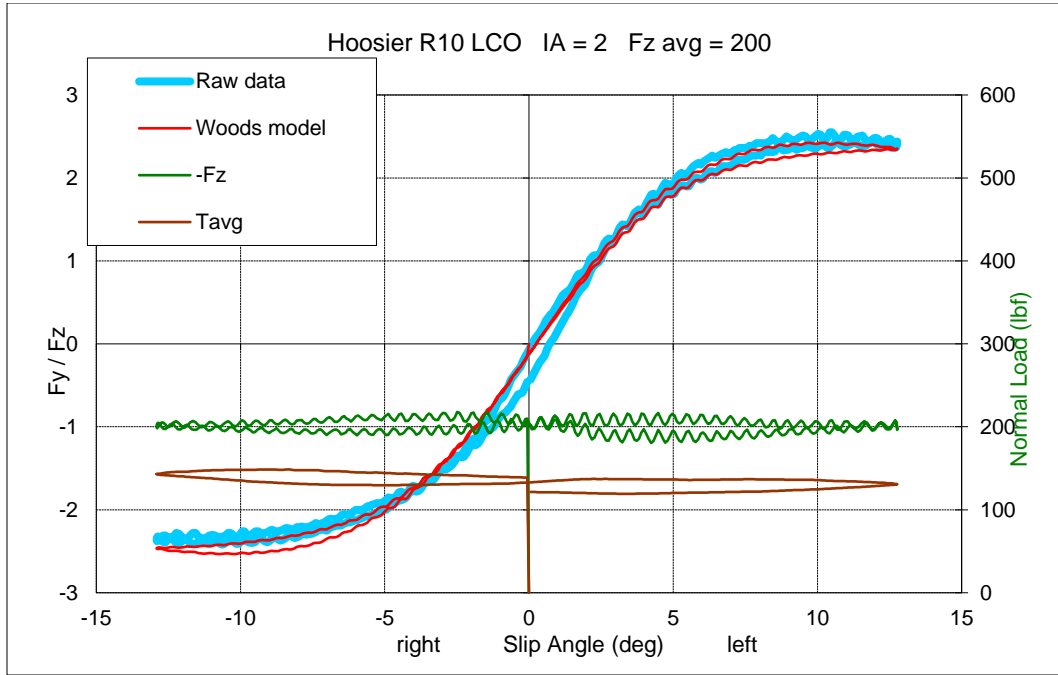


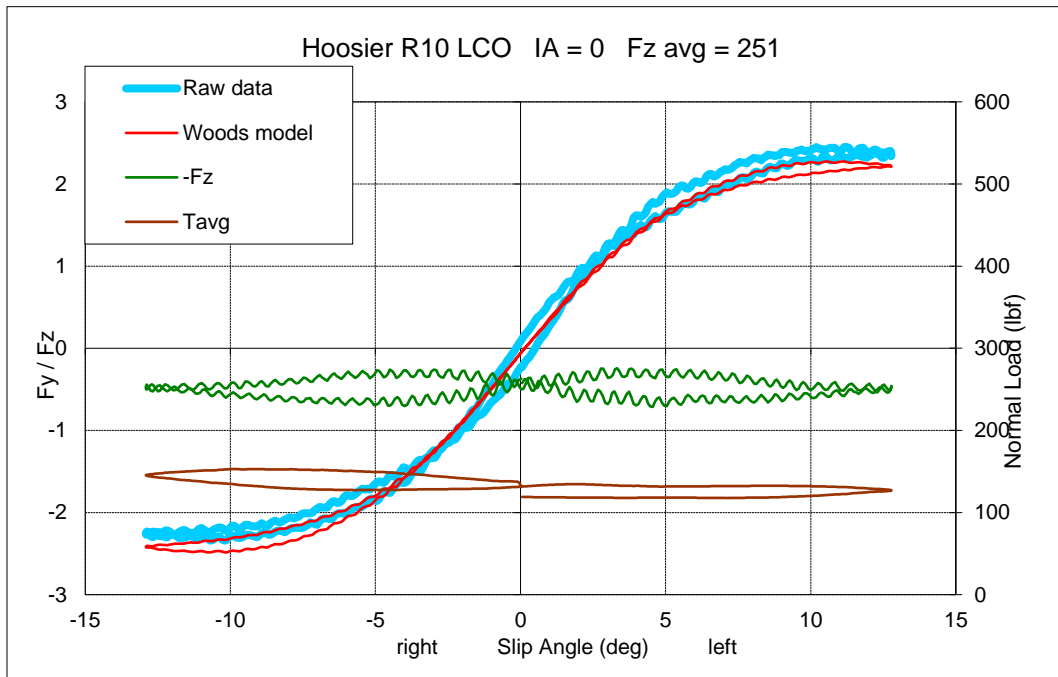
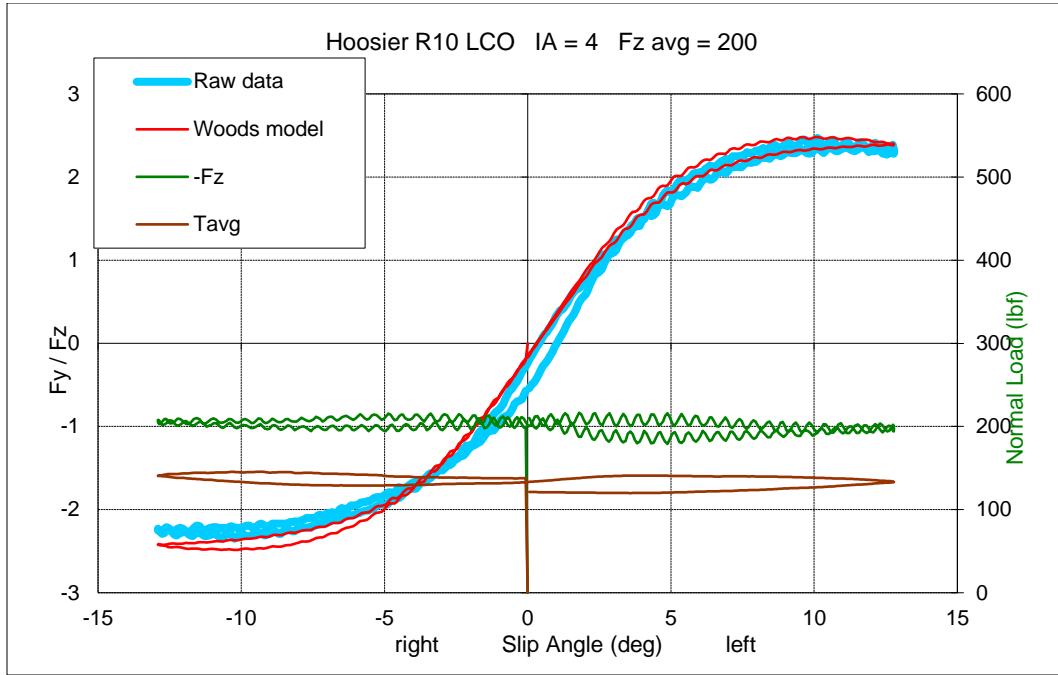


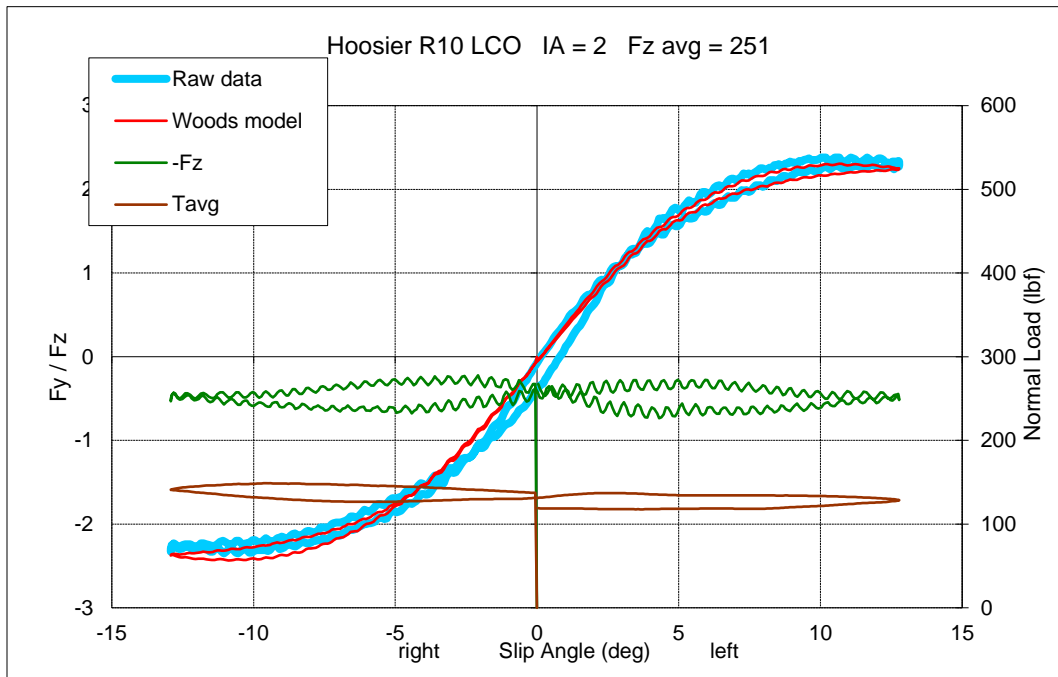
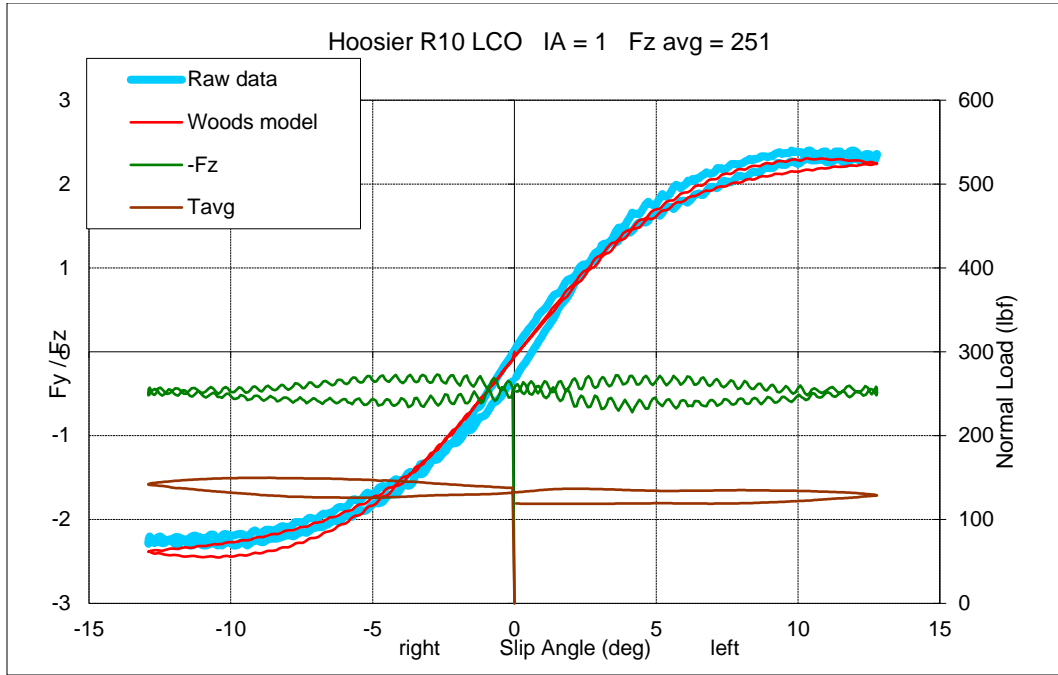


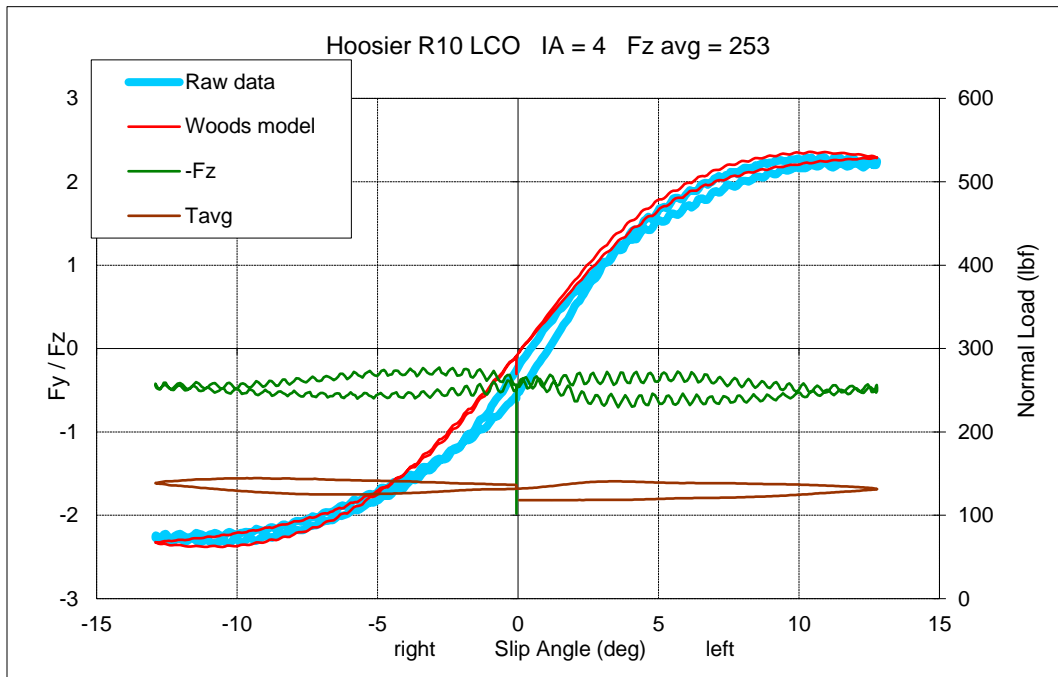
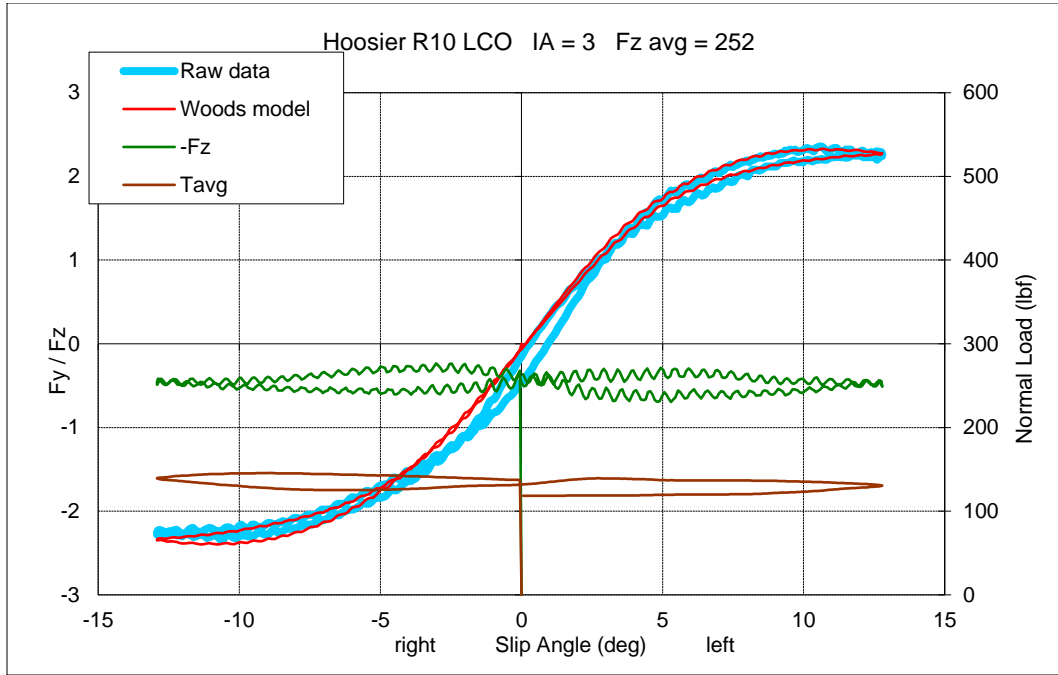


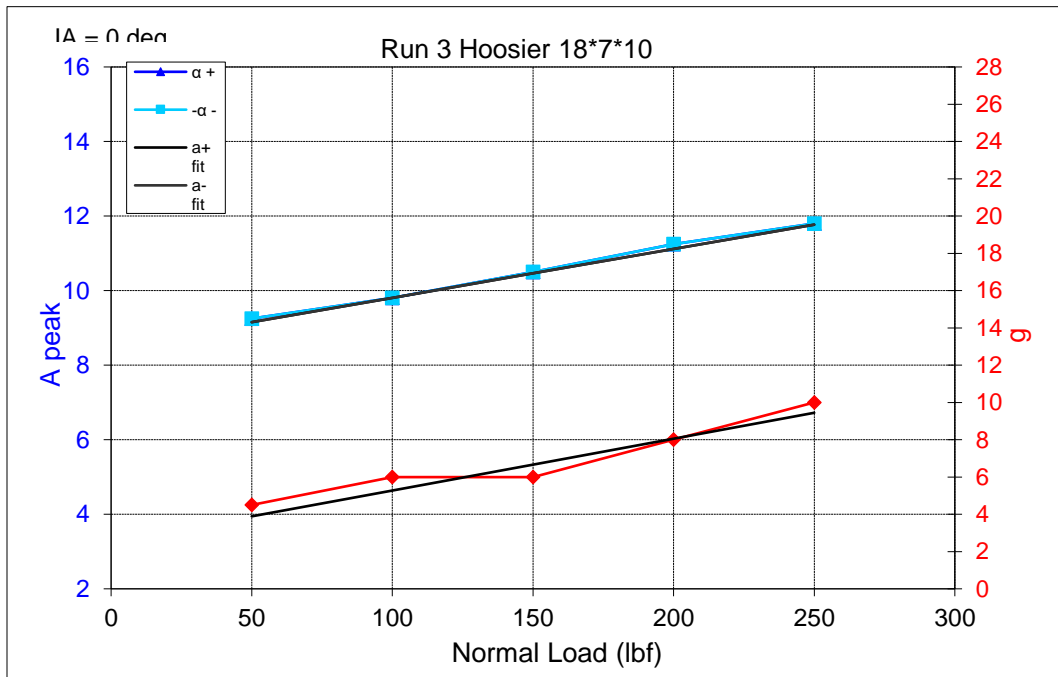
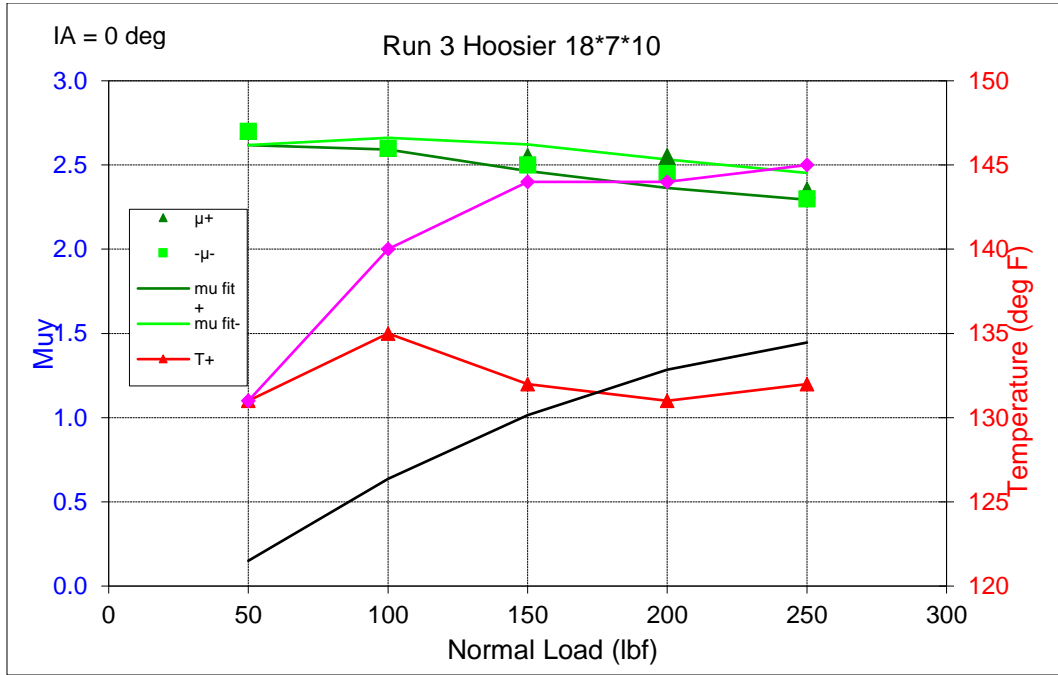


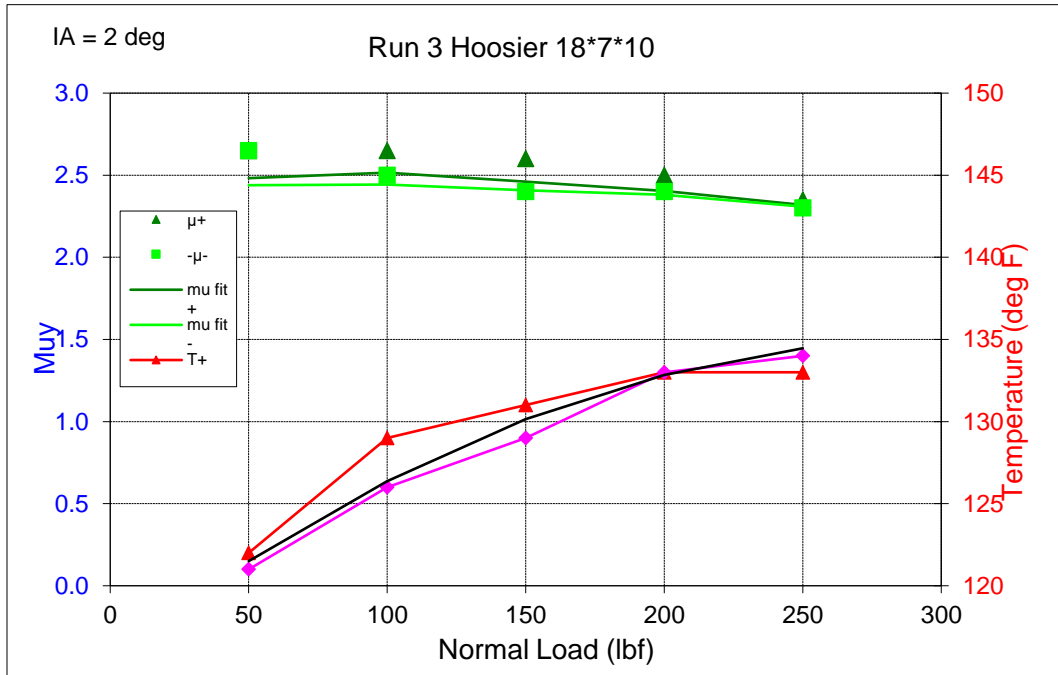
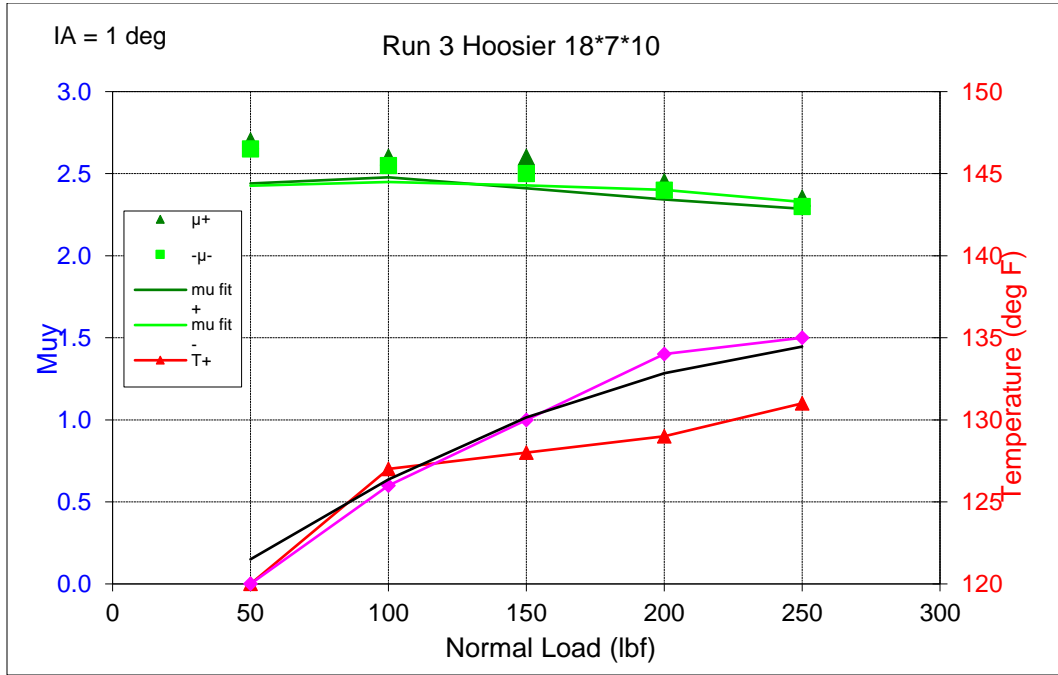


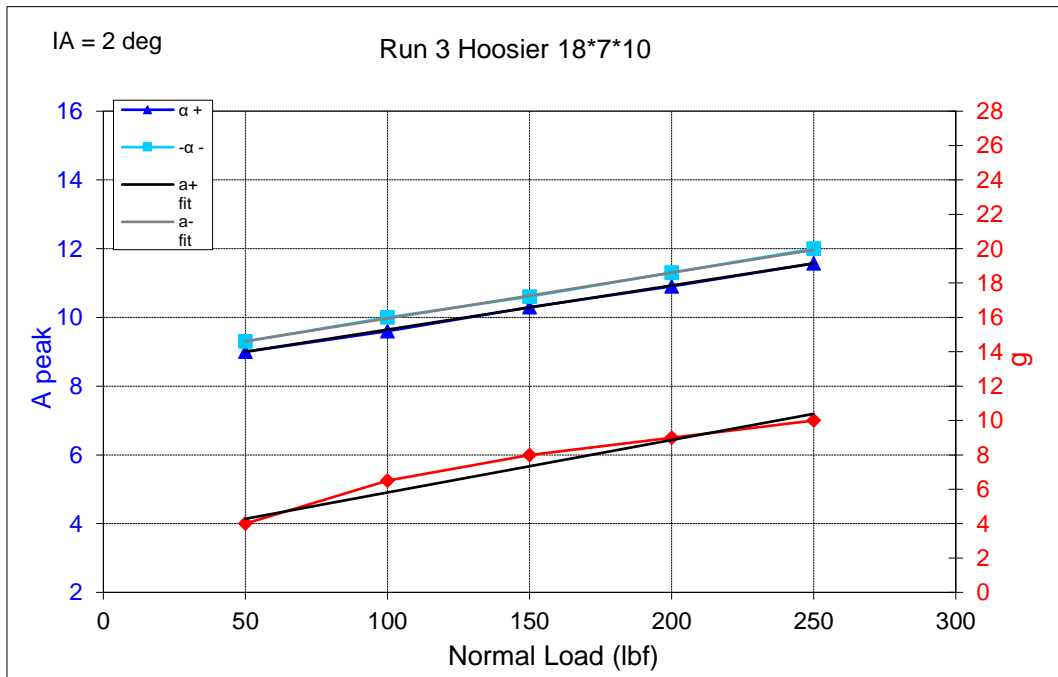
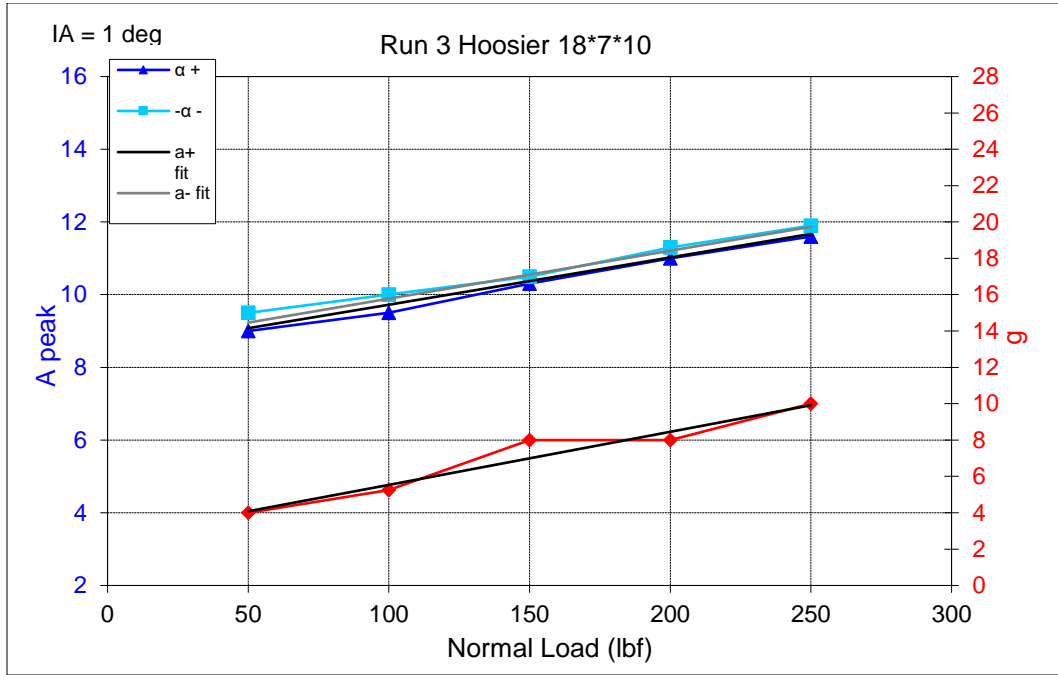


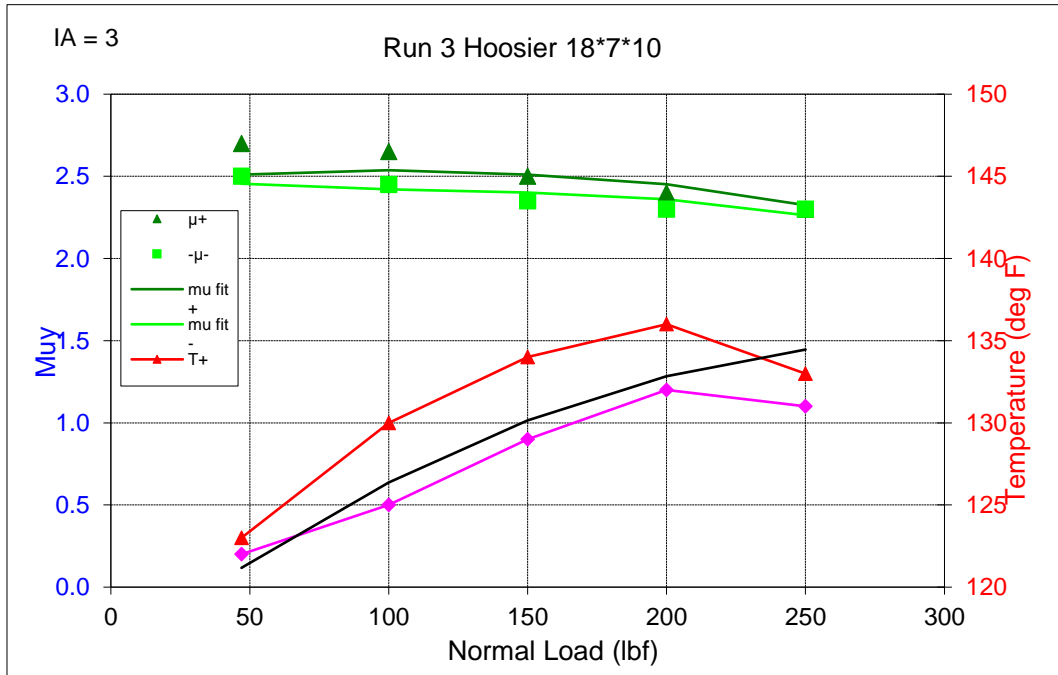
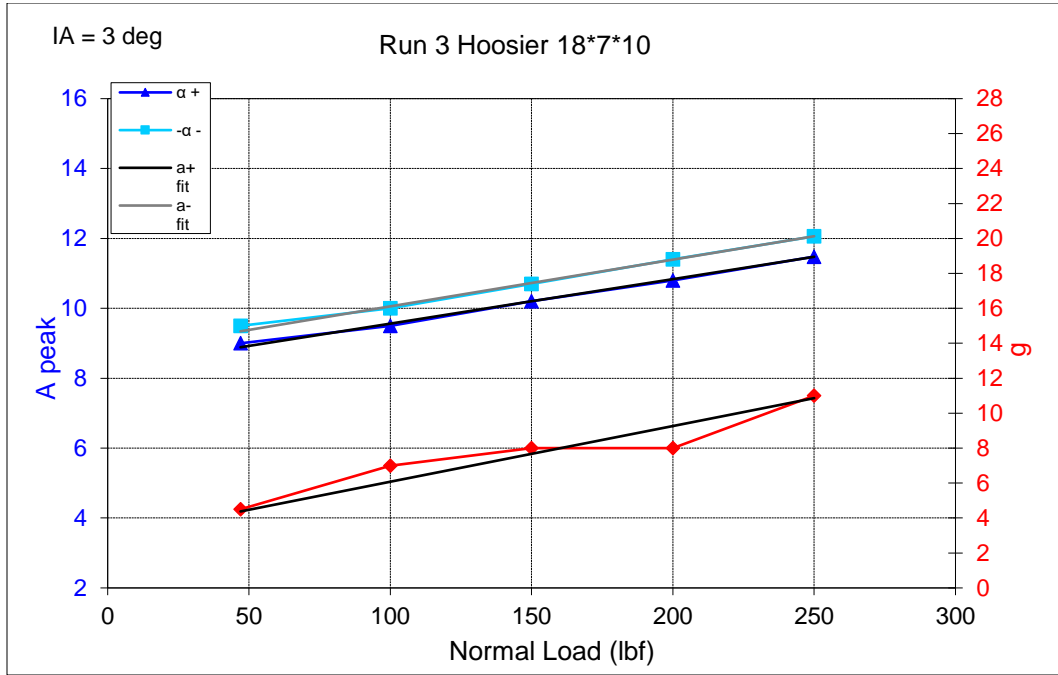


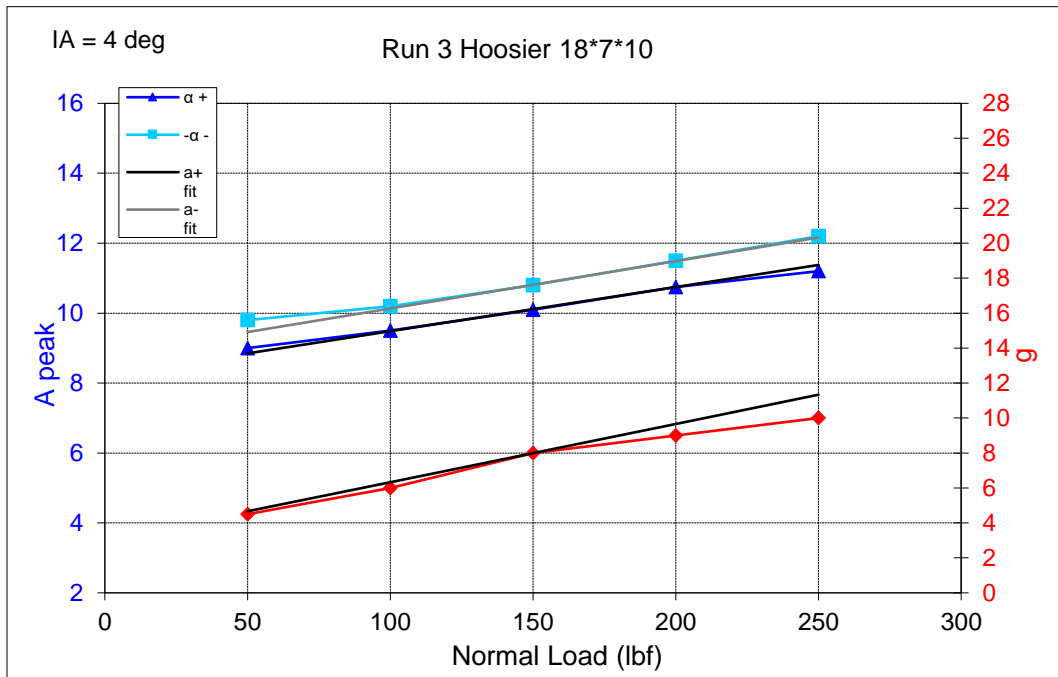
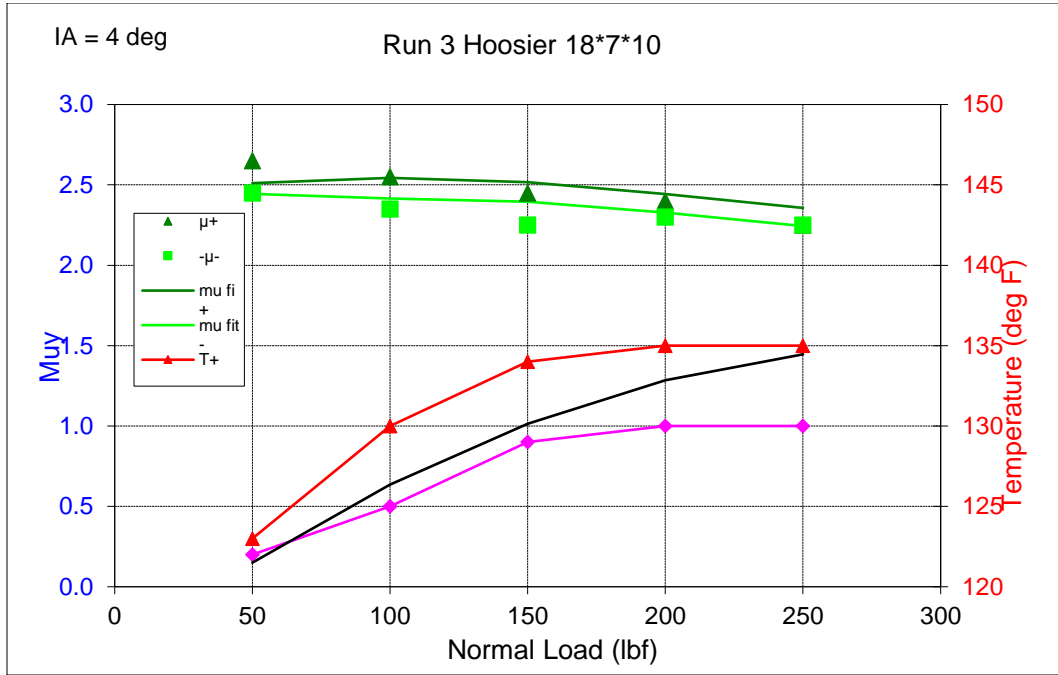




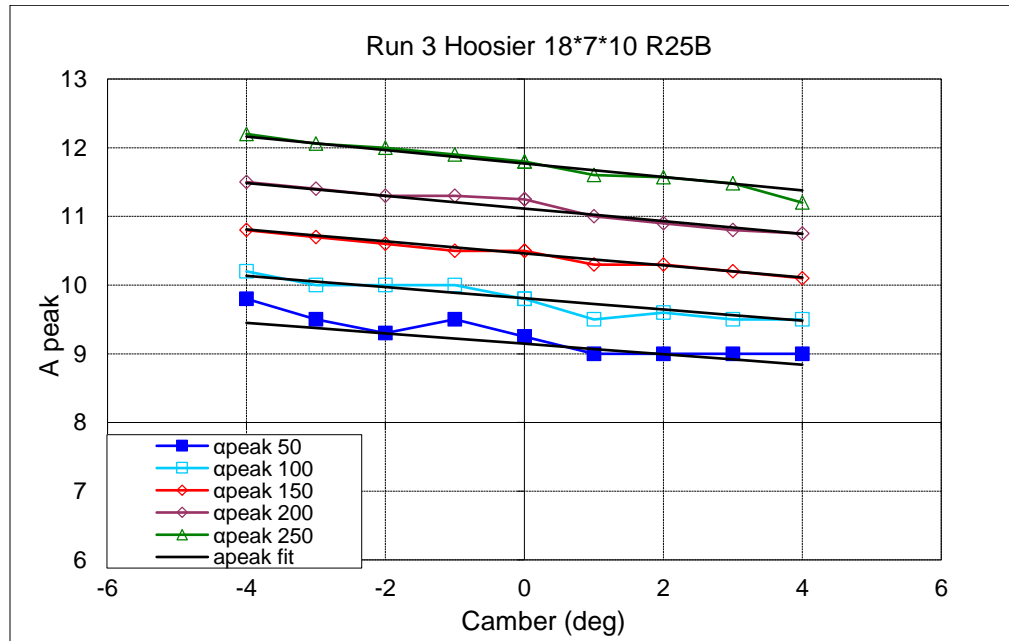
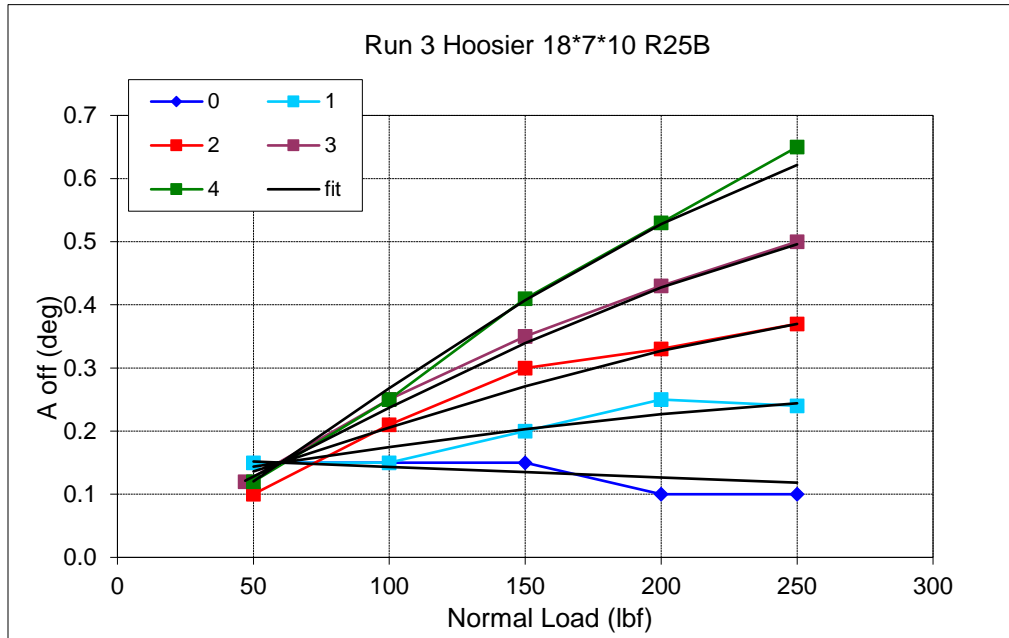


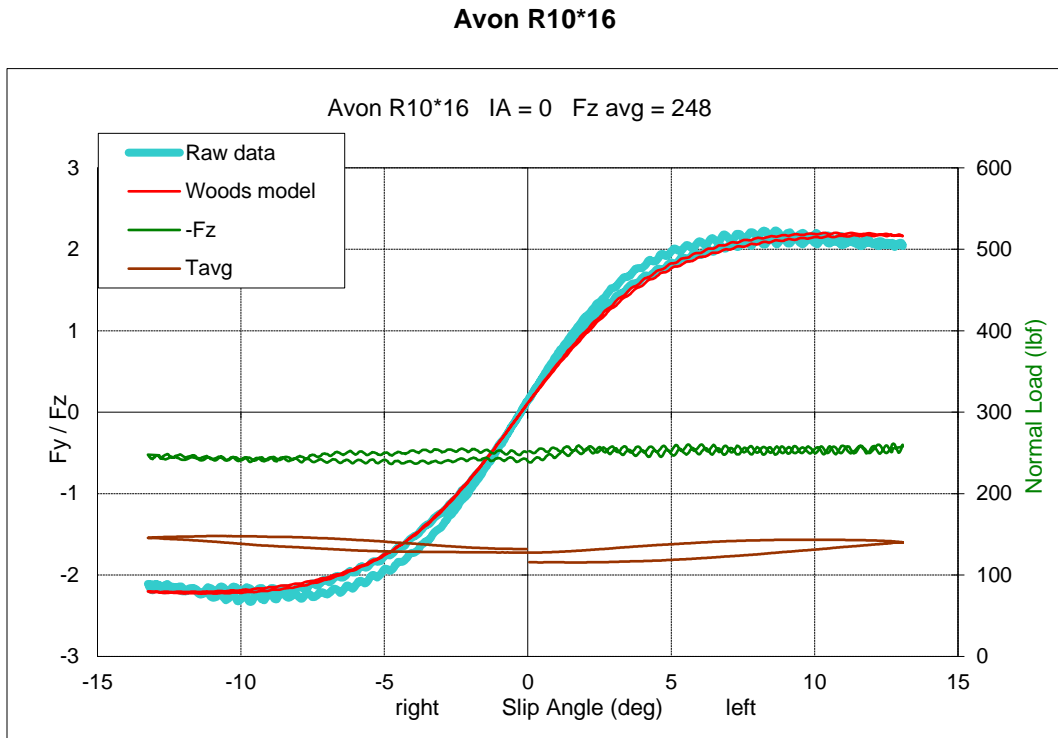
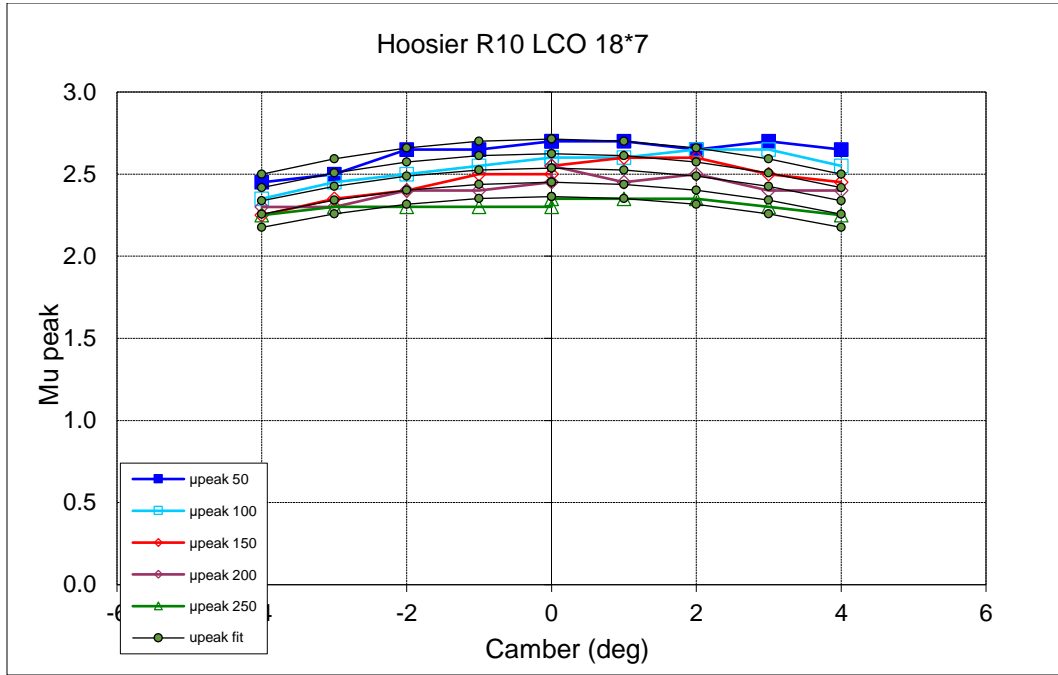


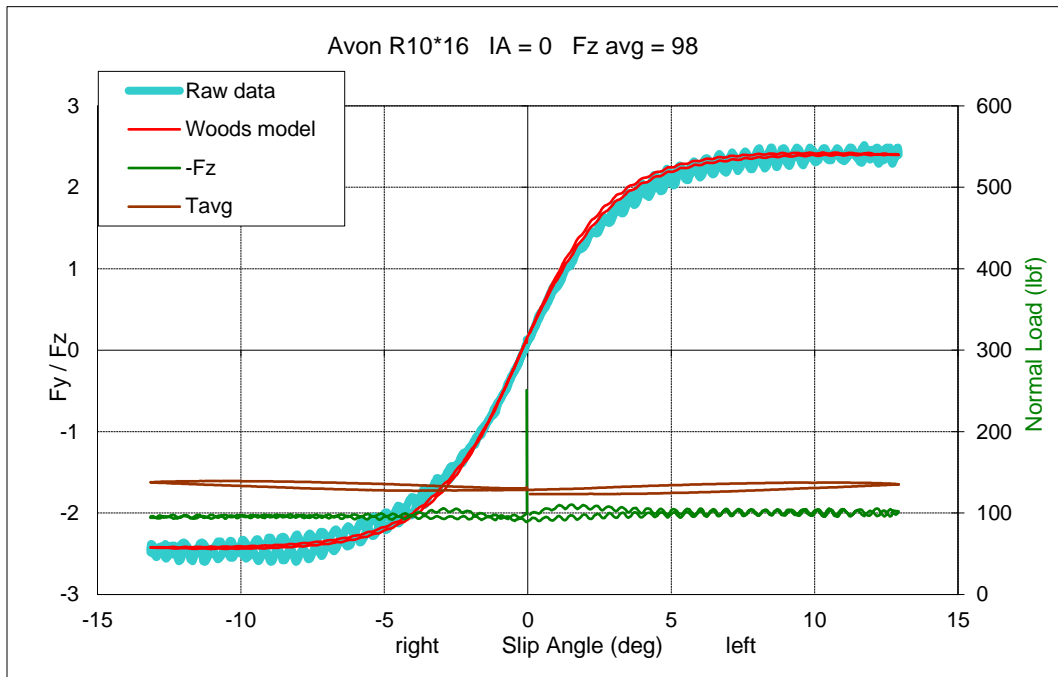
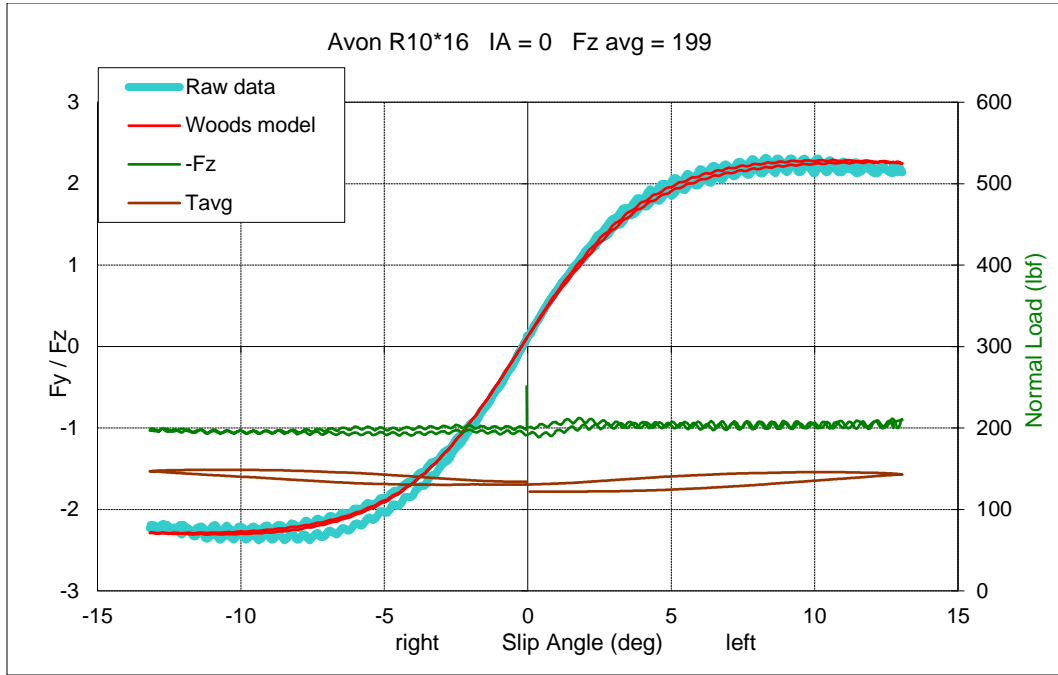


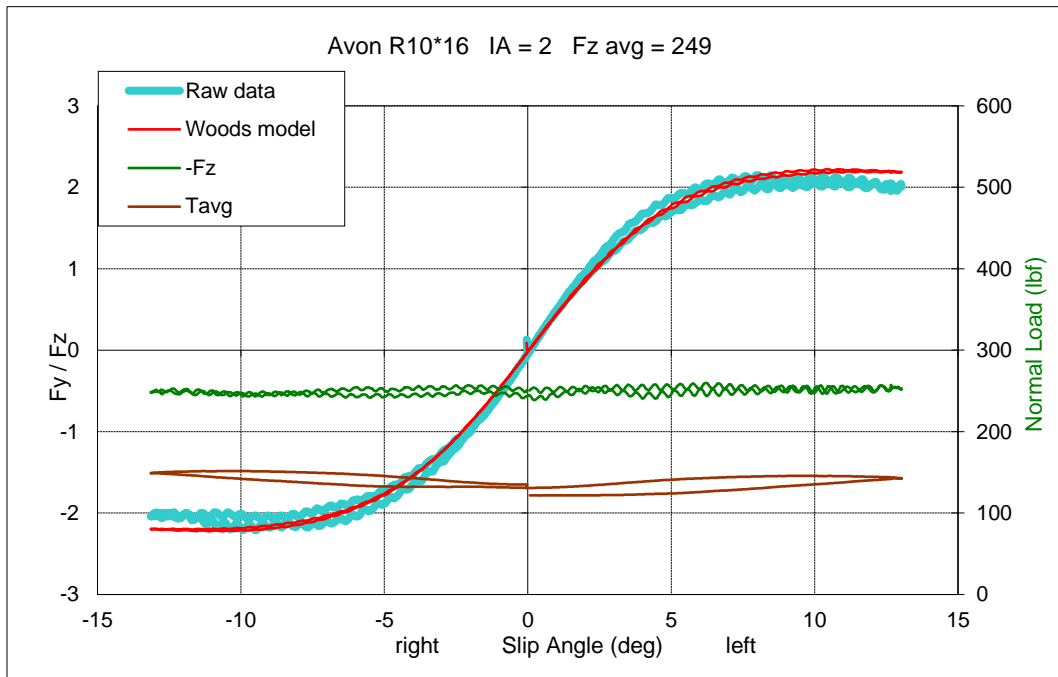
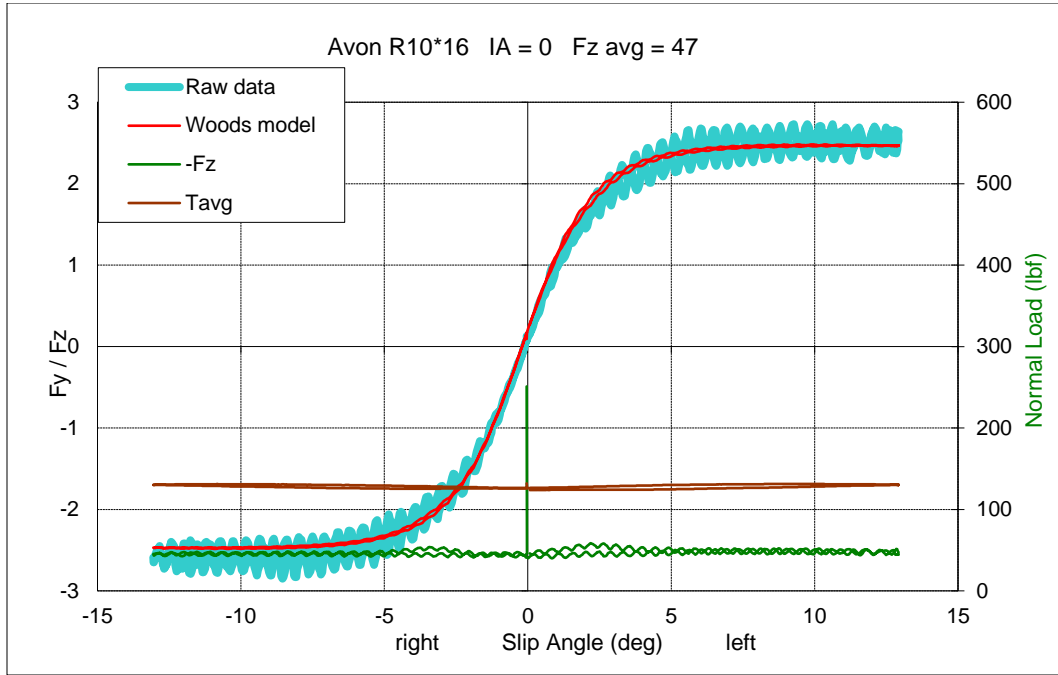


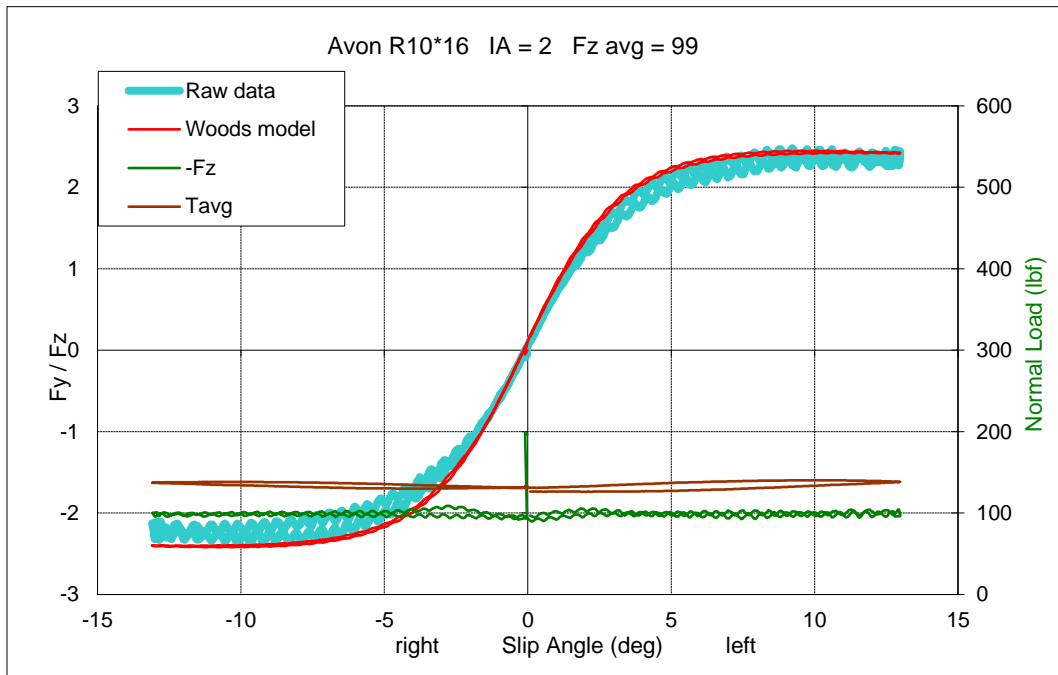
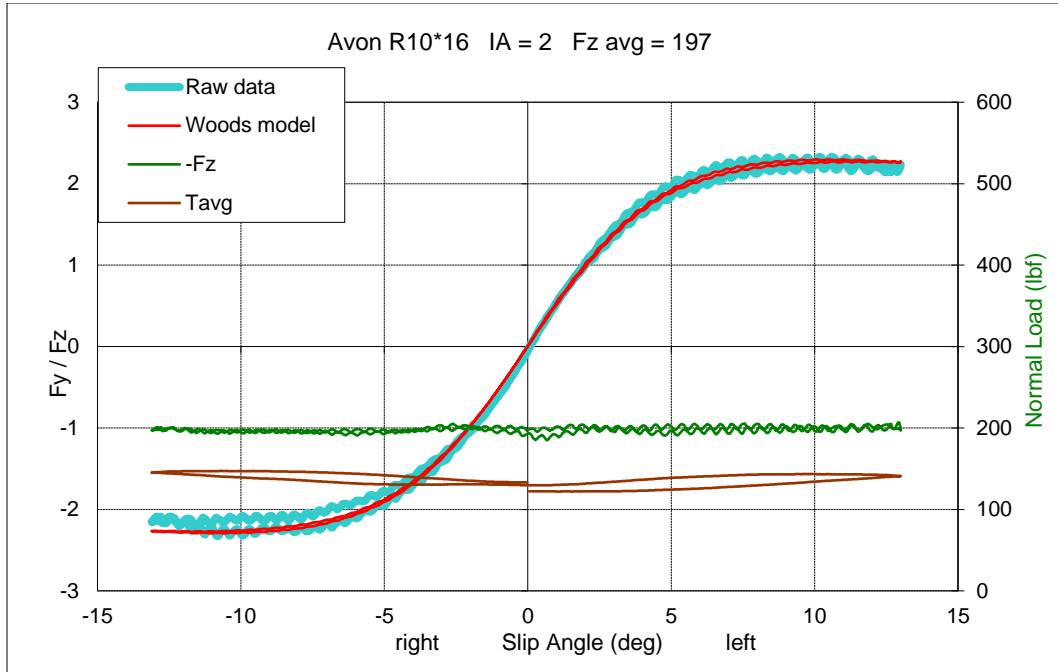
Parametric Graphs

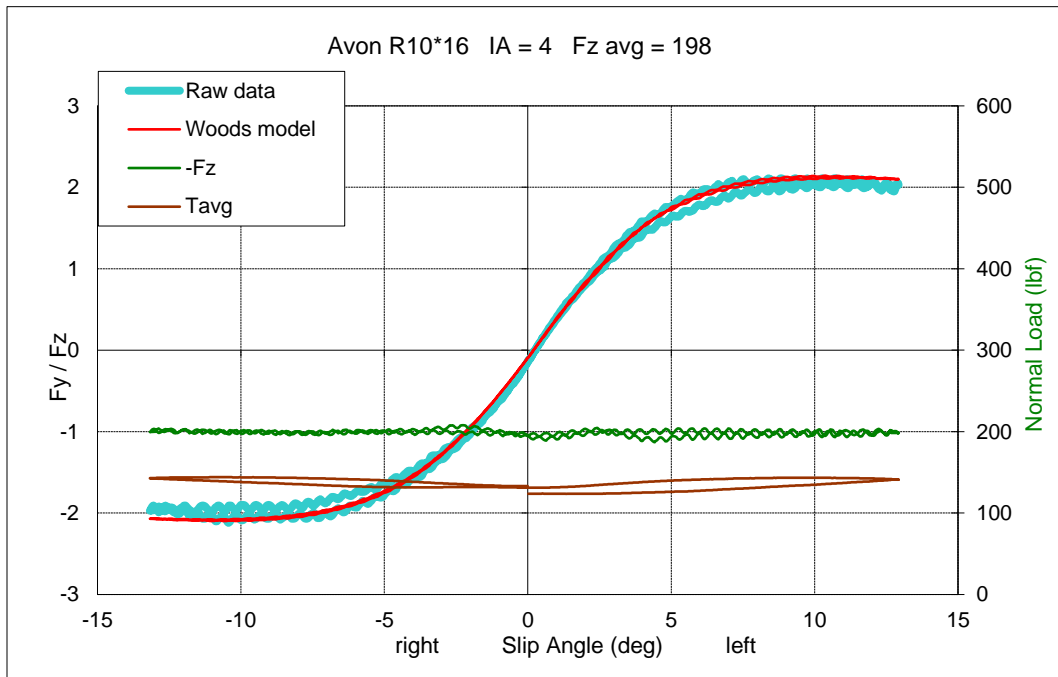
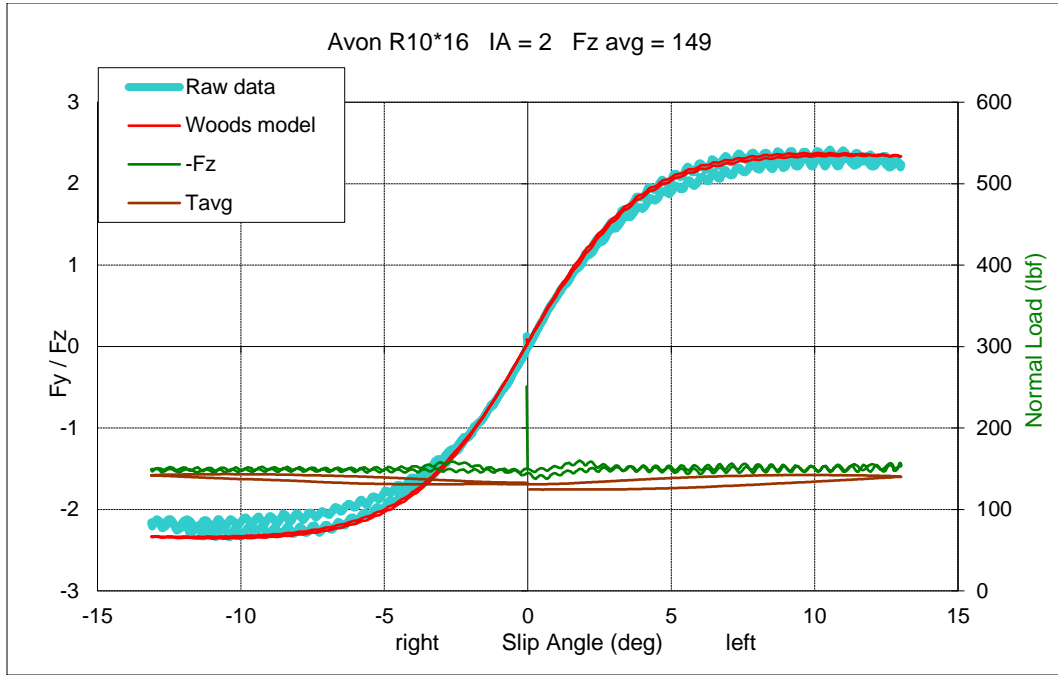


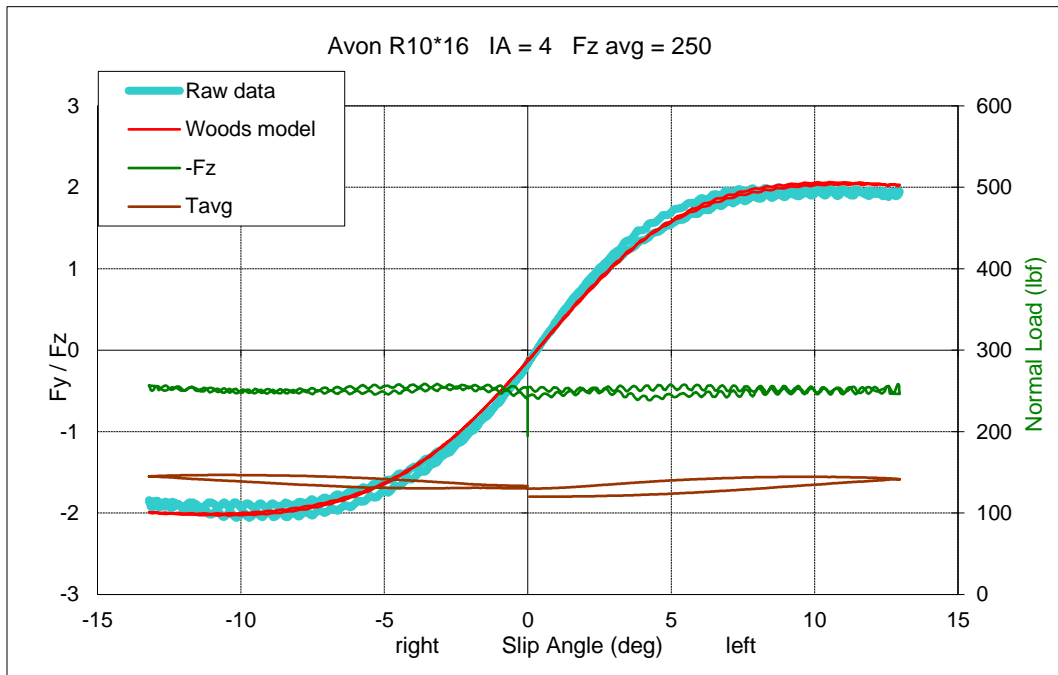
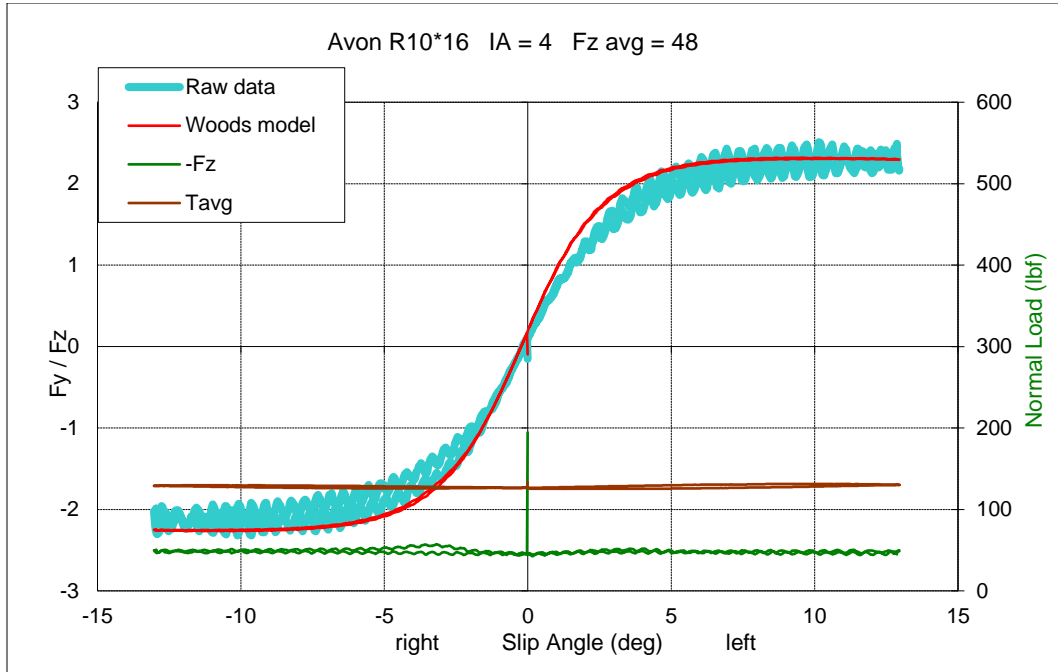


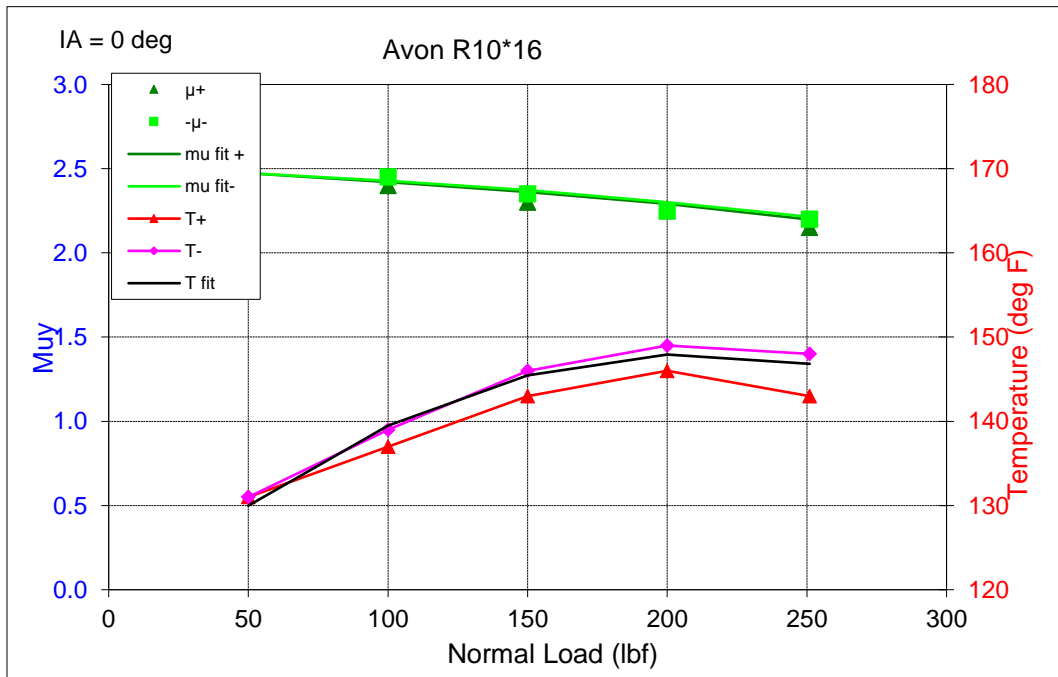
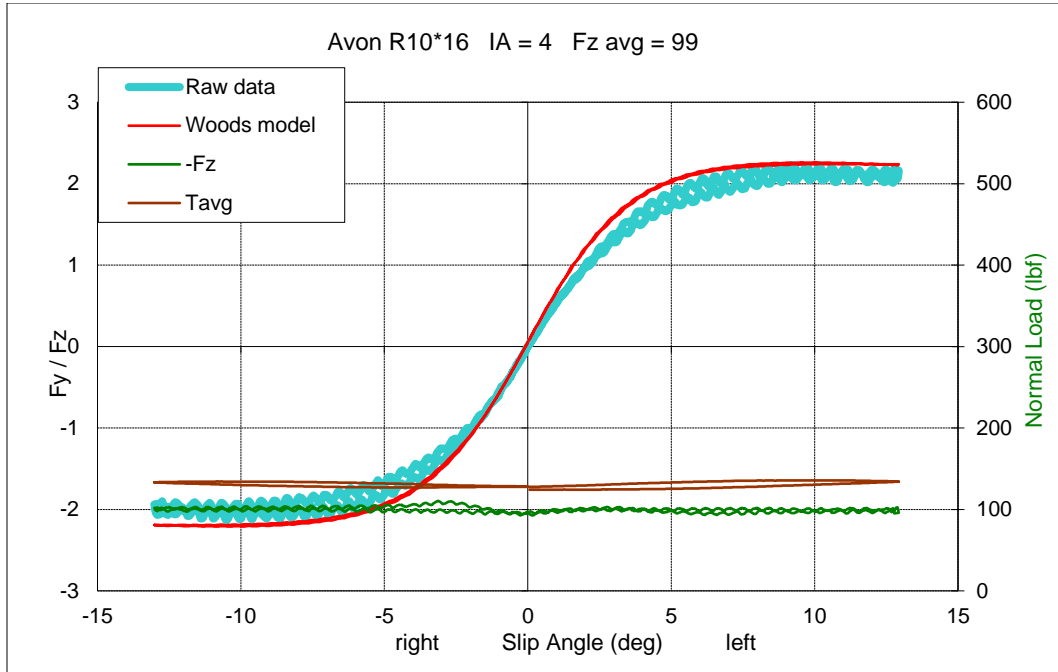


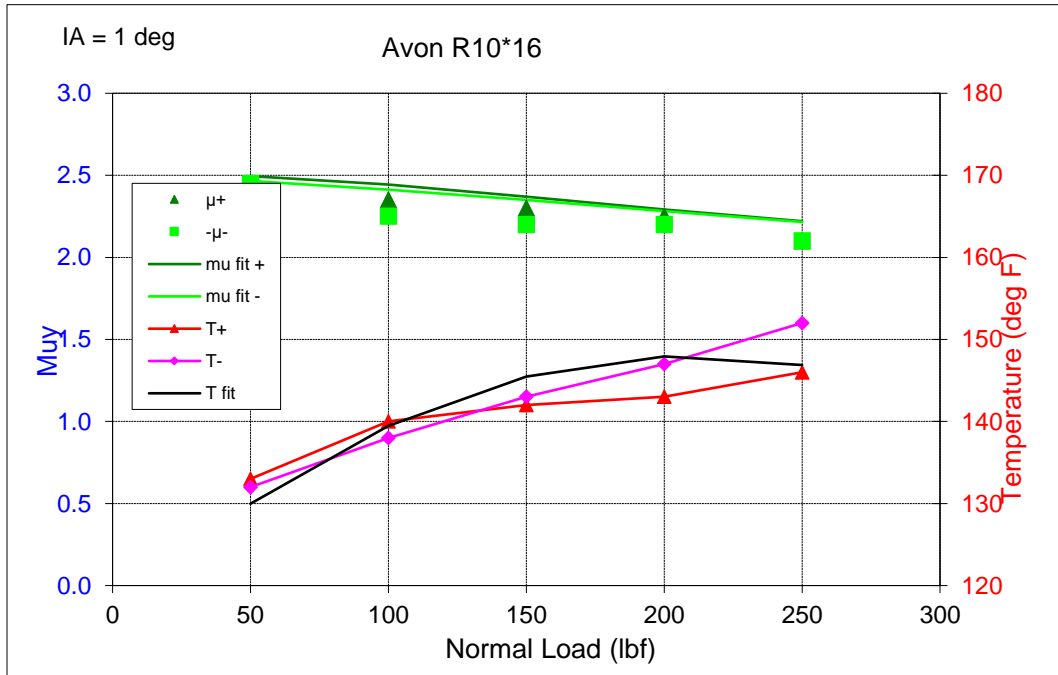
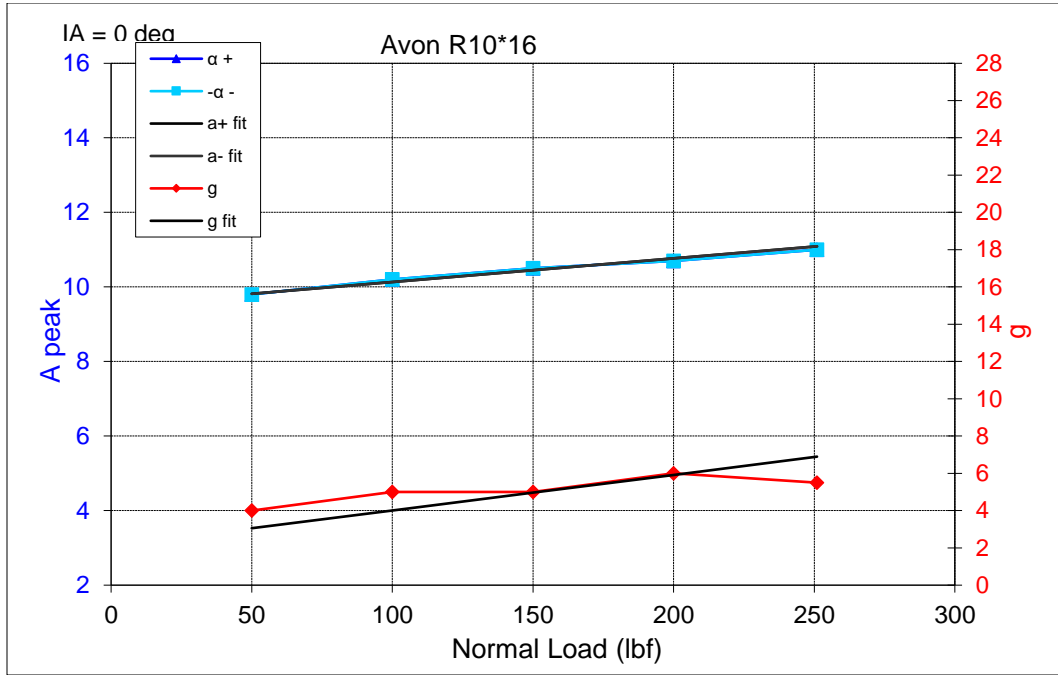


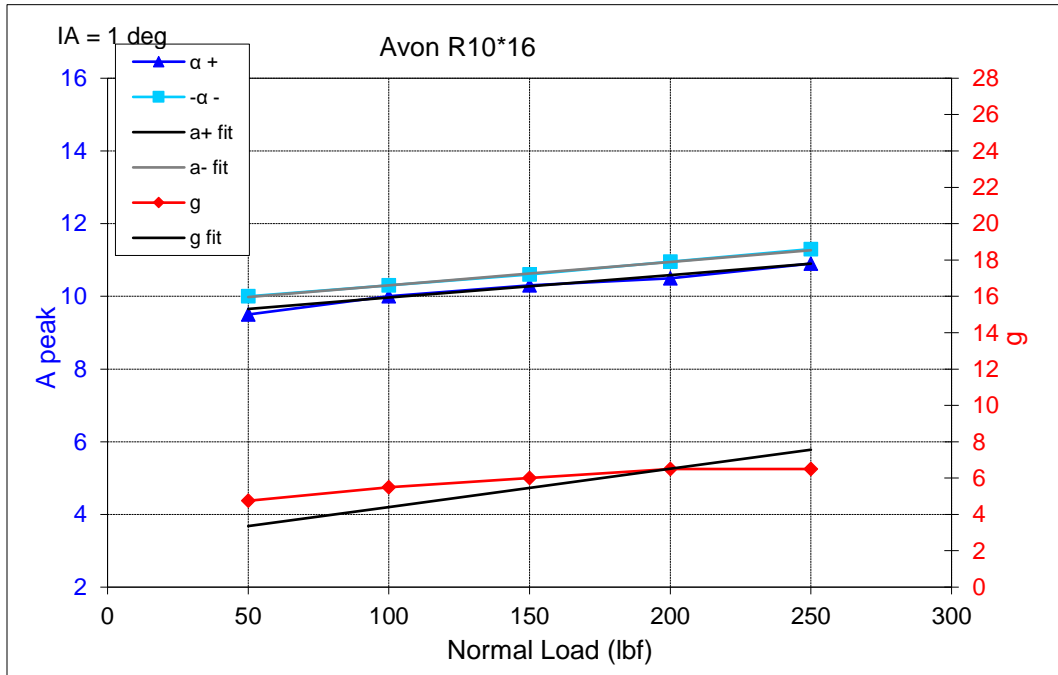
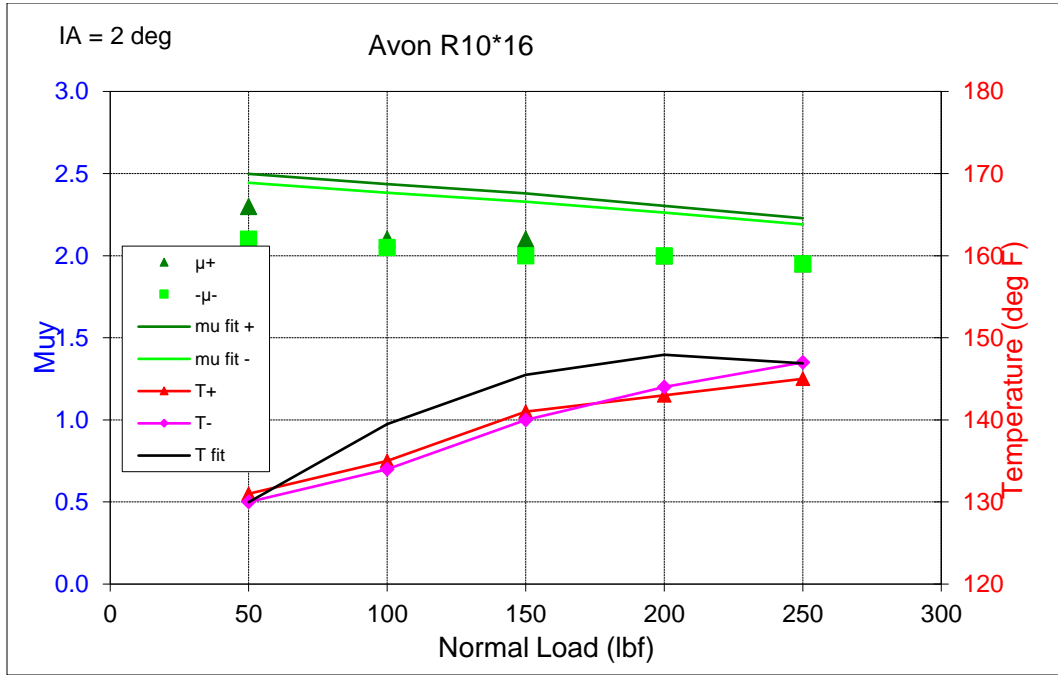


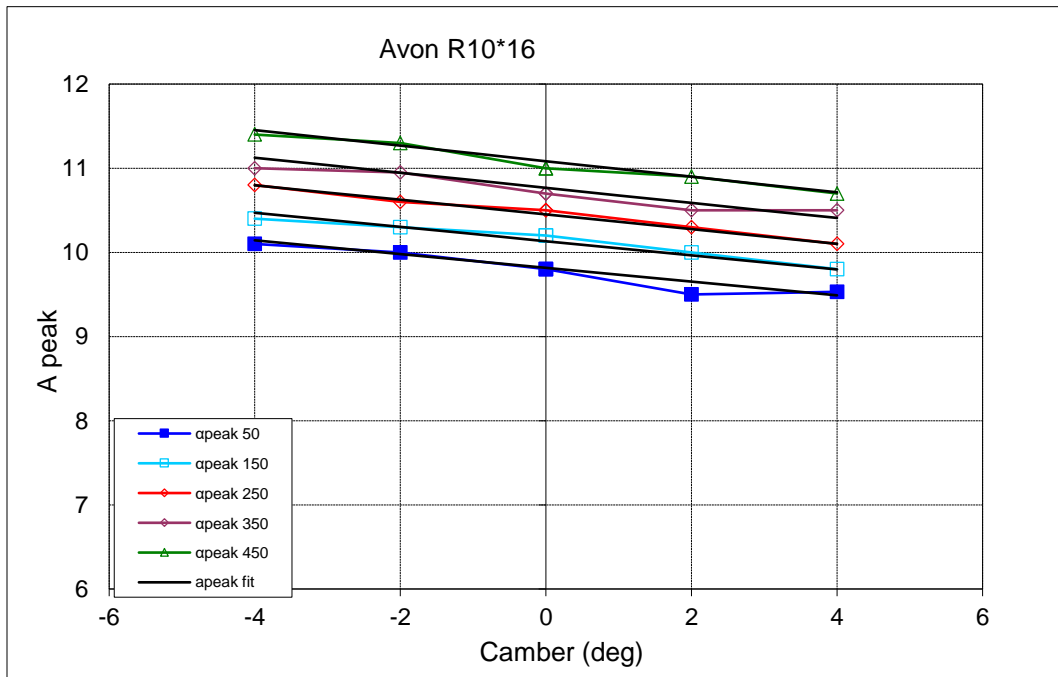
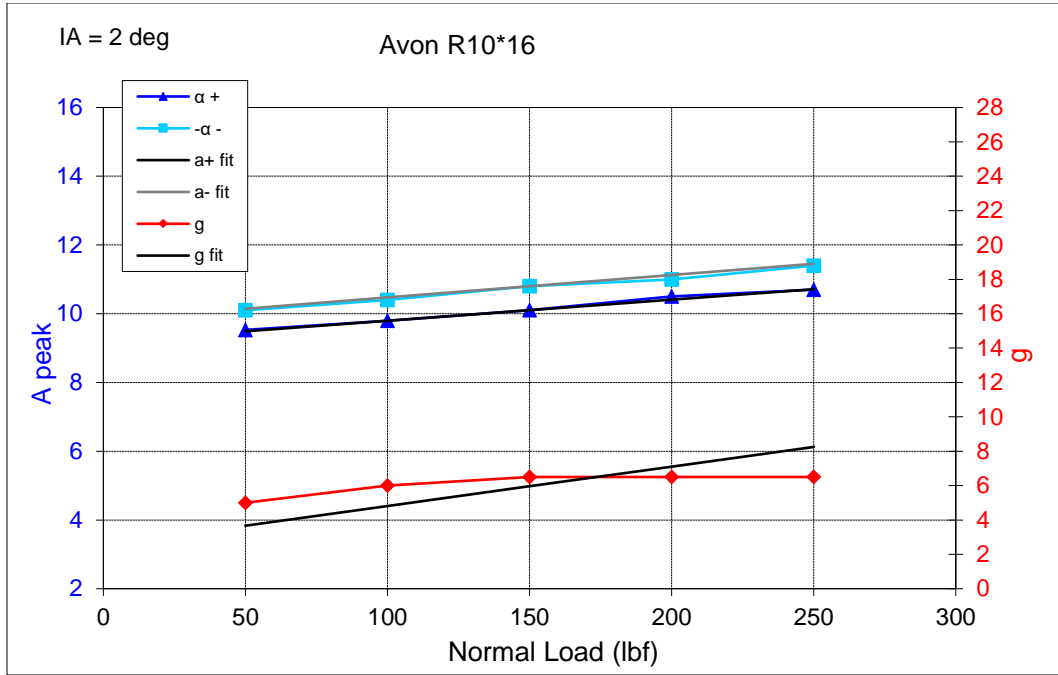


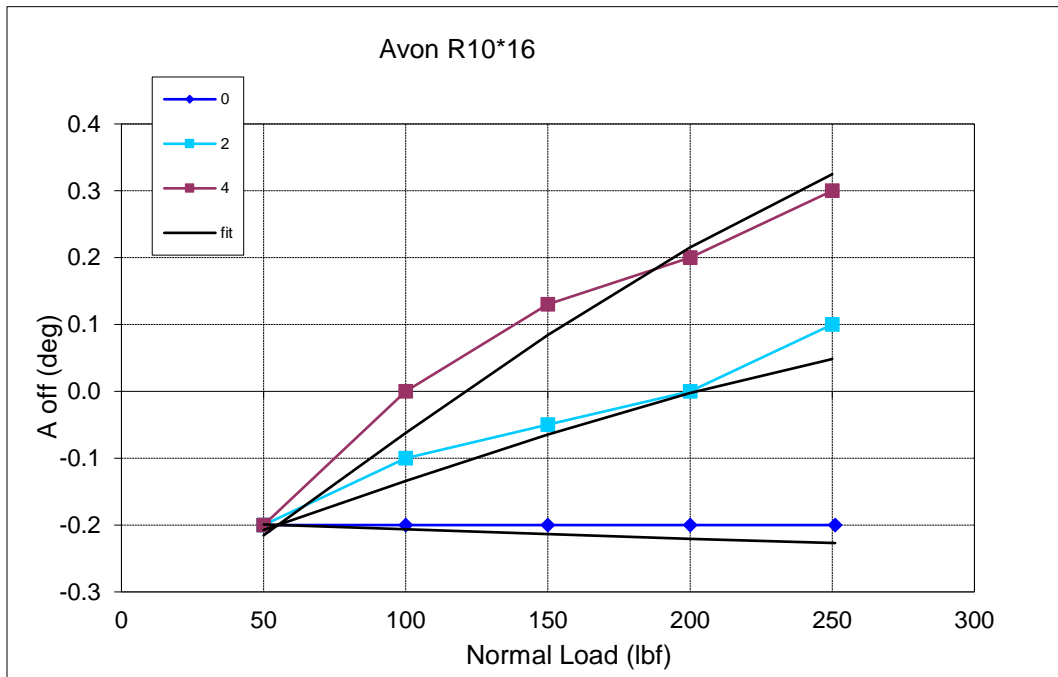
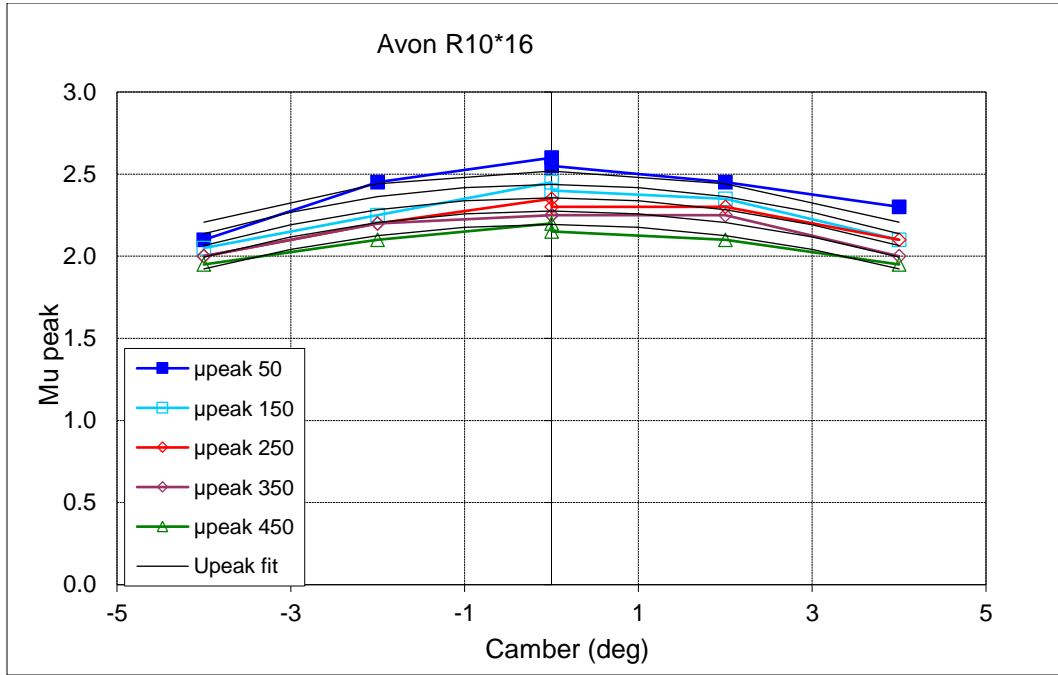




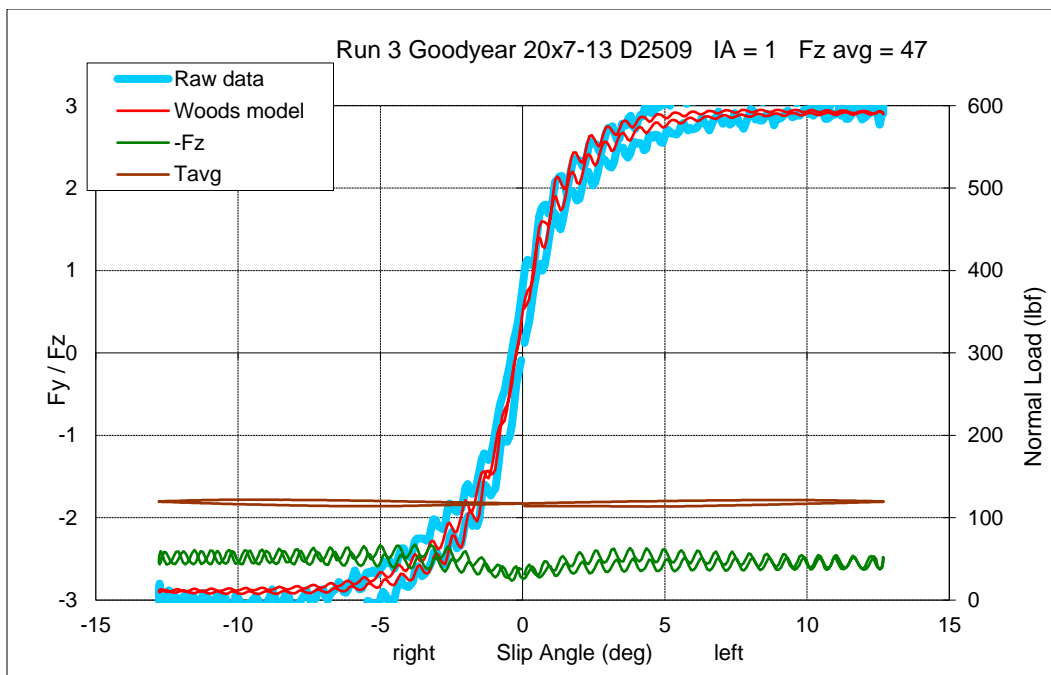
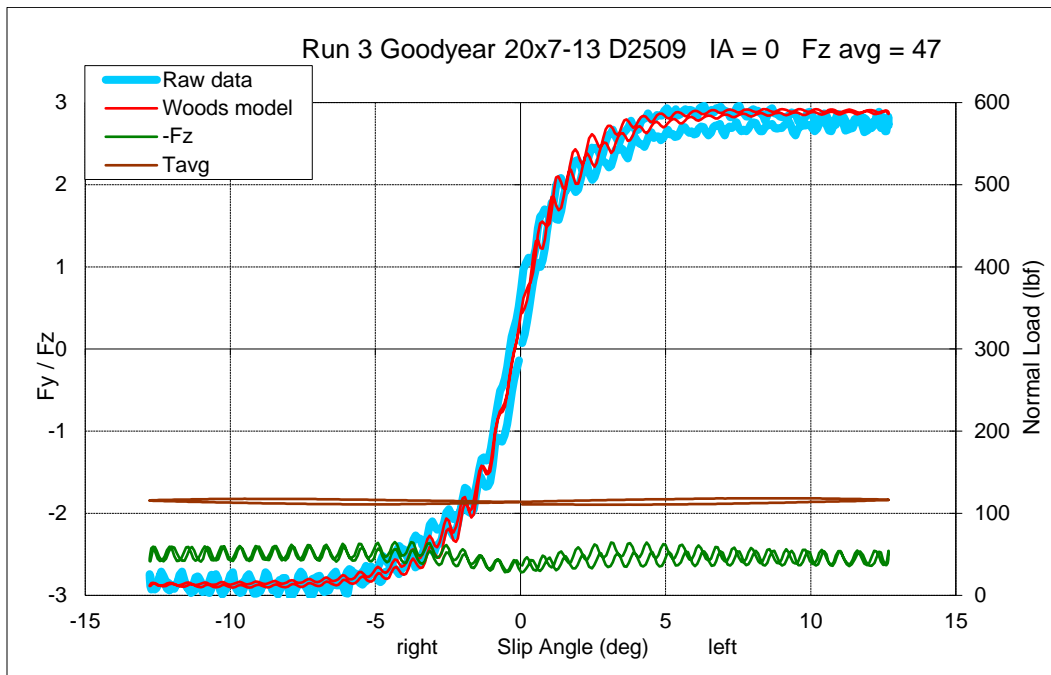


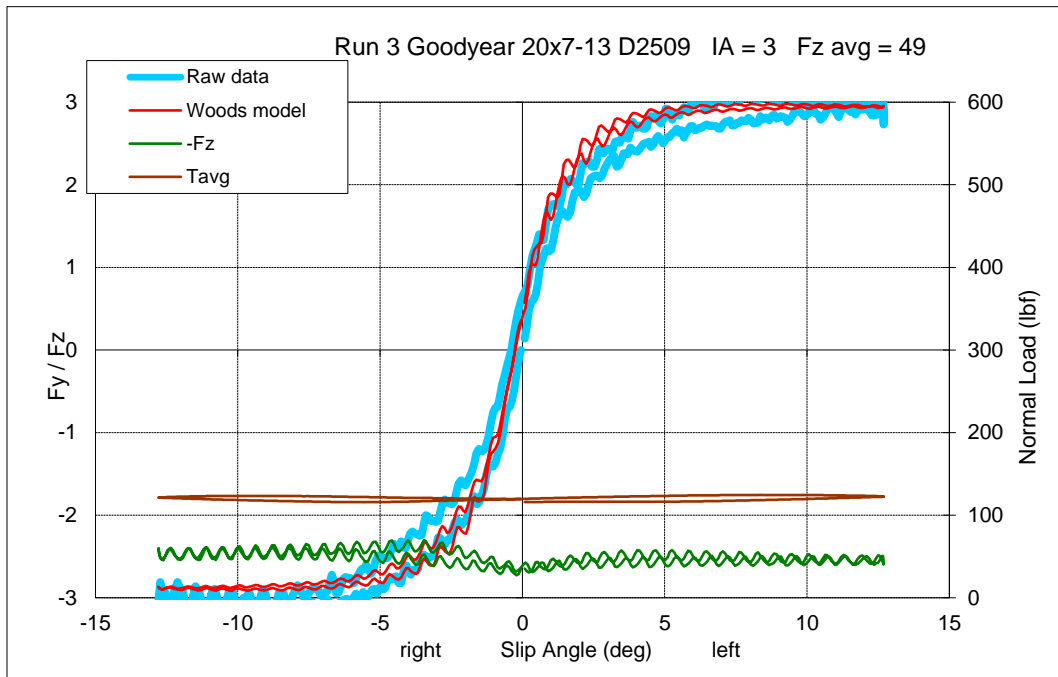
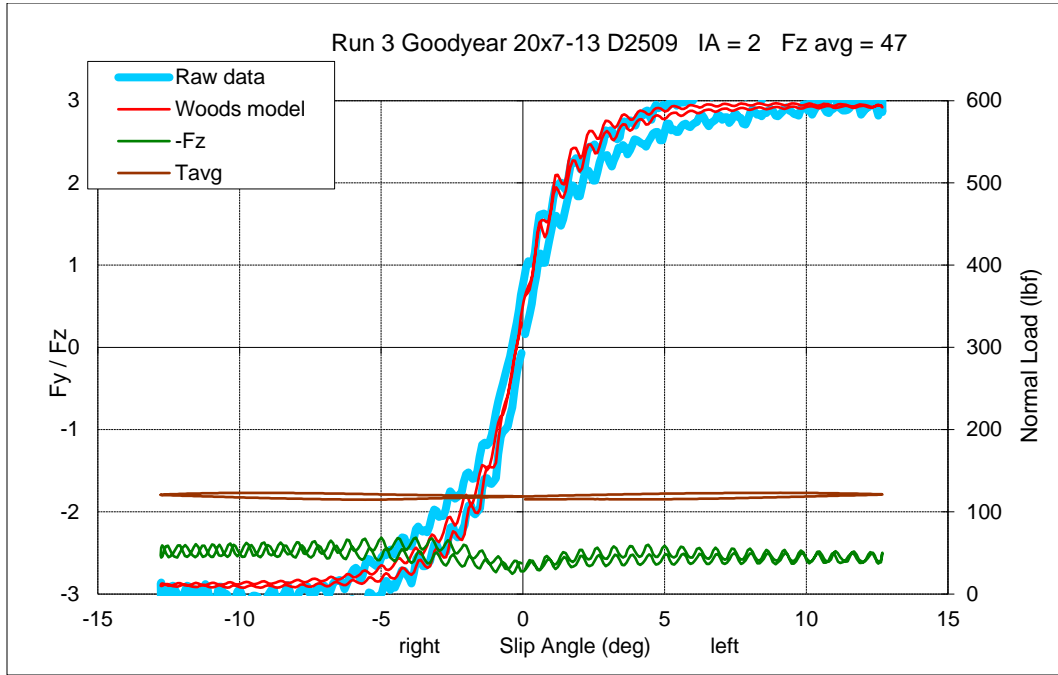


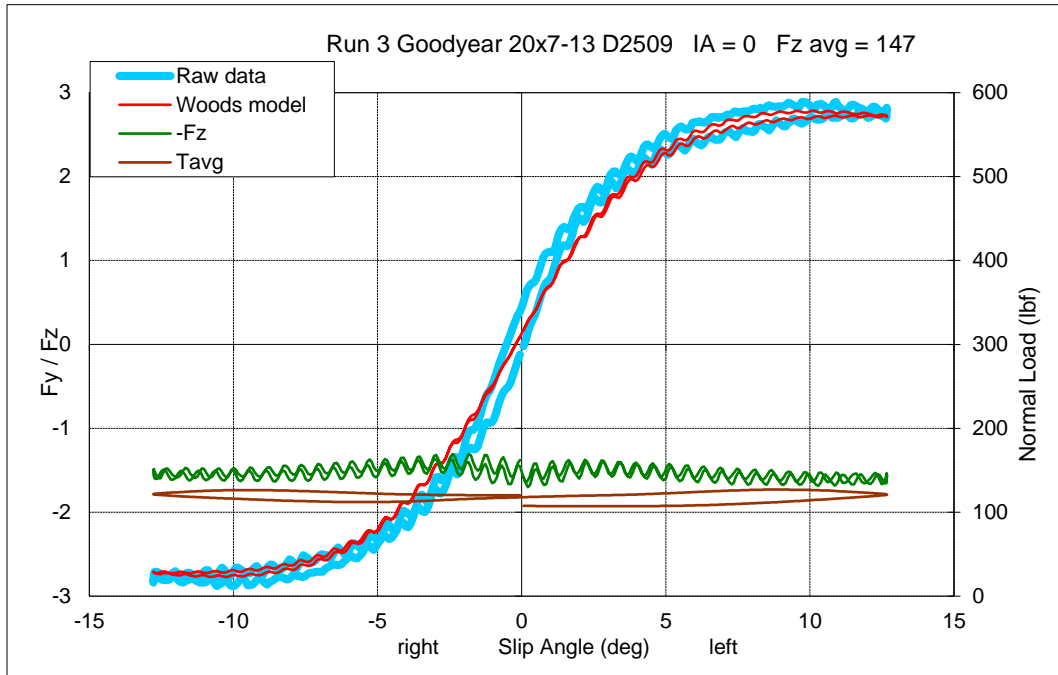
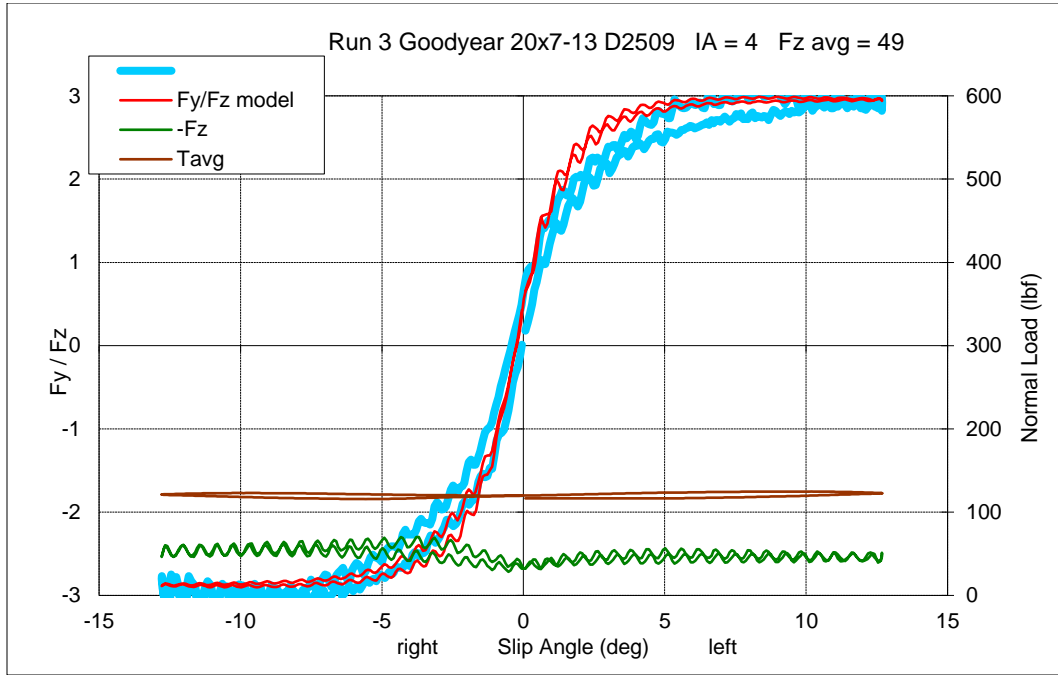


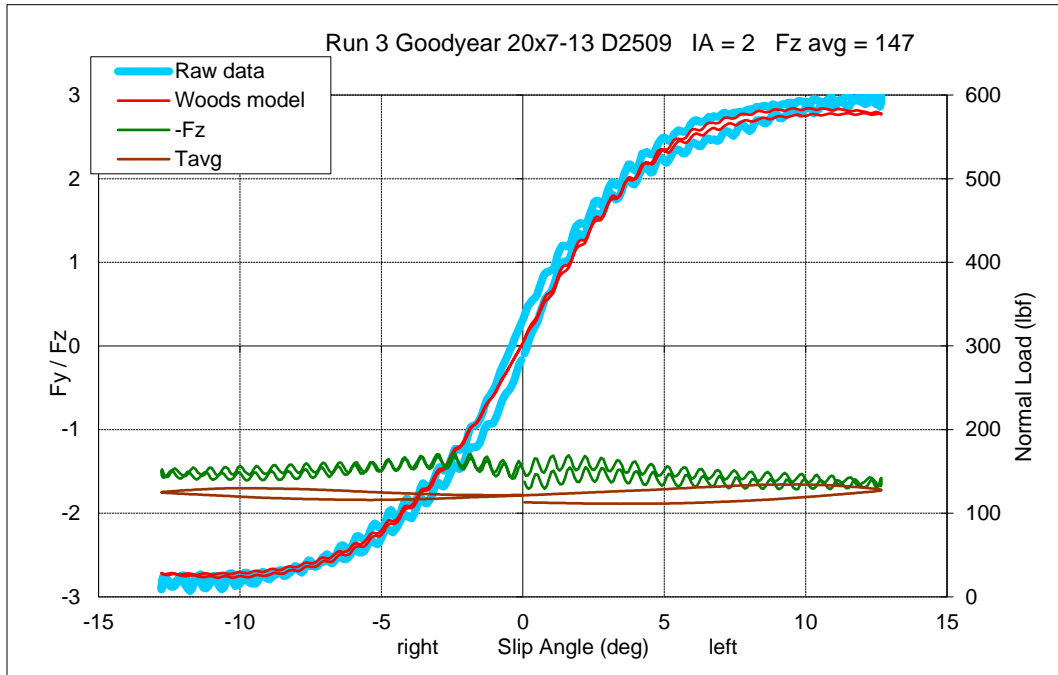
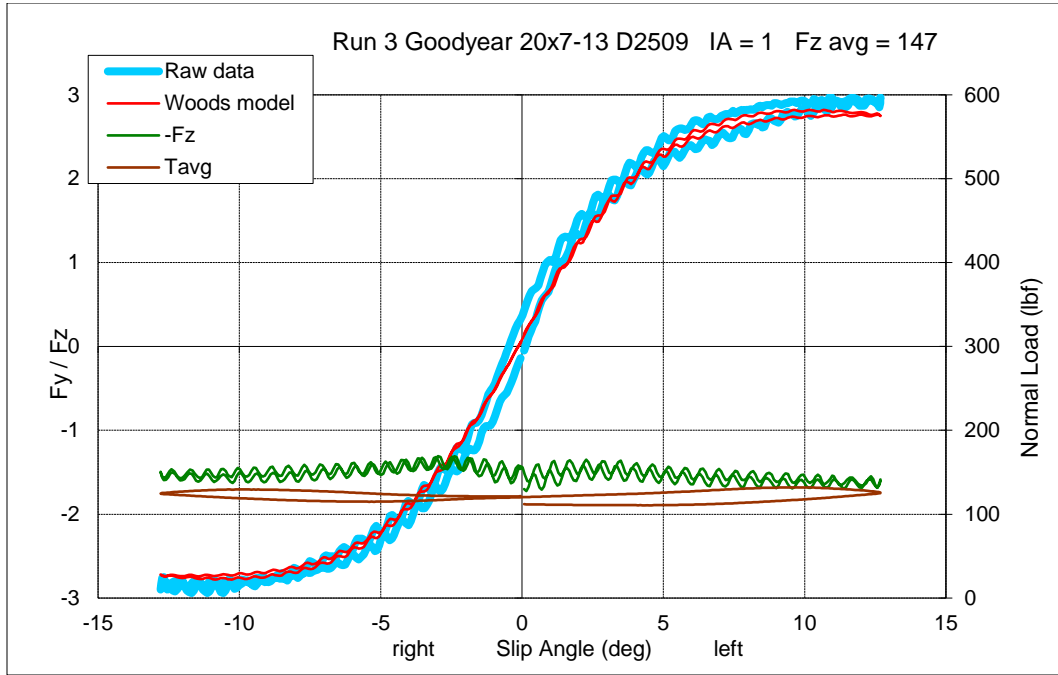


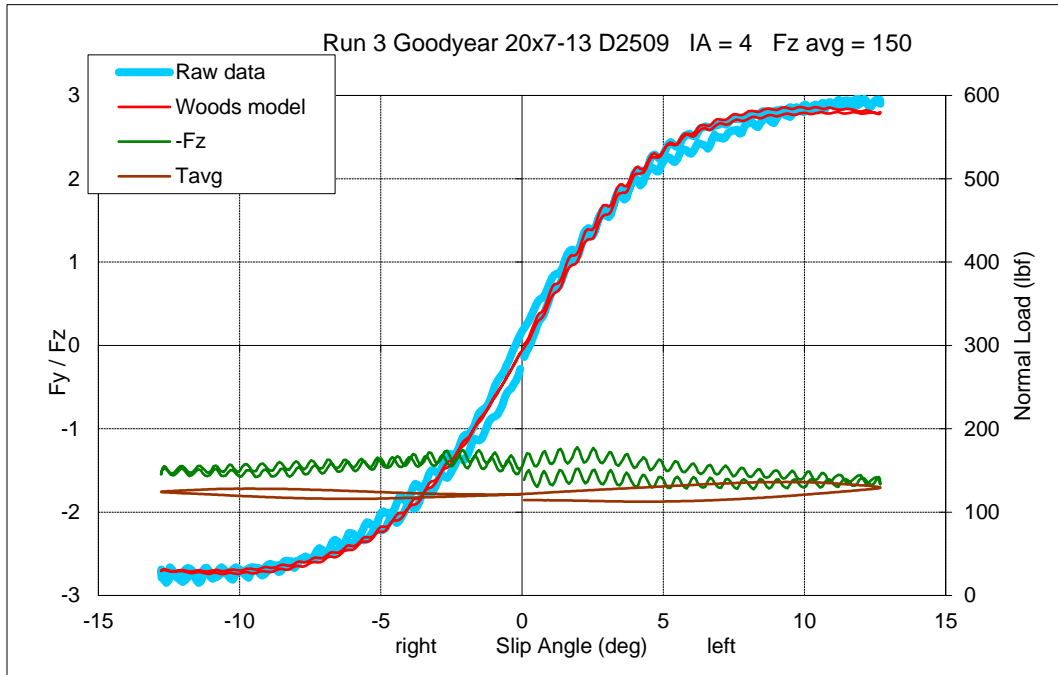
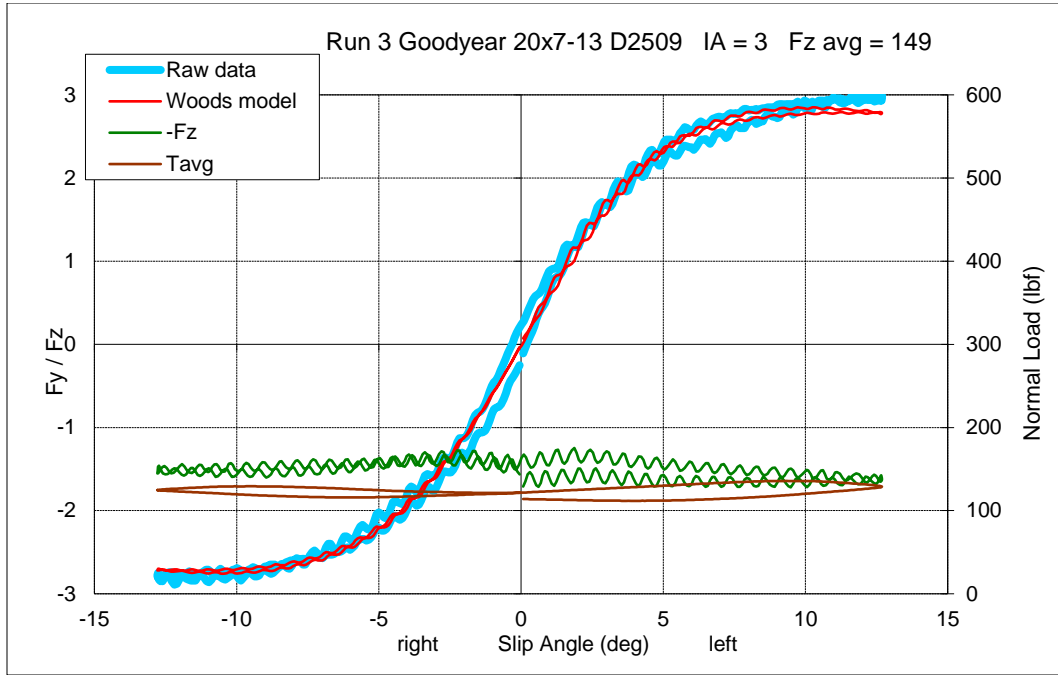
Goodyear 20x7-13 D2509

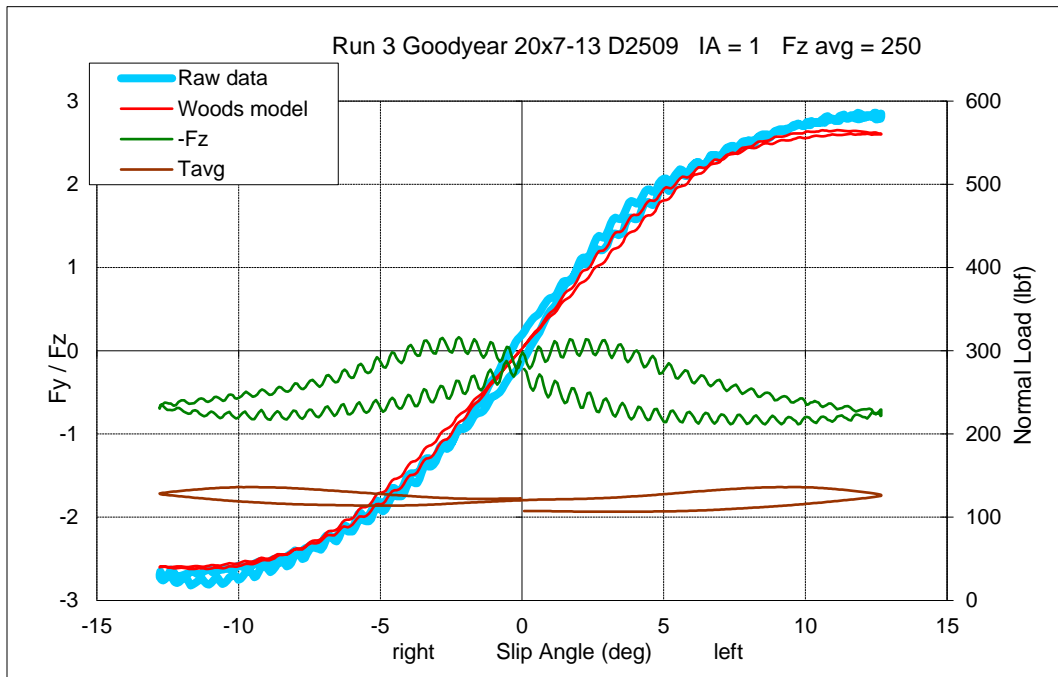
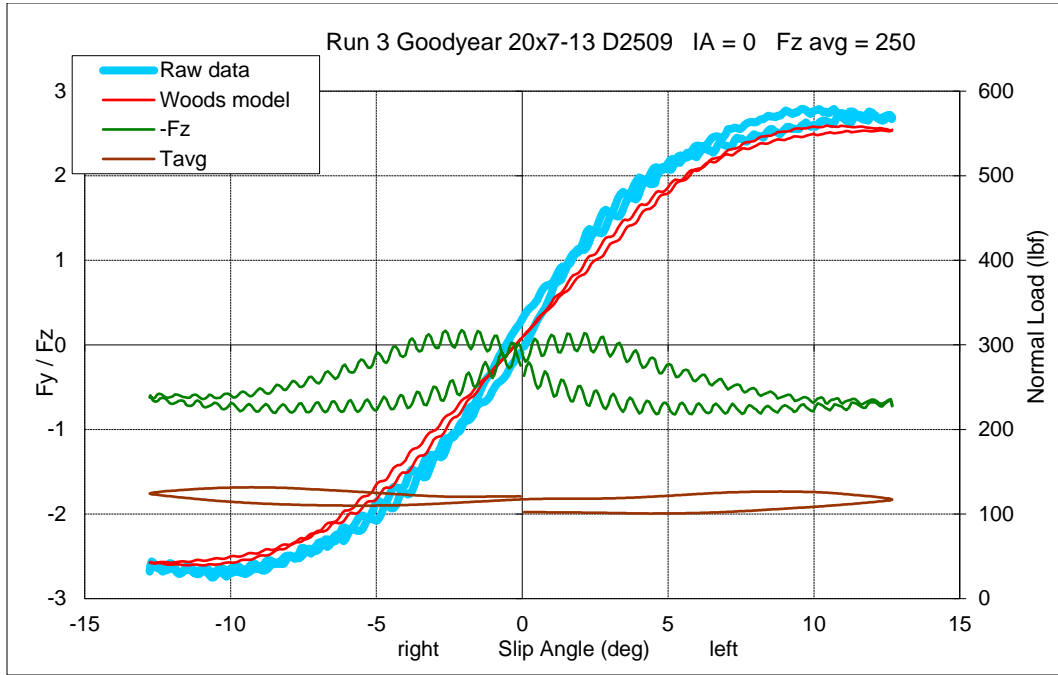


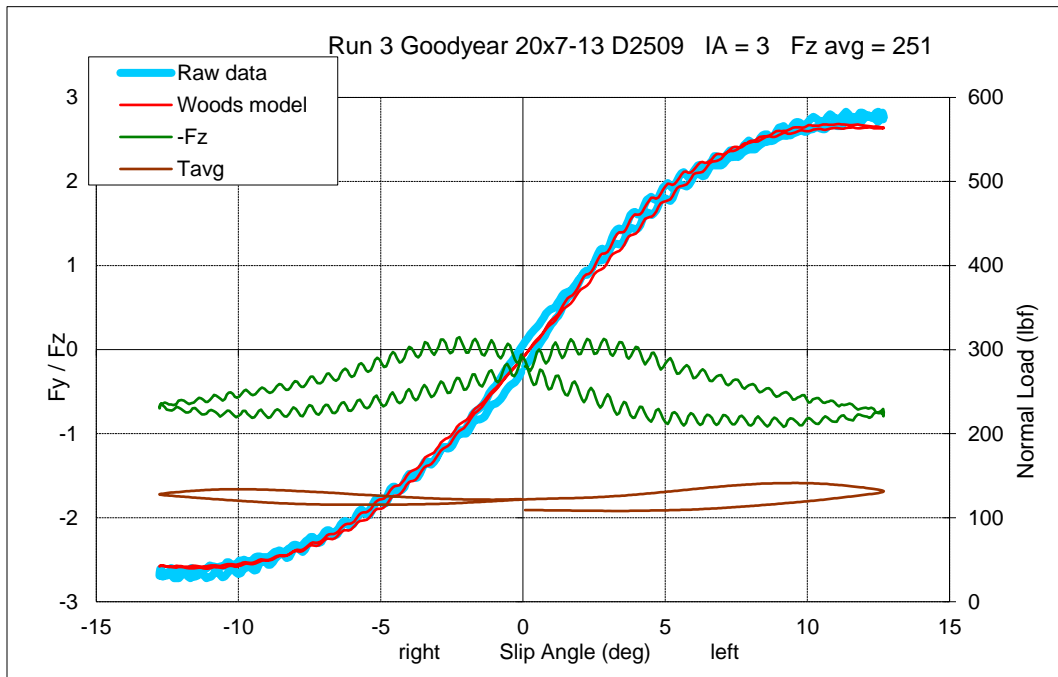
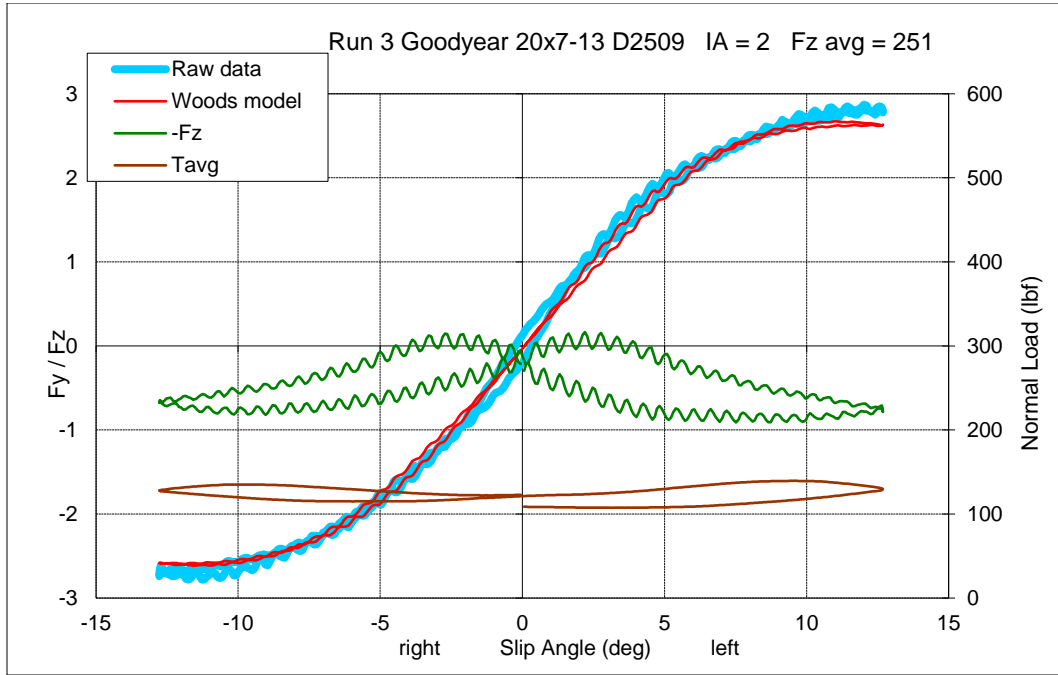


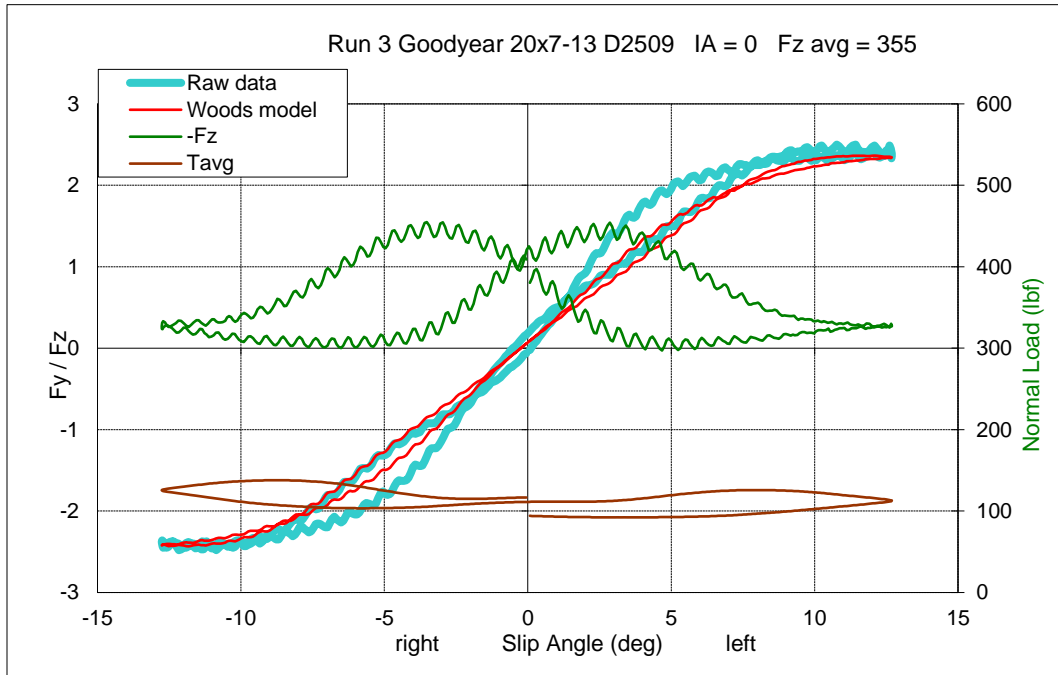
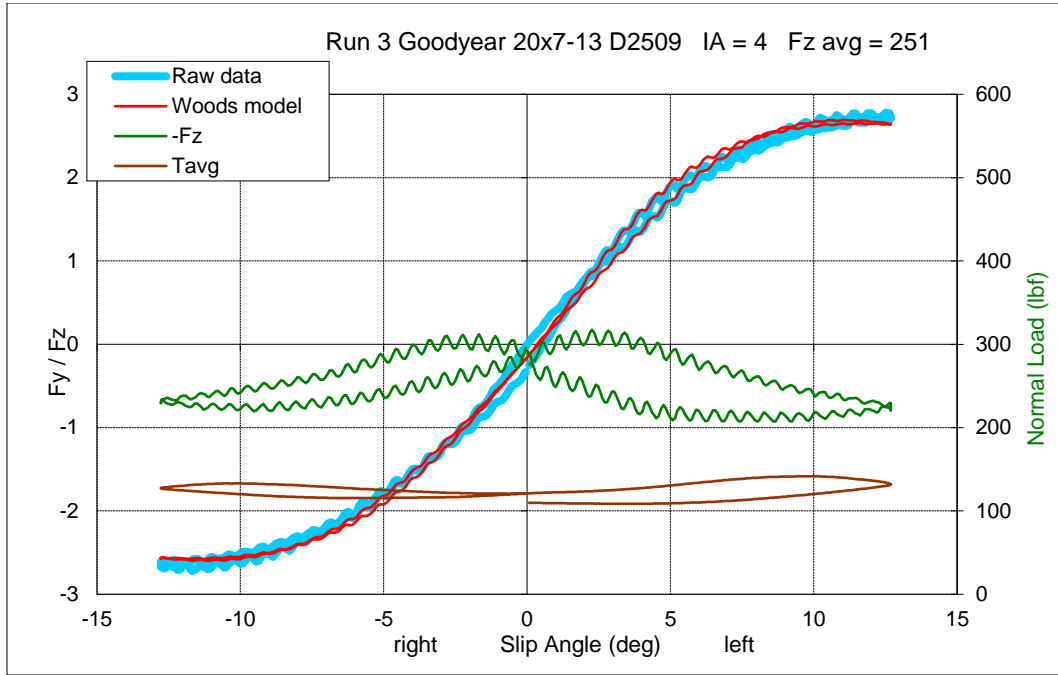


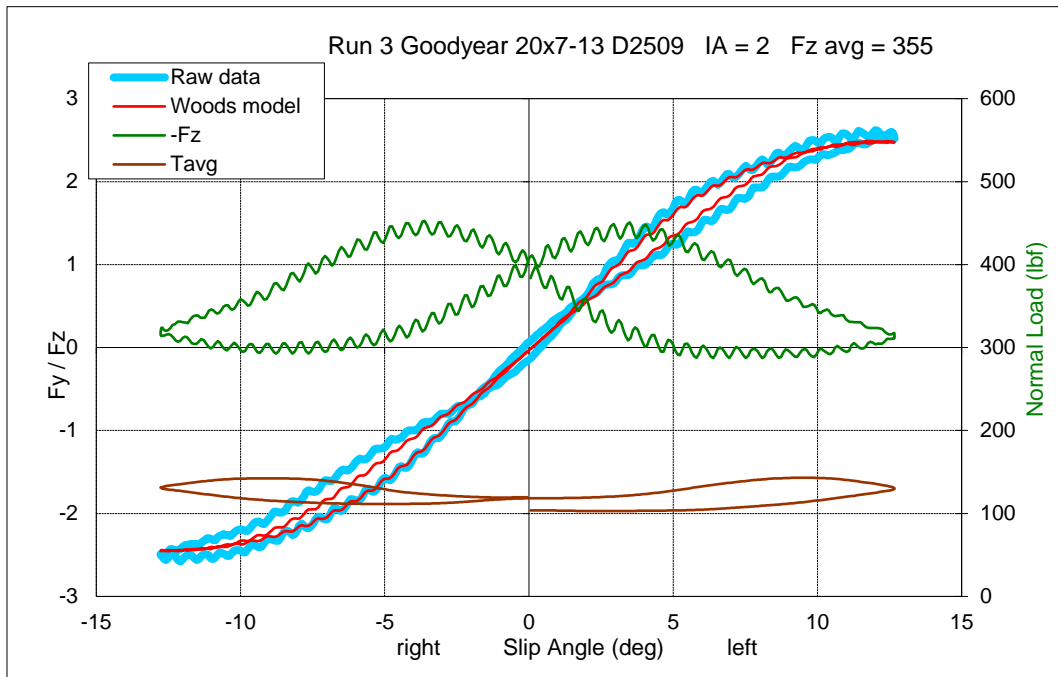
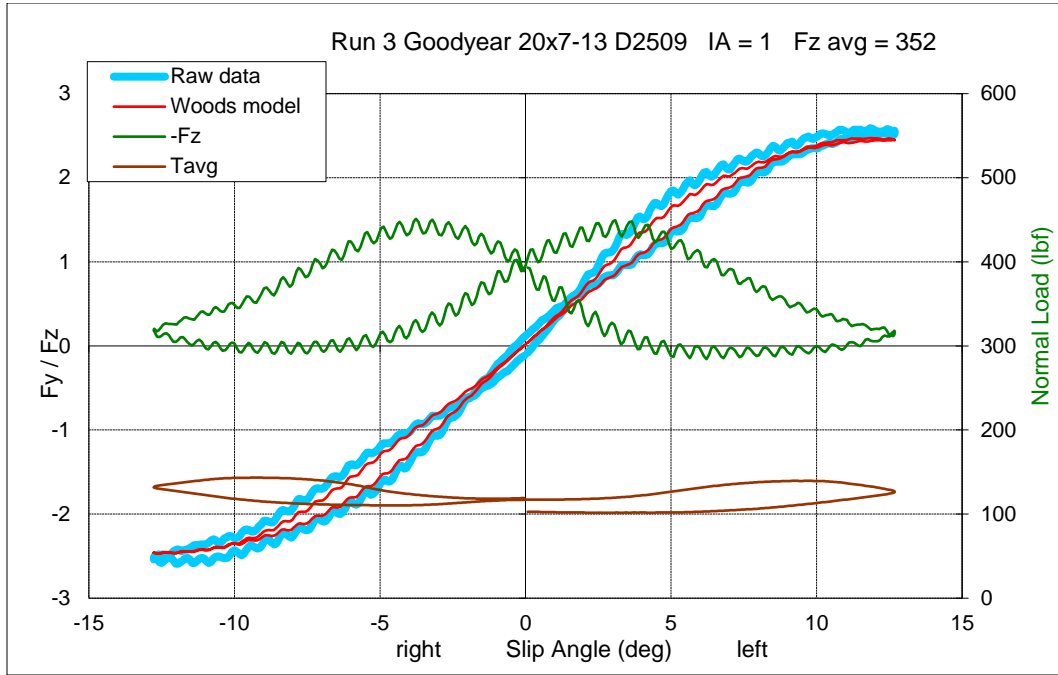


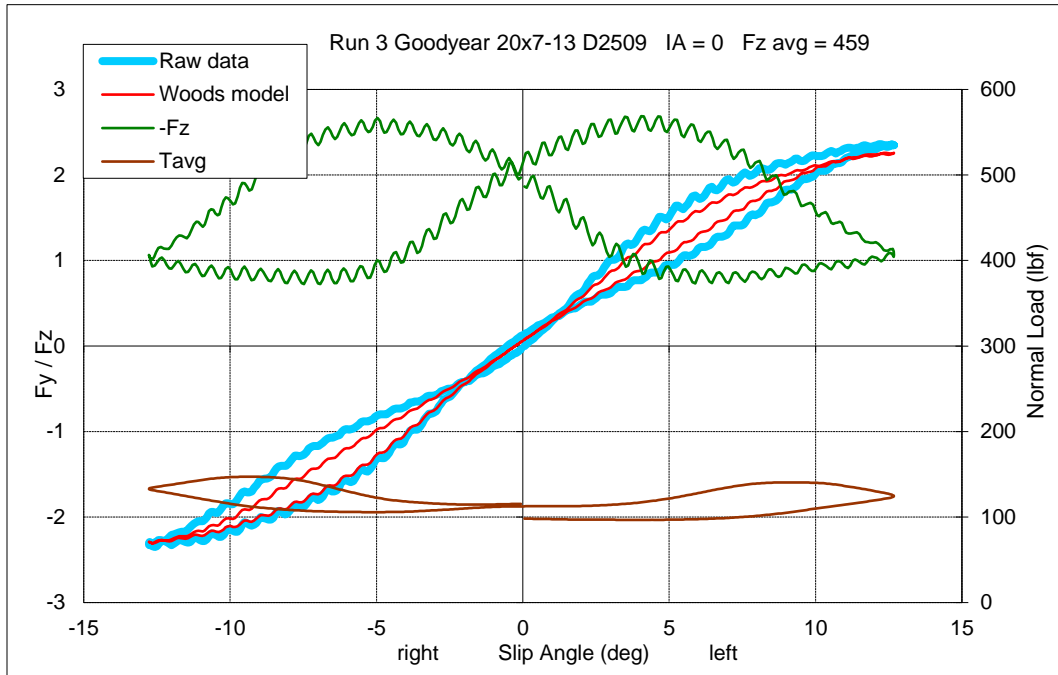
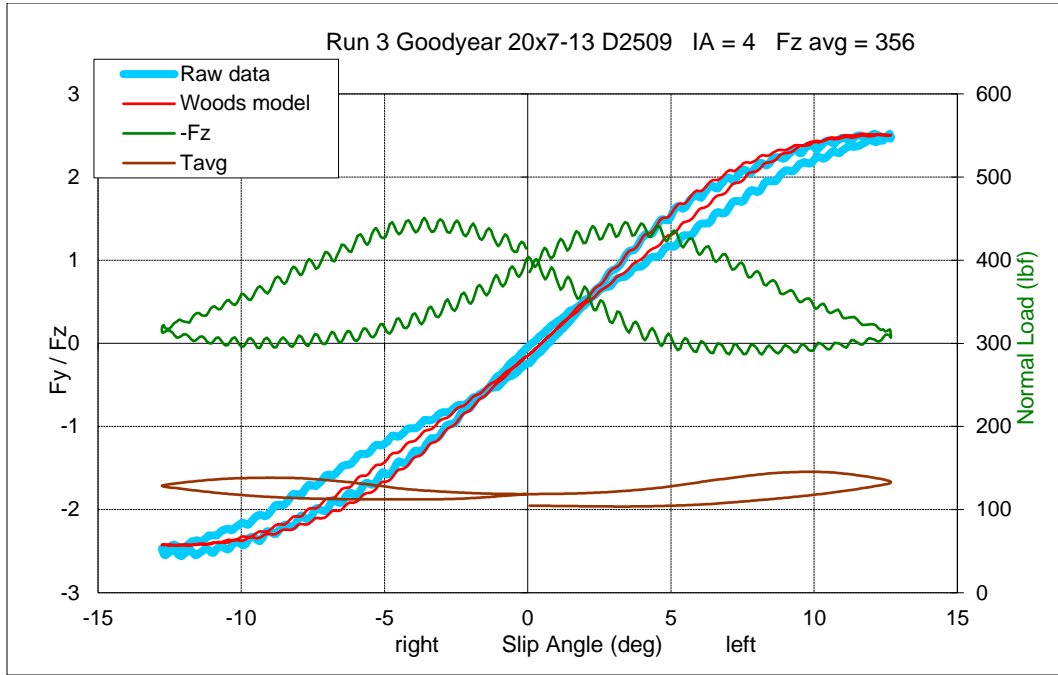


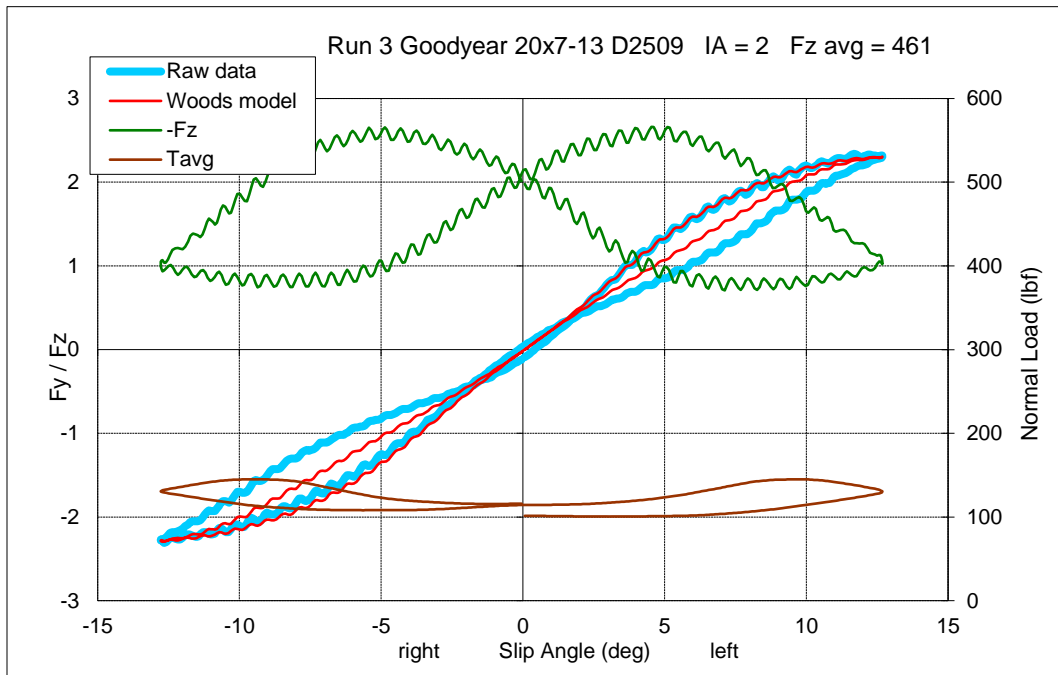
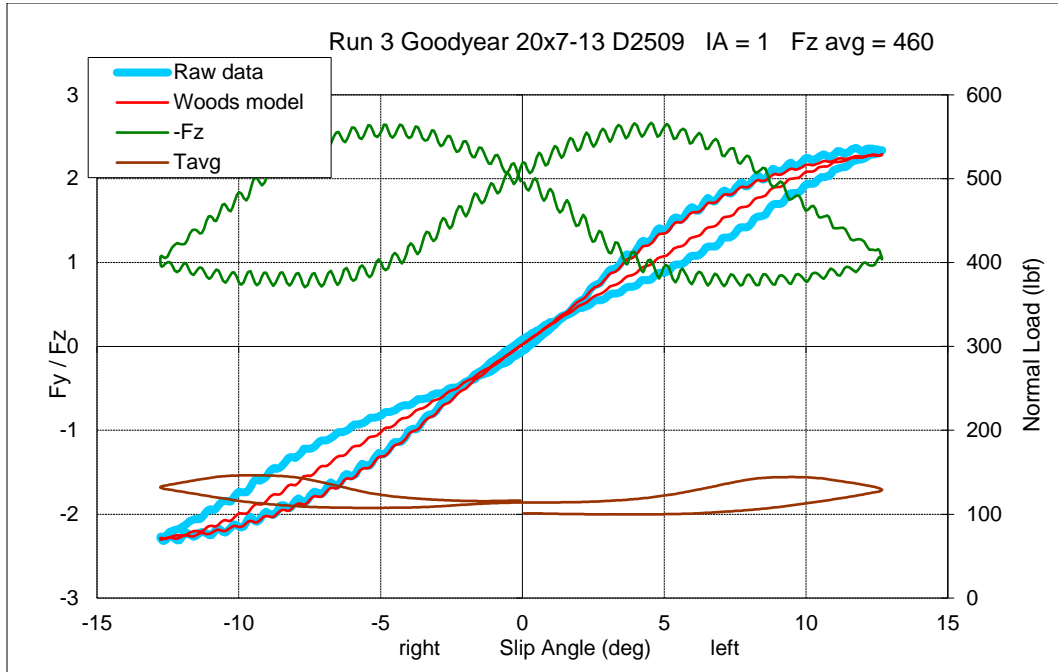


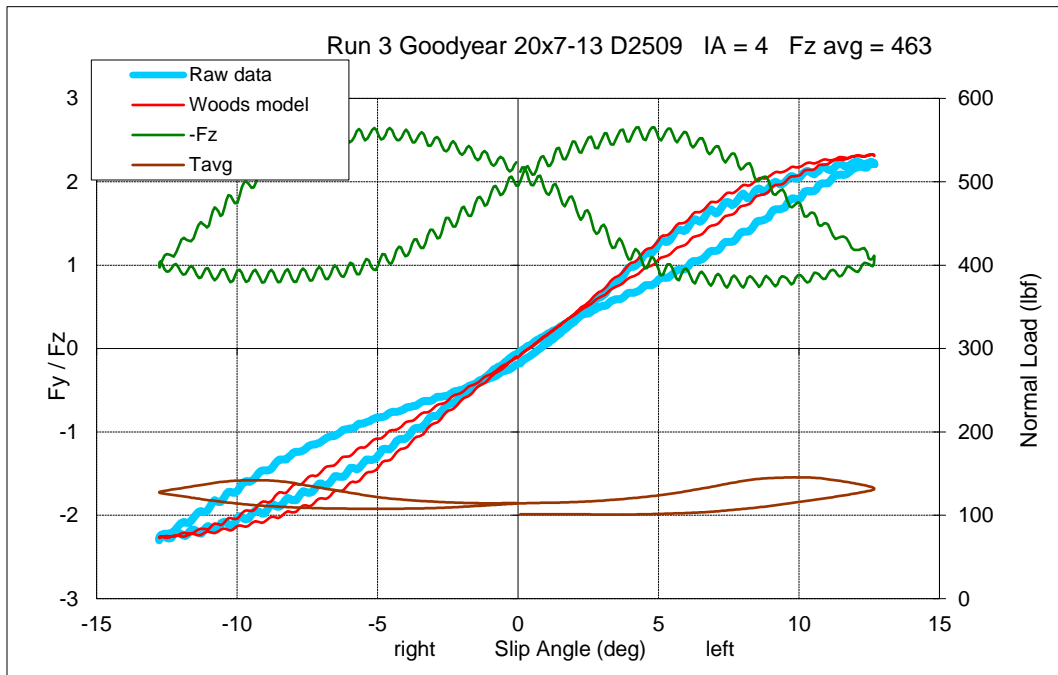
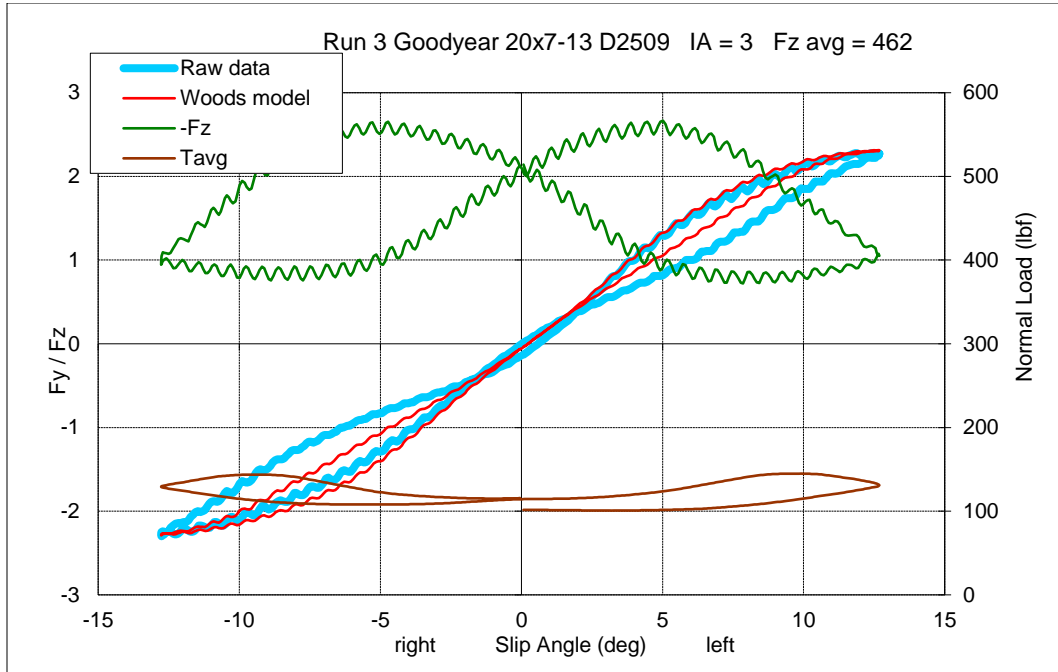


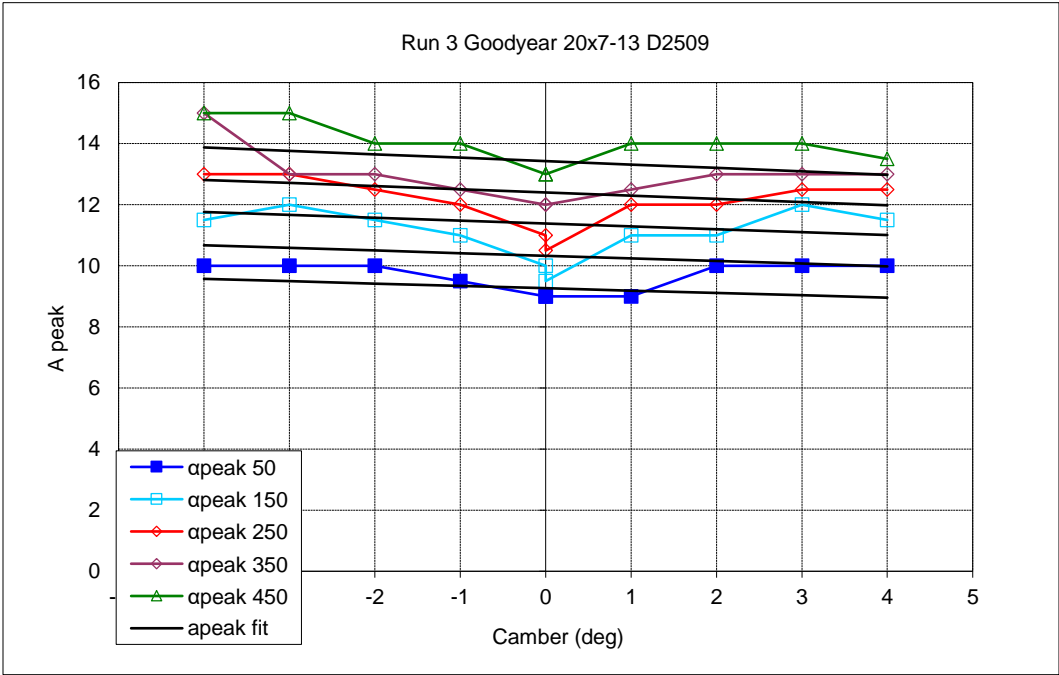
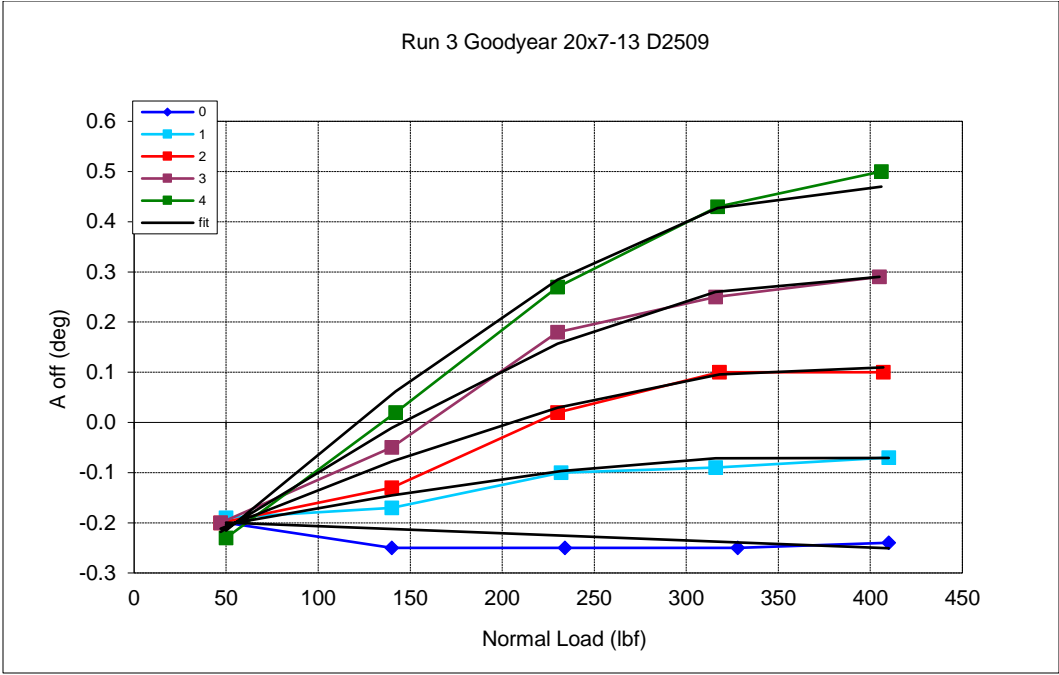


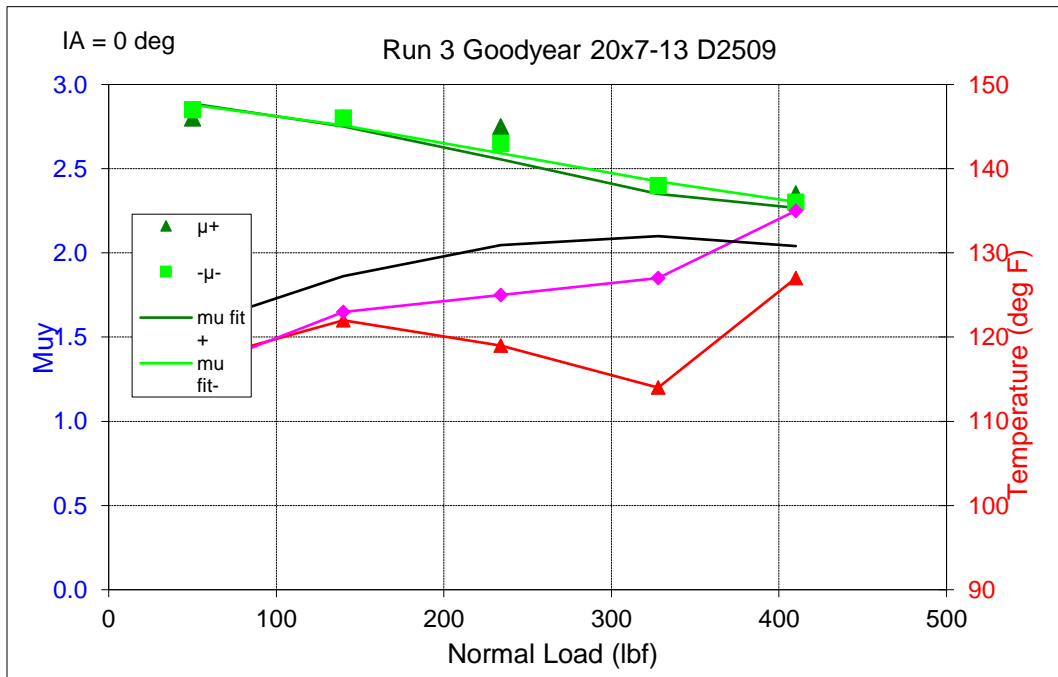
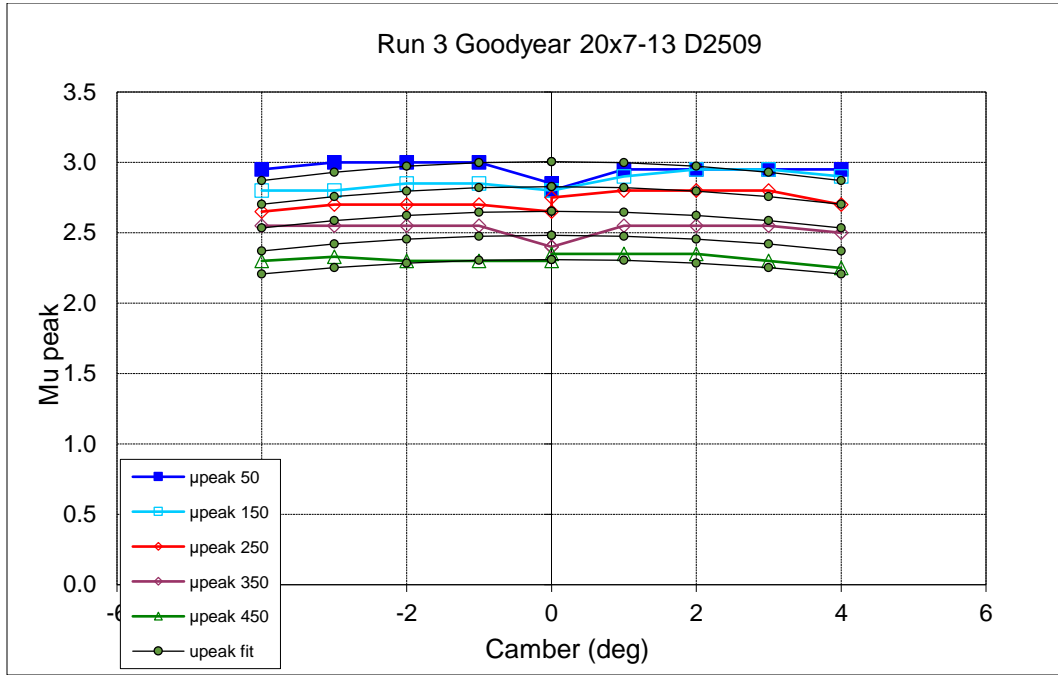


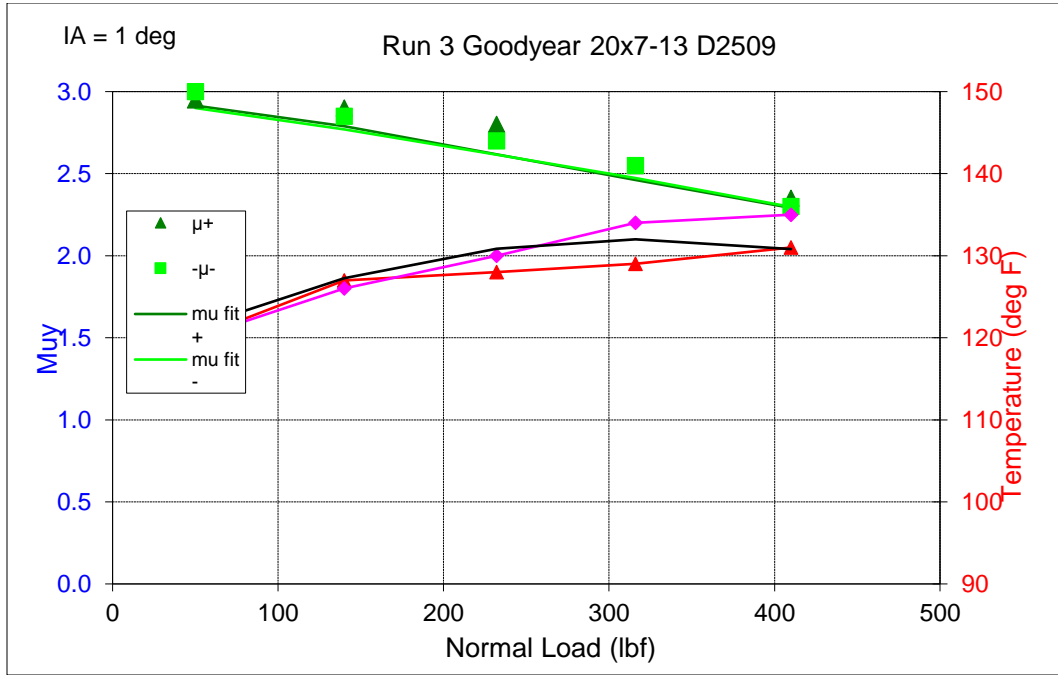


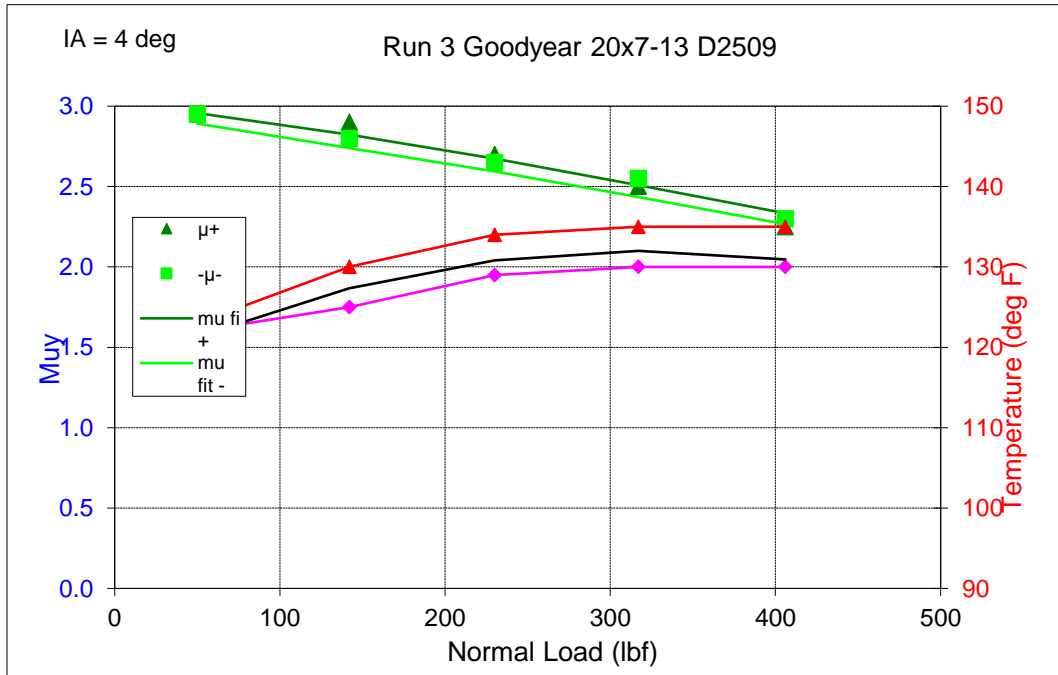
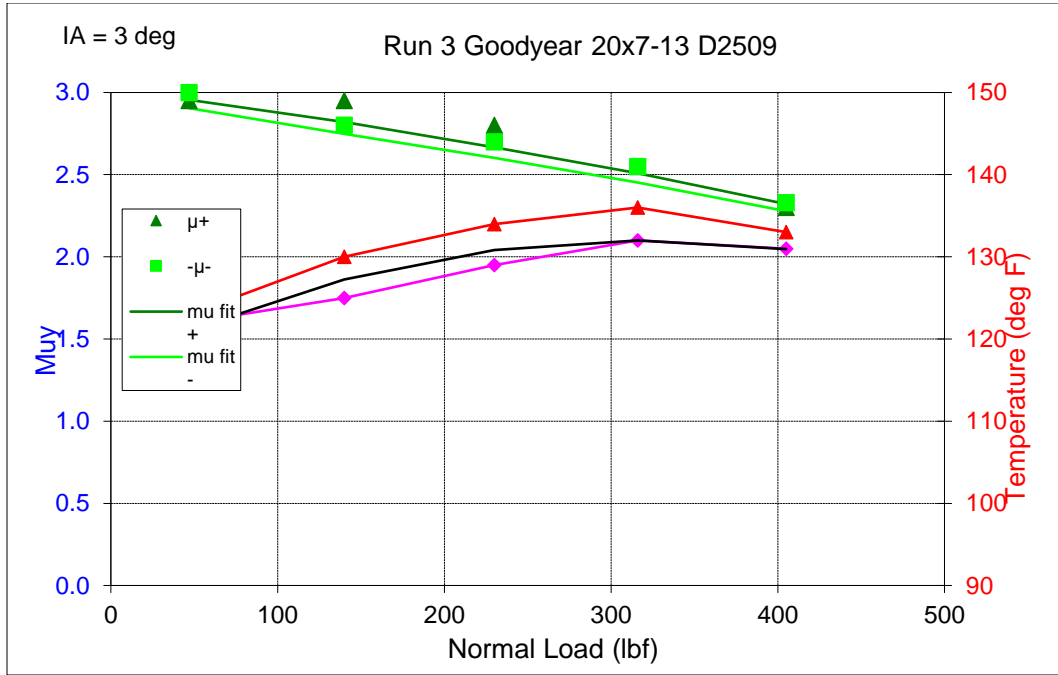


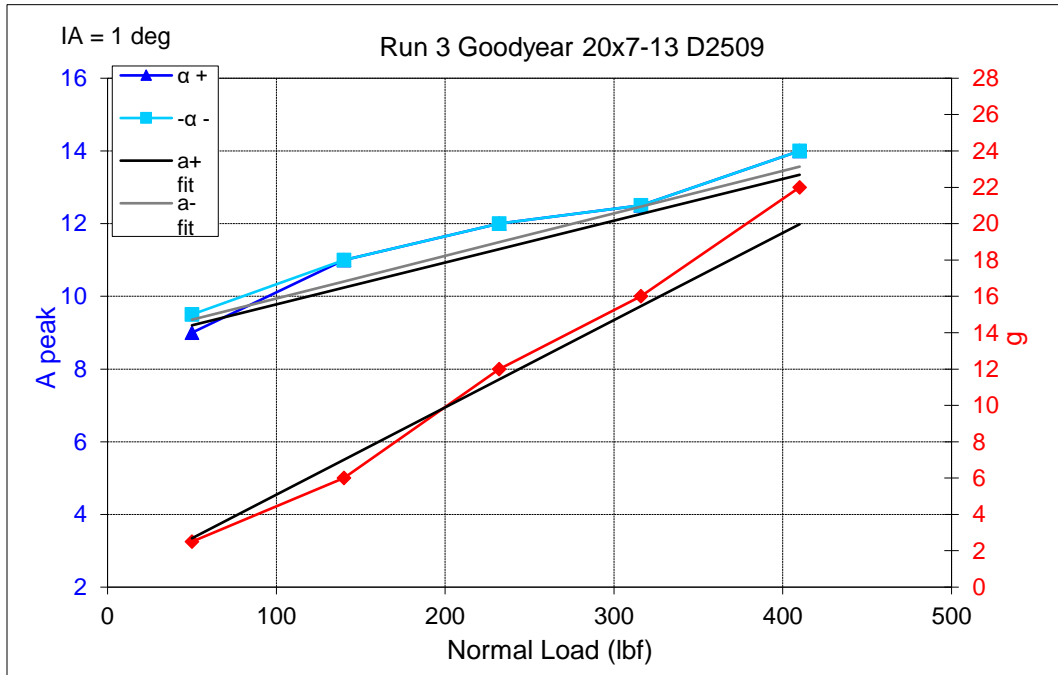


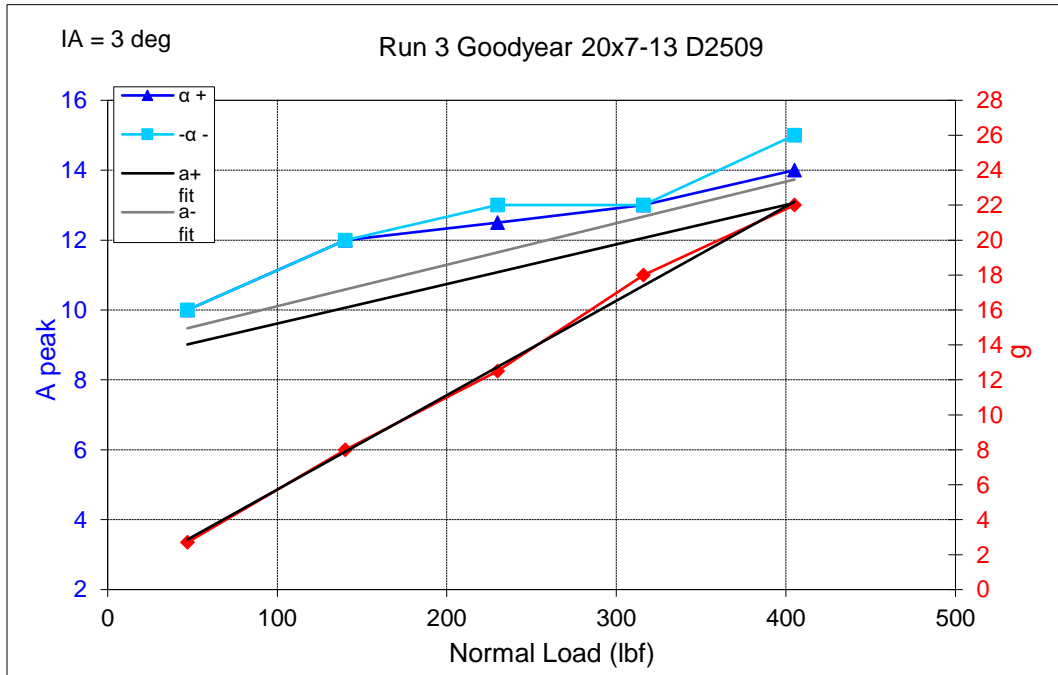
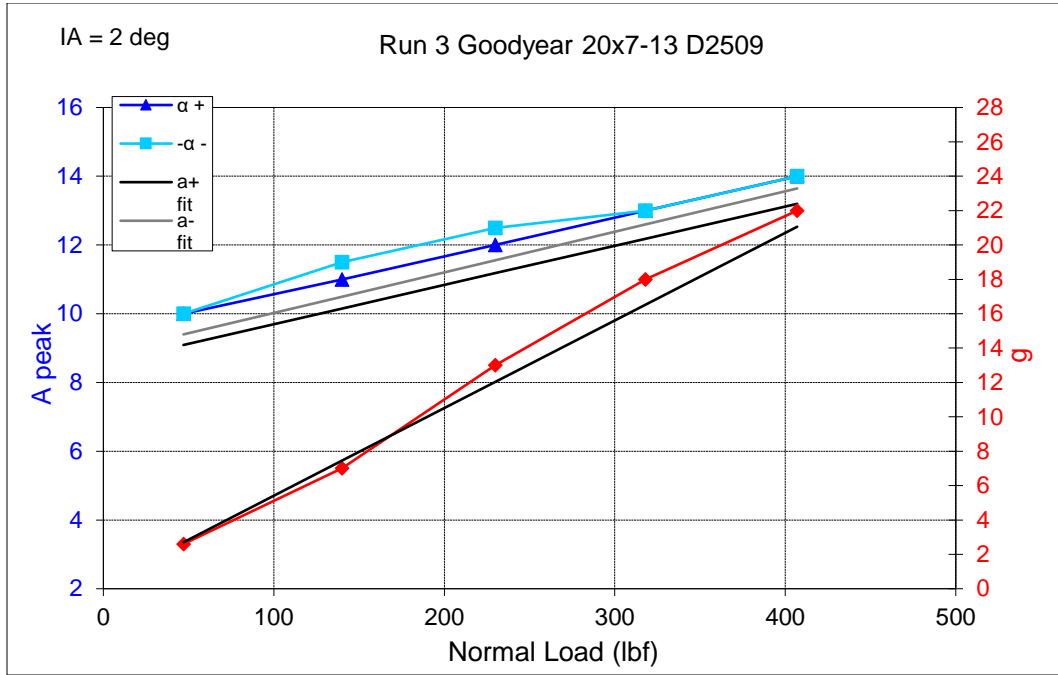


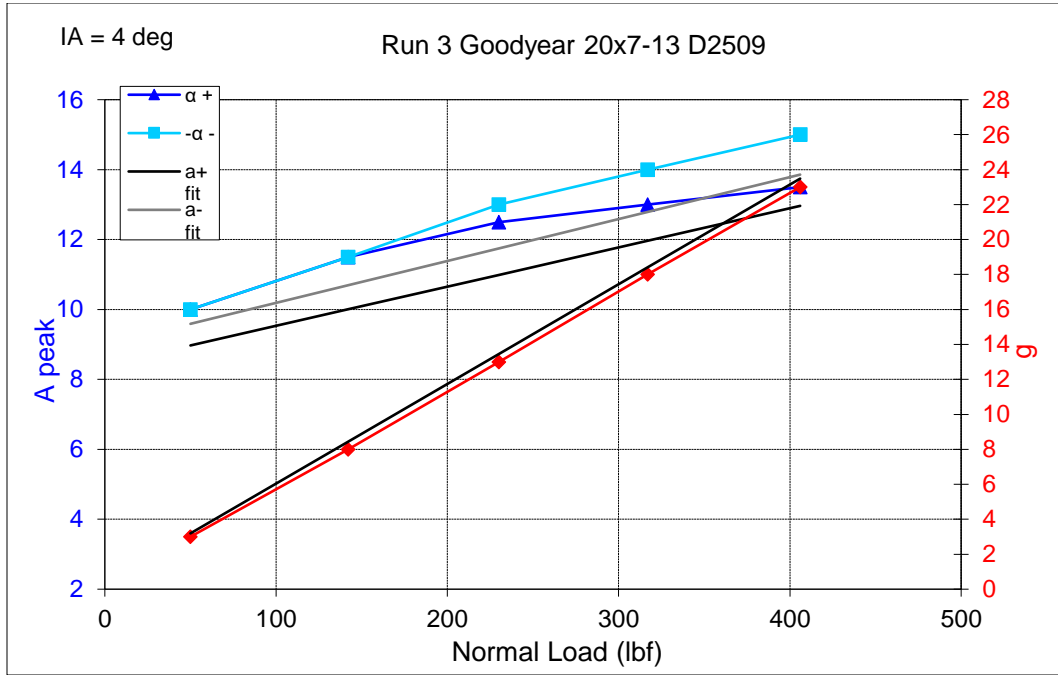




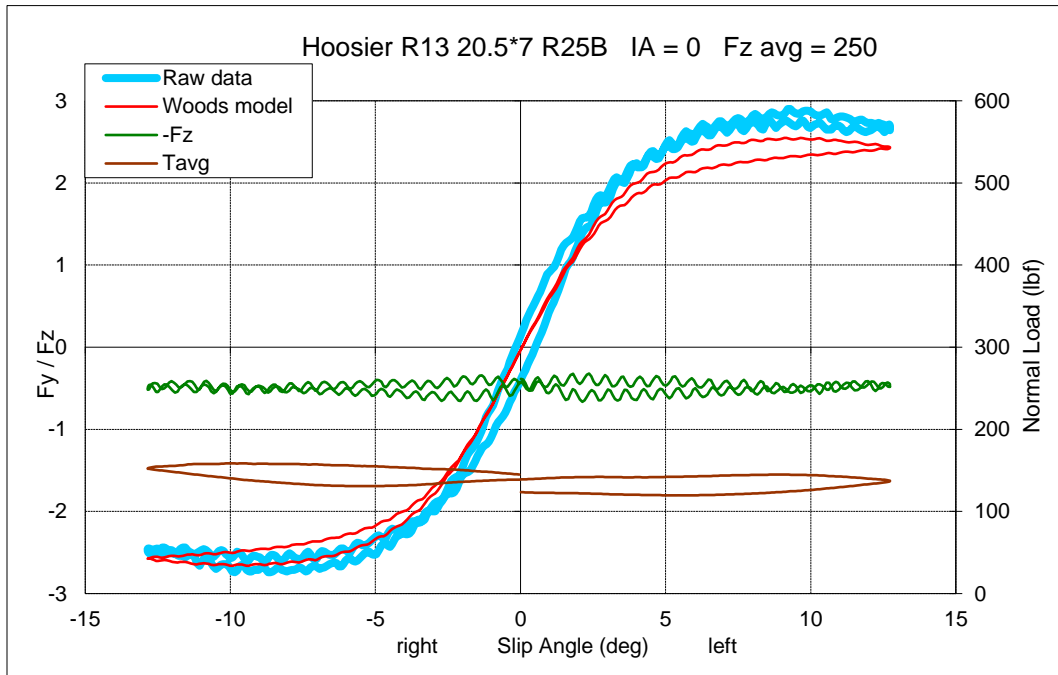


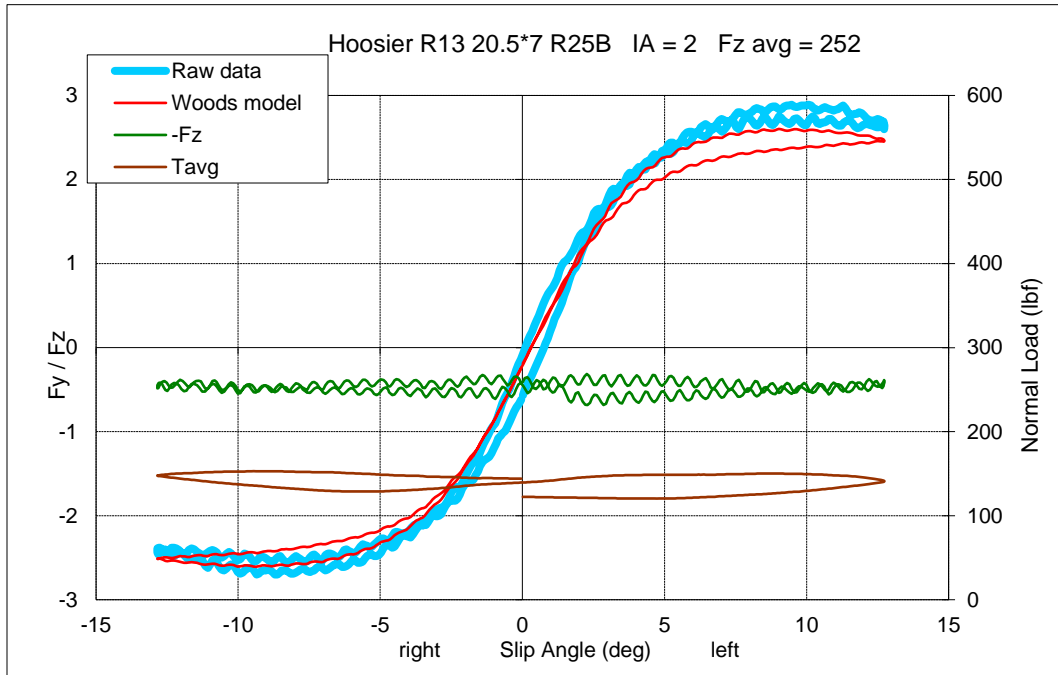
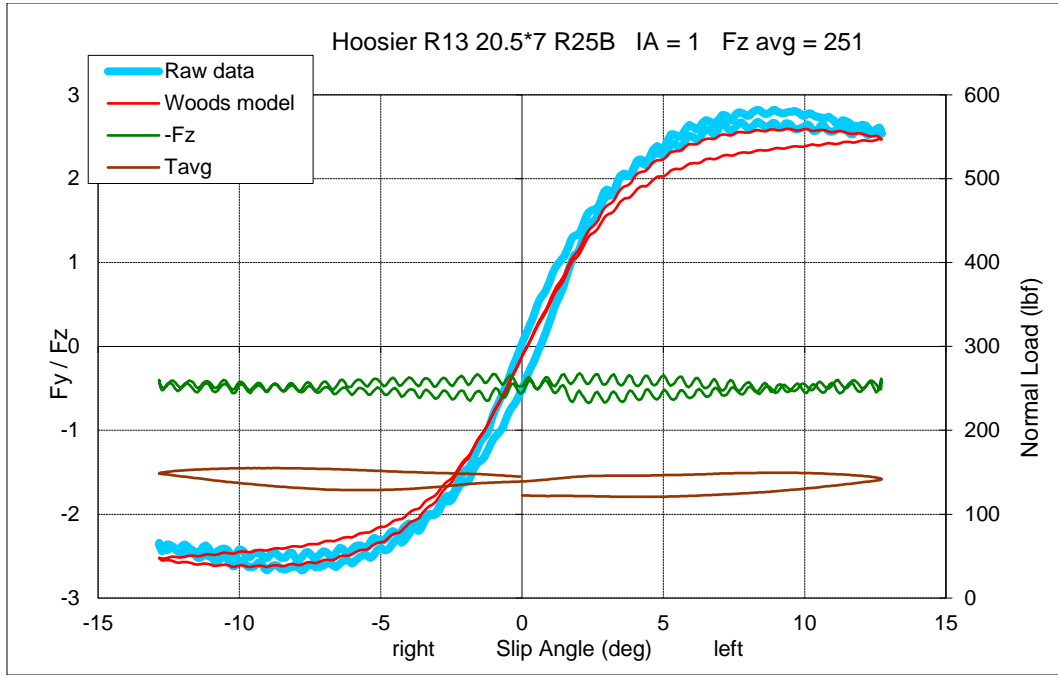


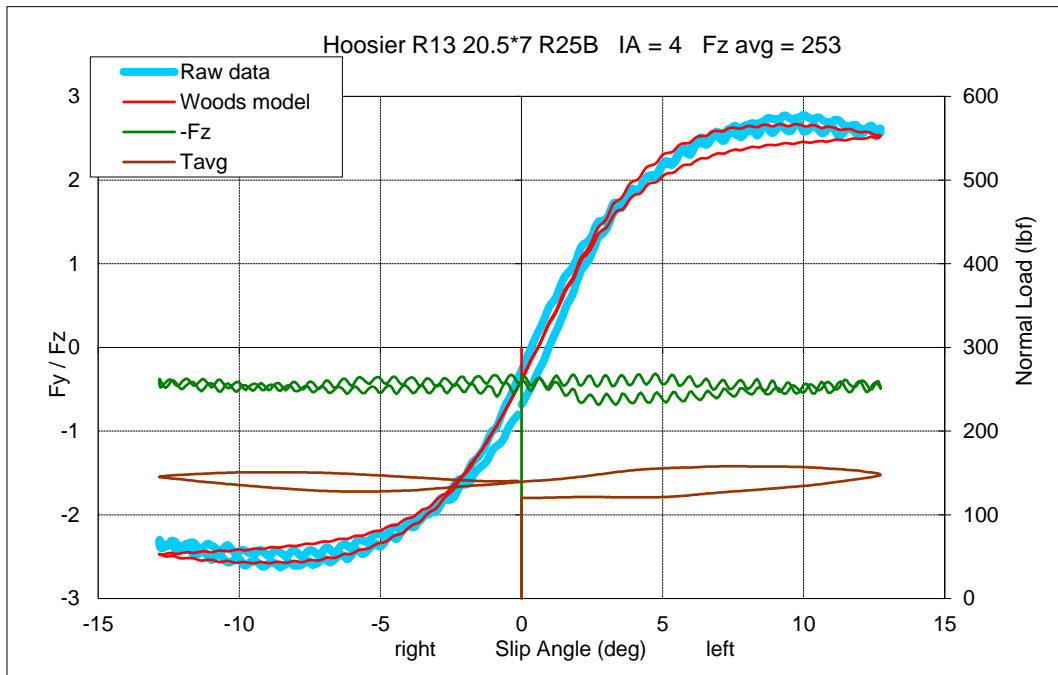
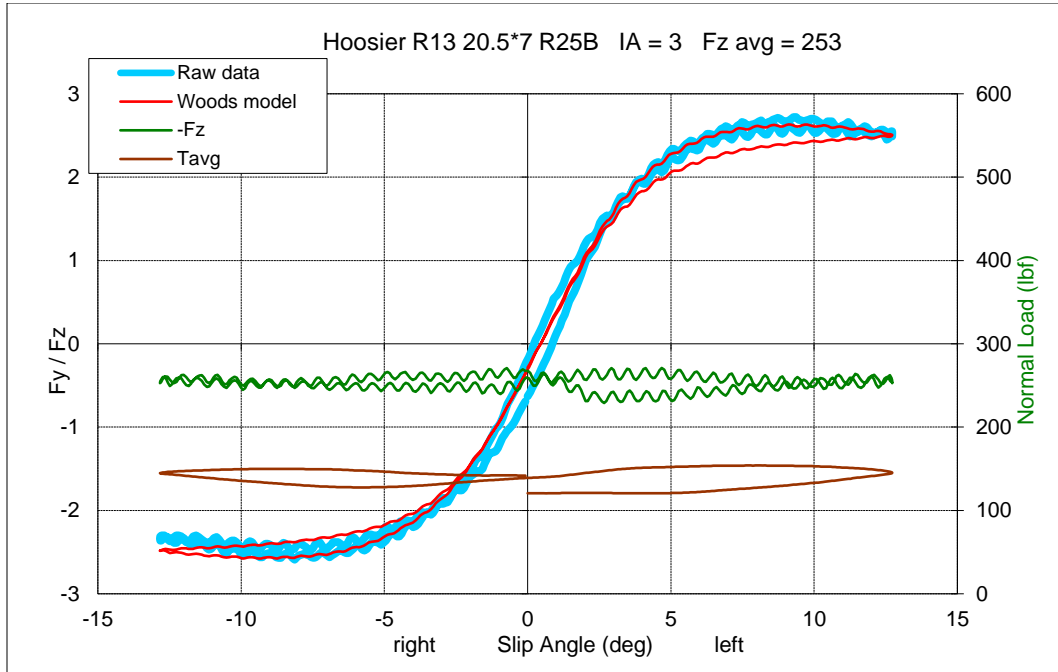


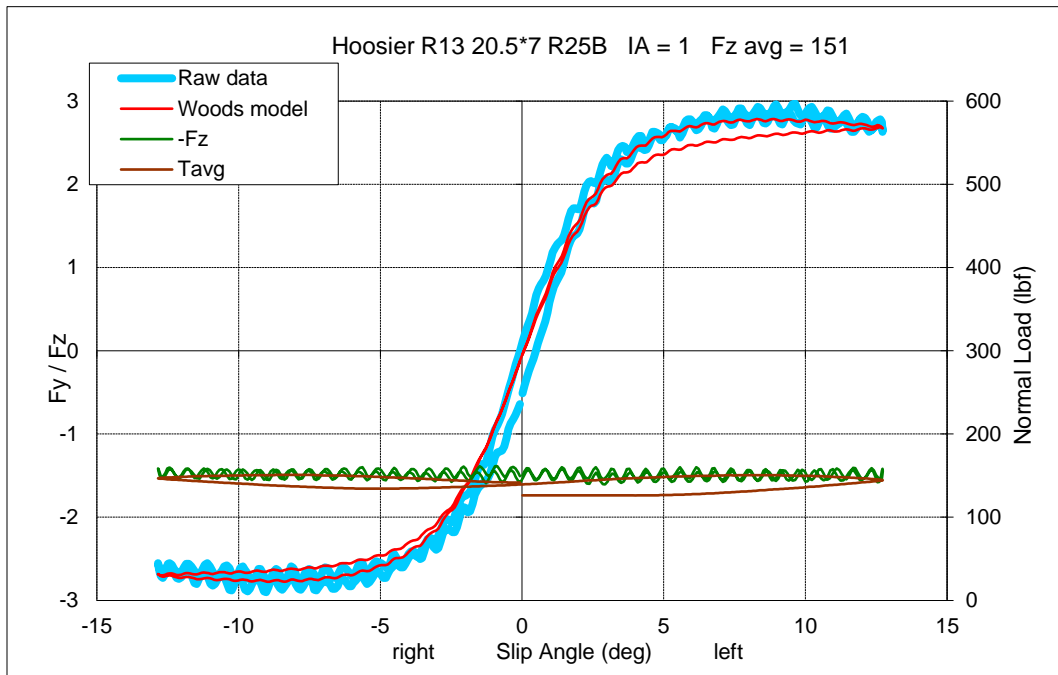
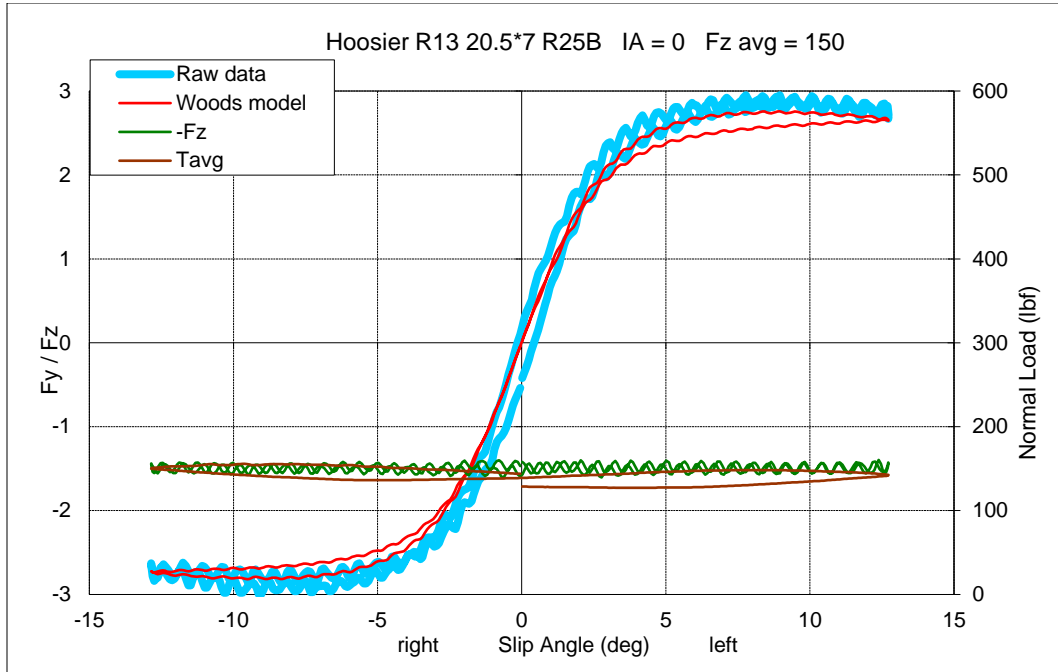


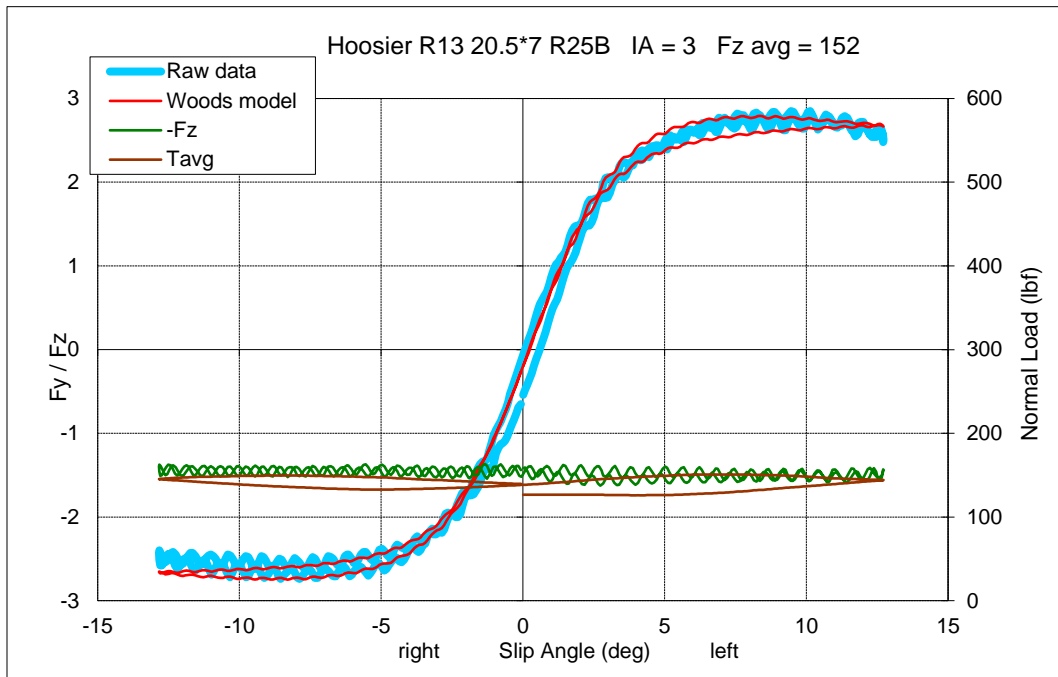
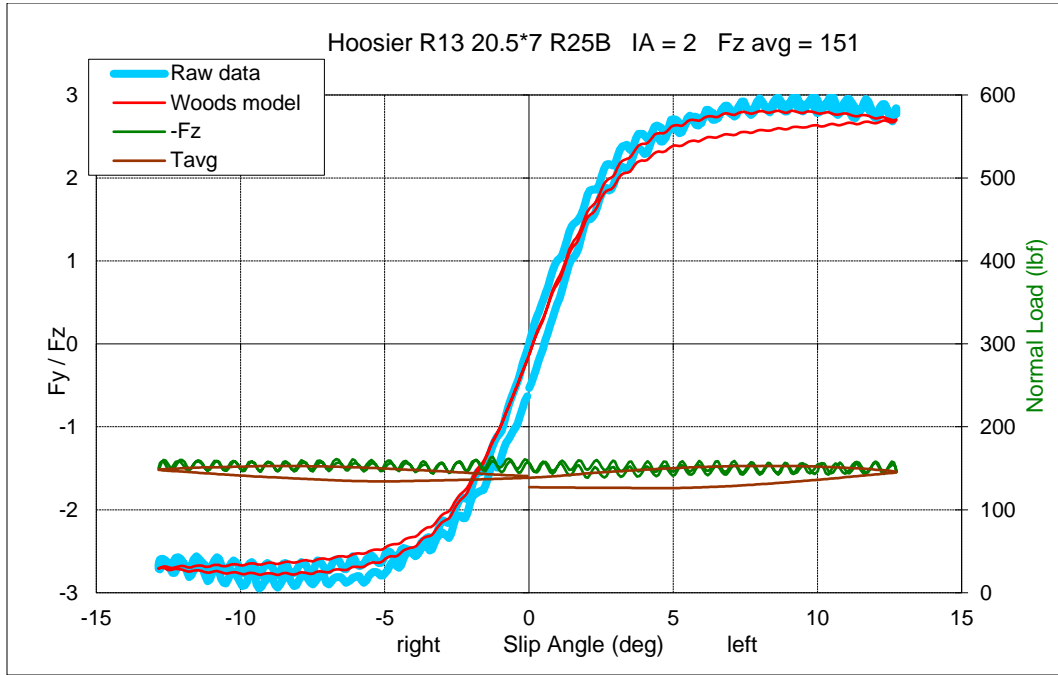
Hoosier R13 20.5*7 R25B

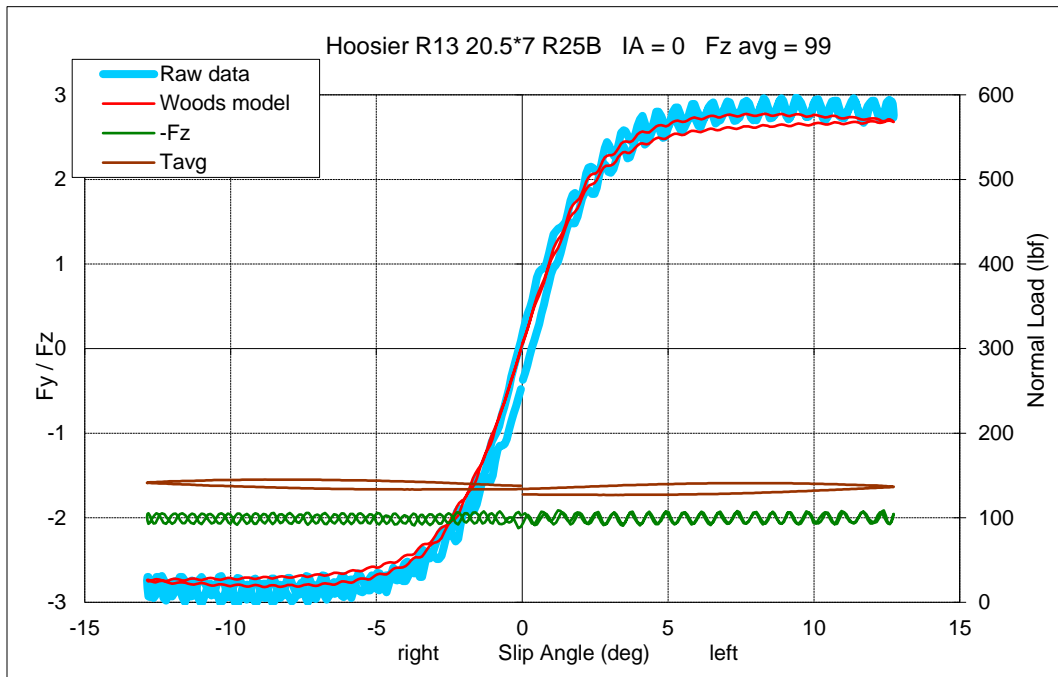
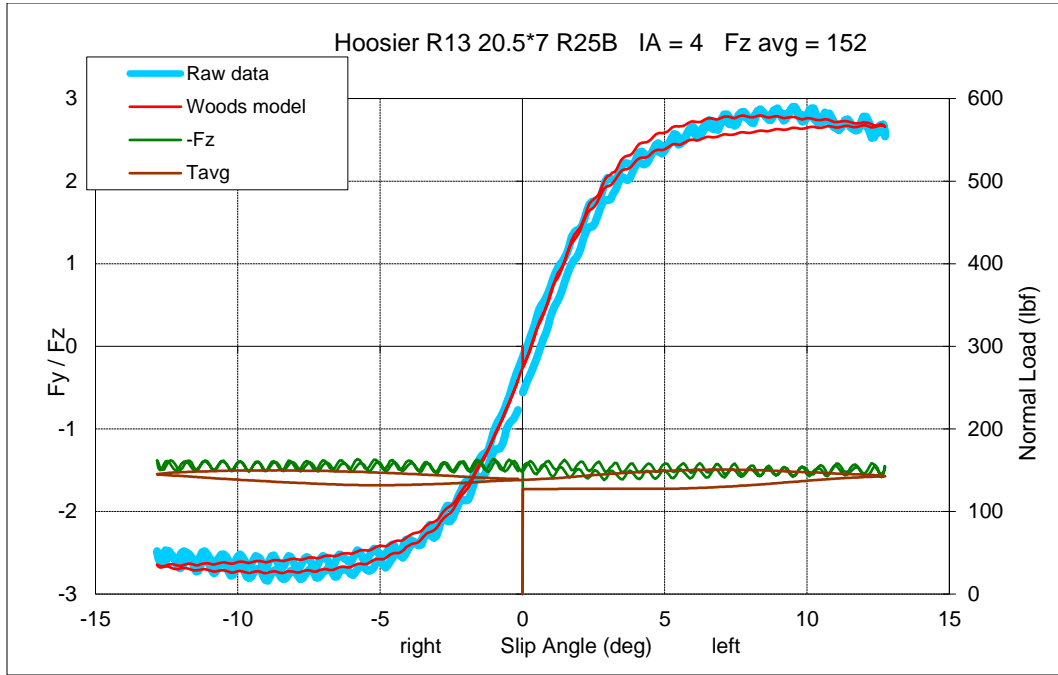


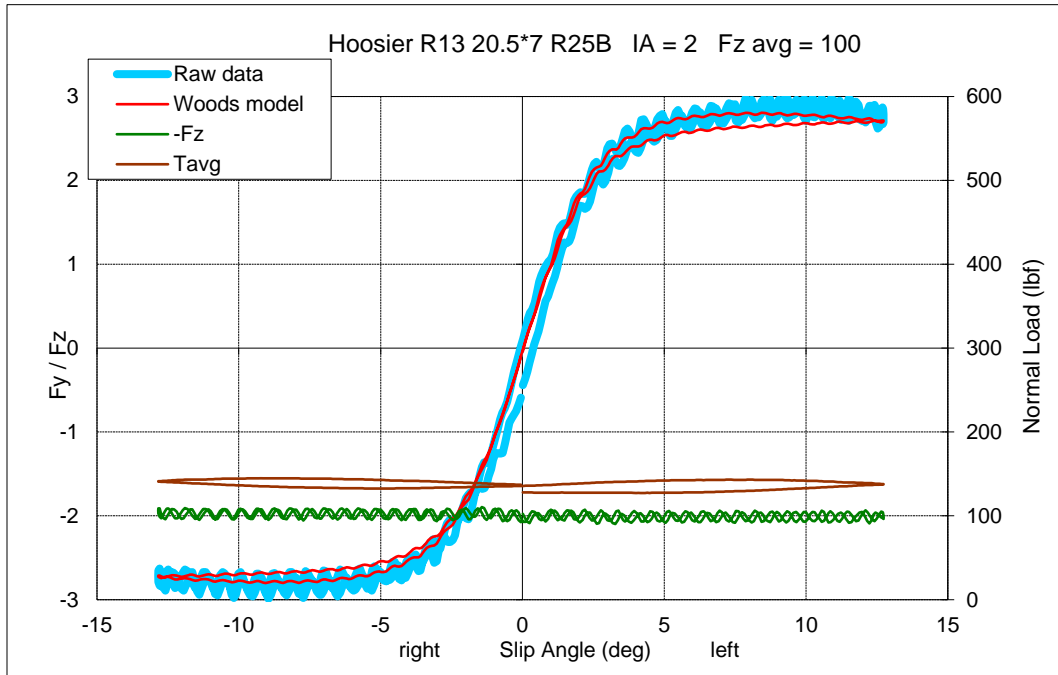
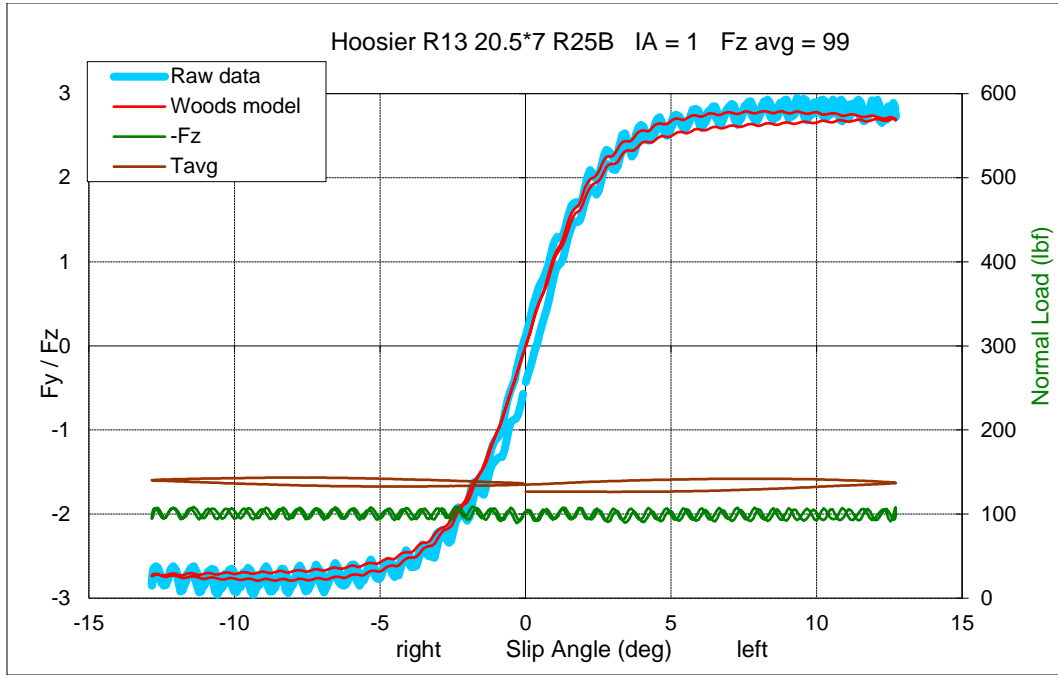


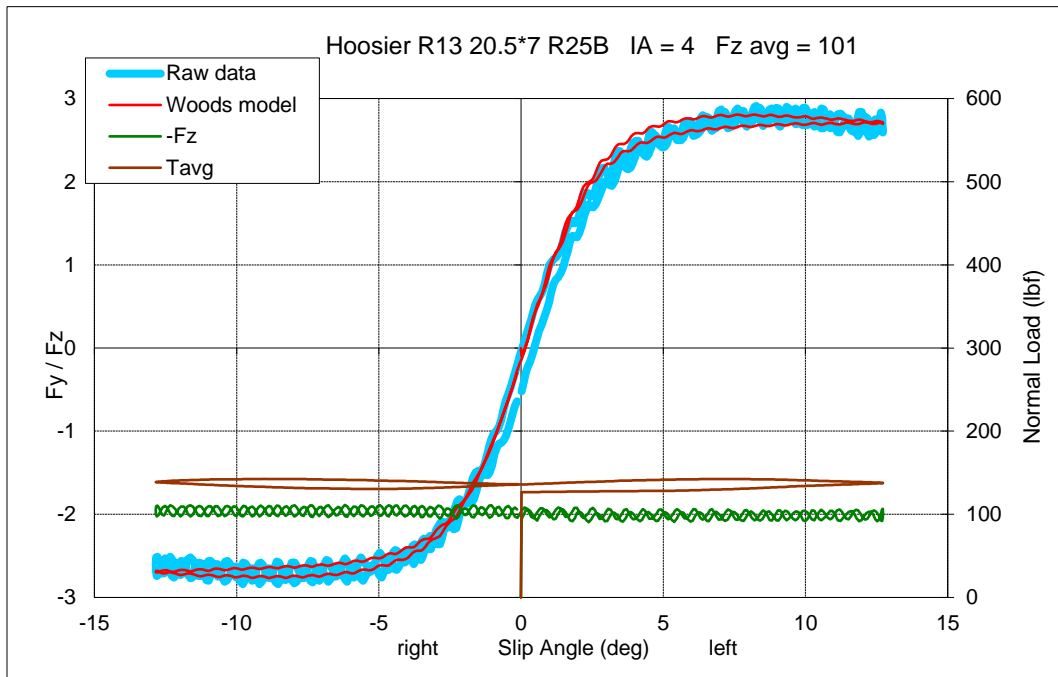
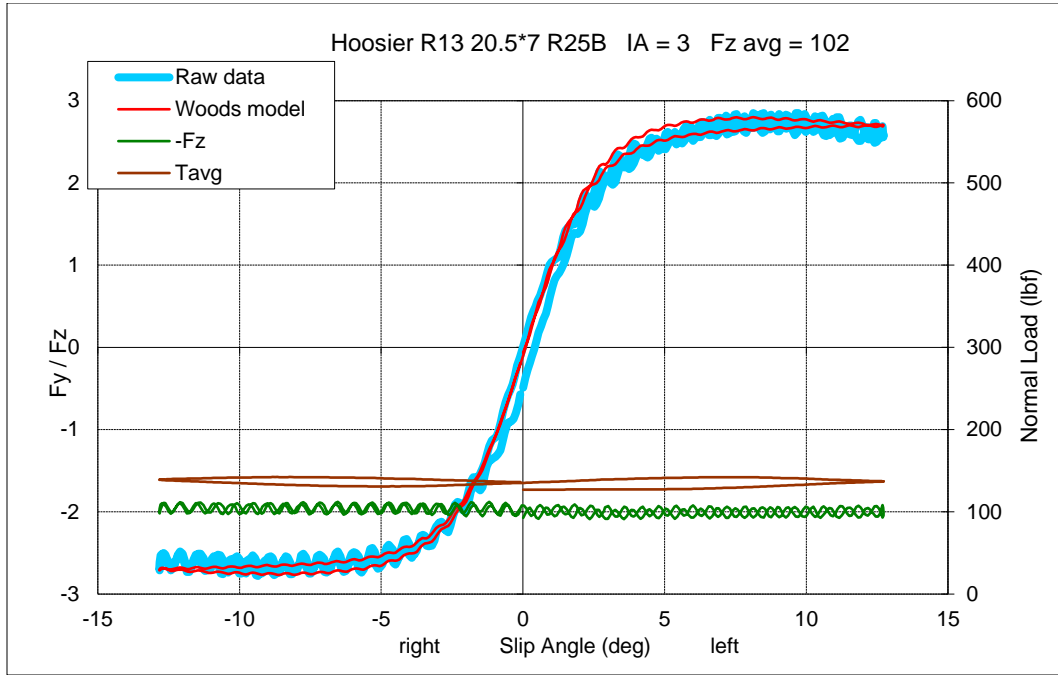


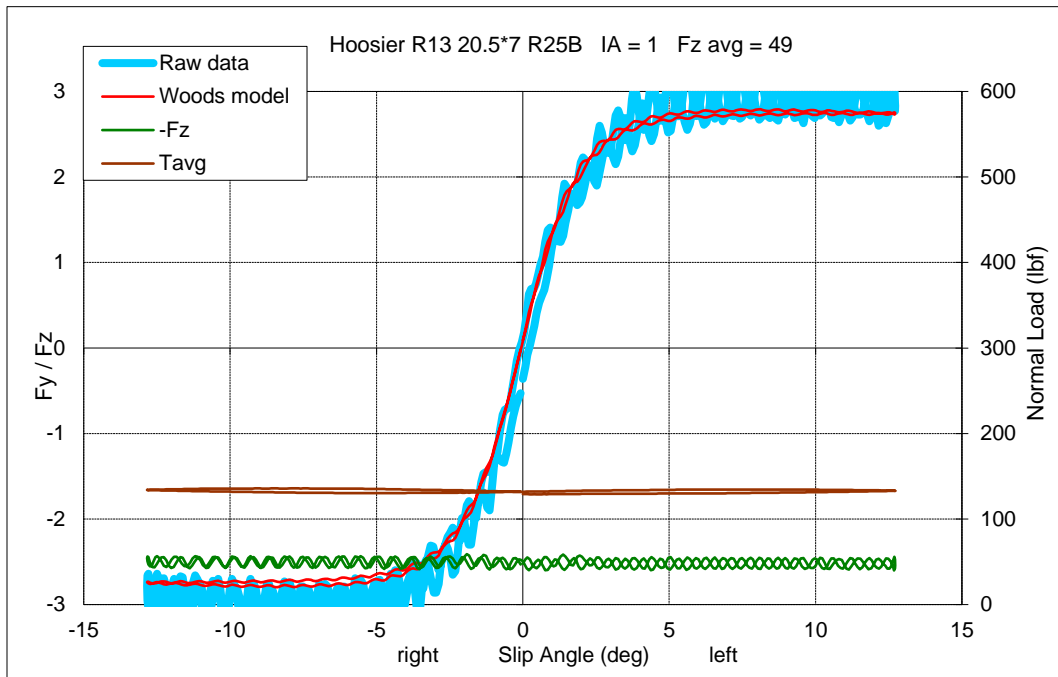
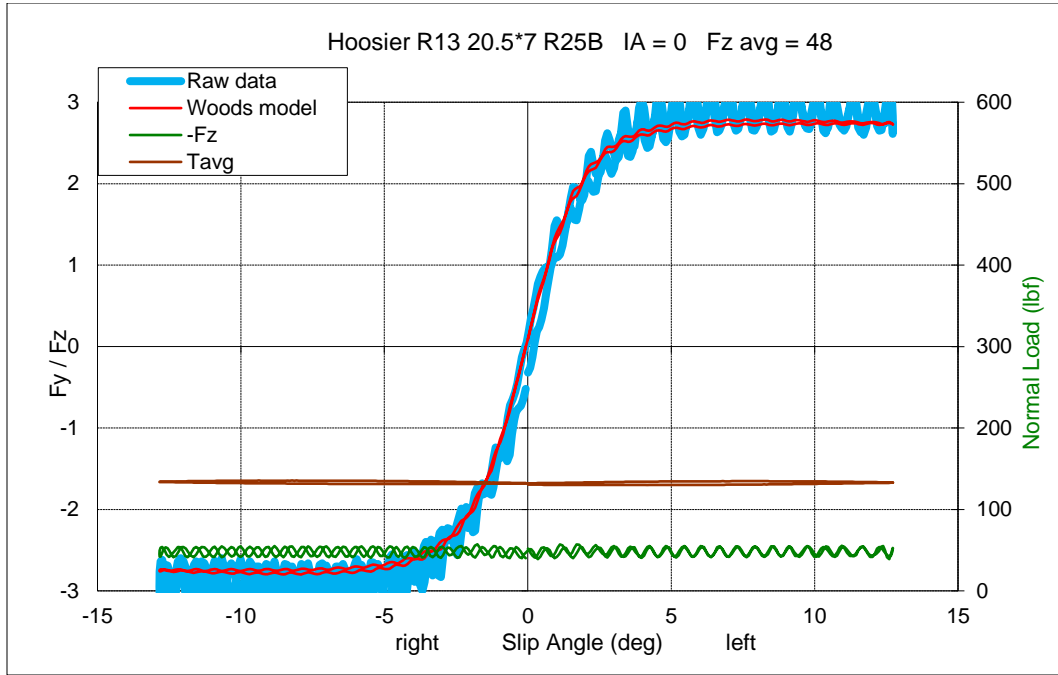


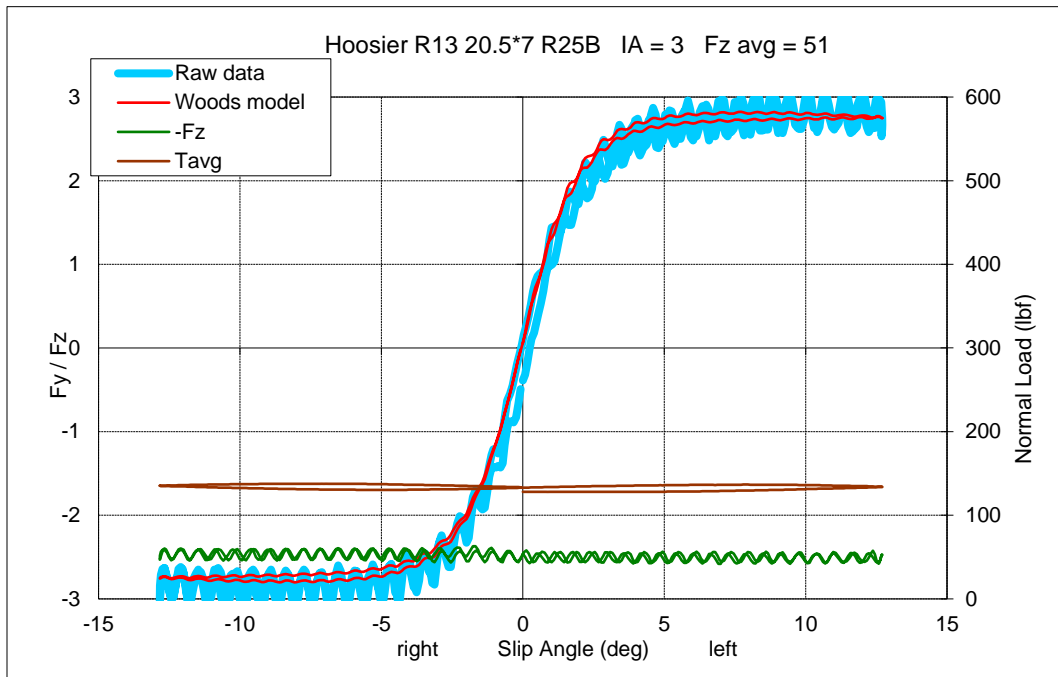
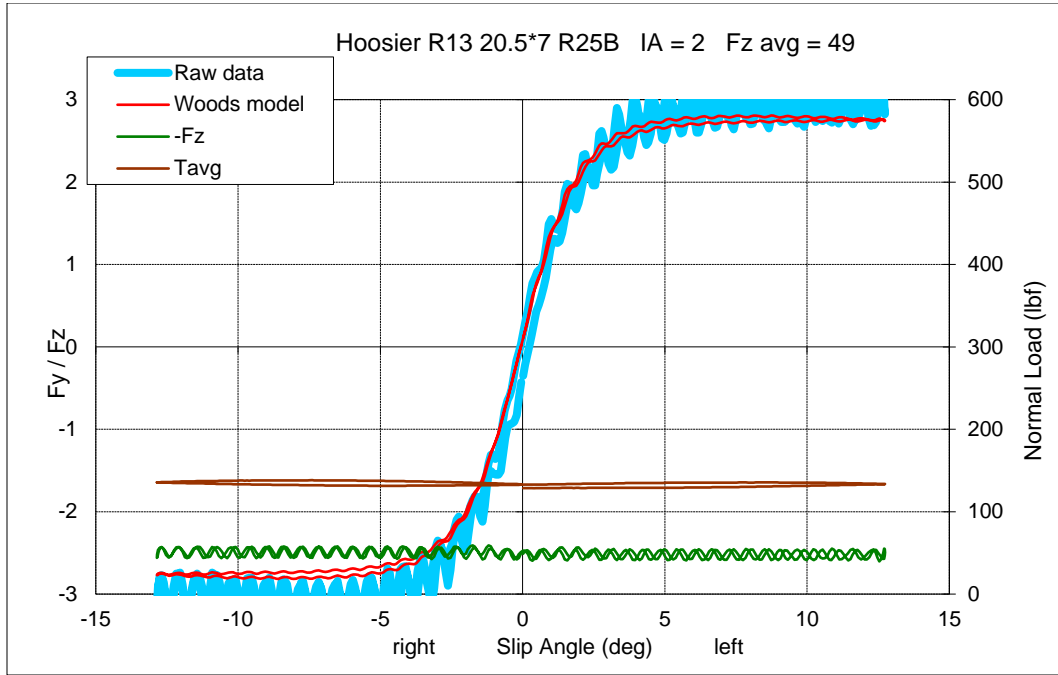


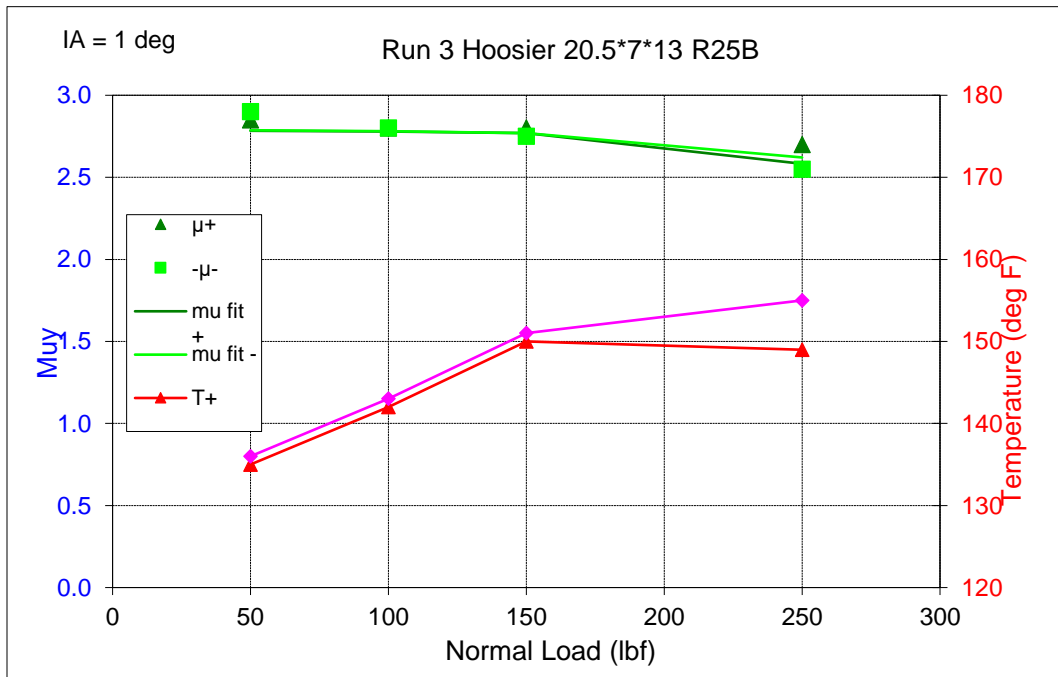
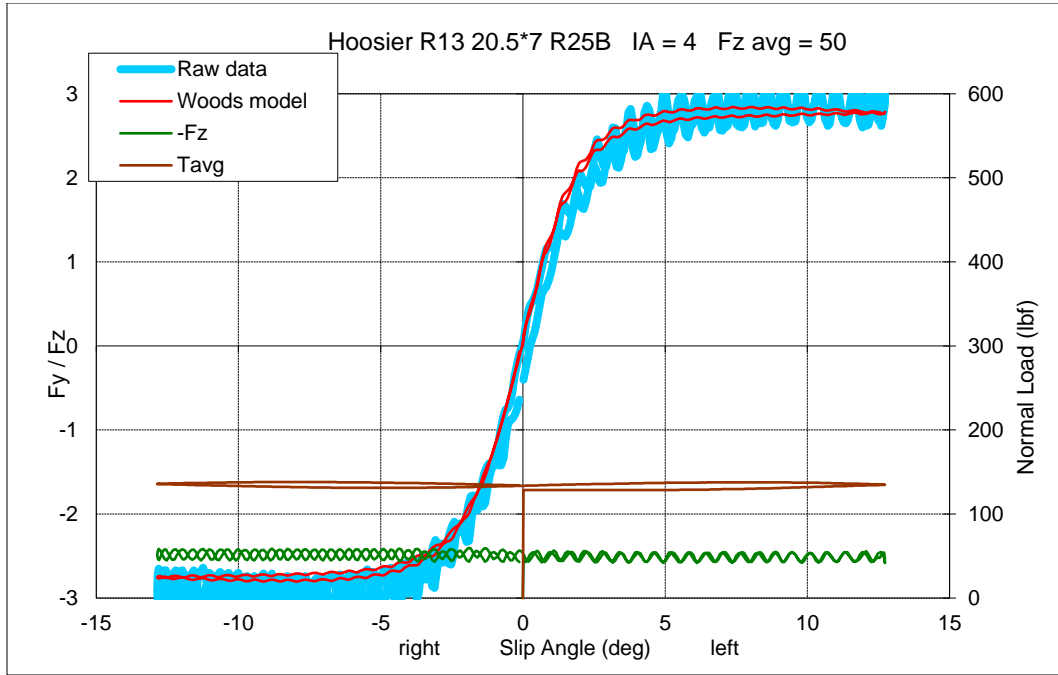


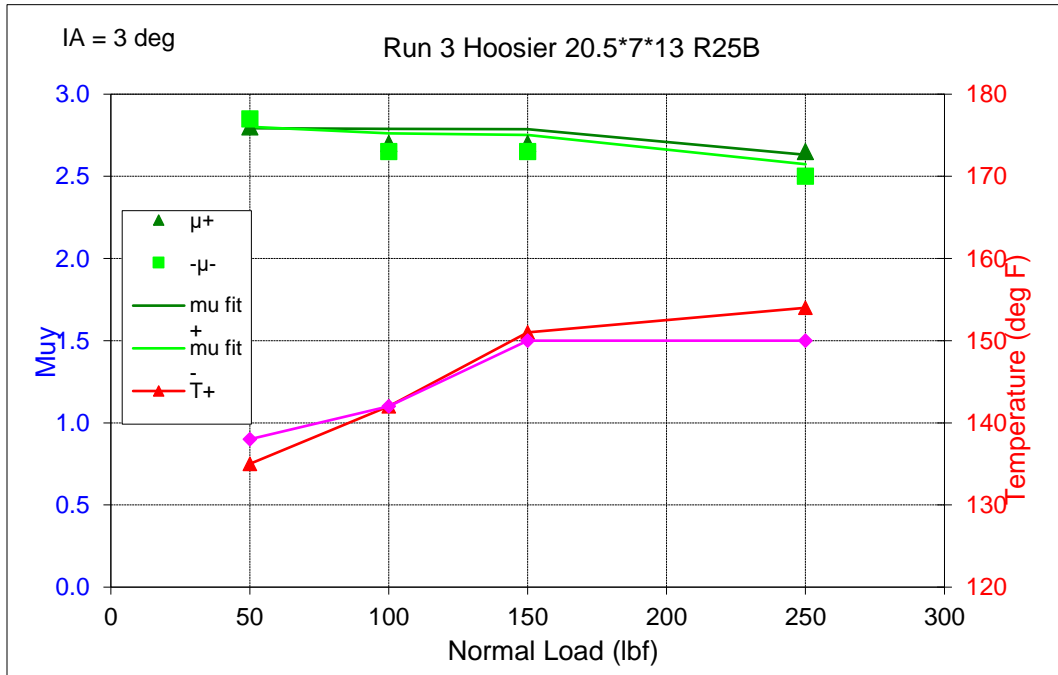
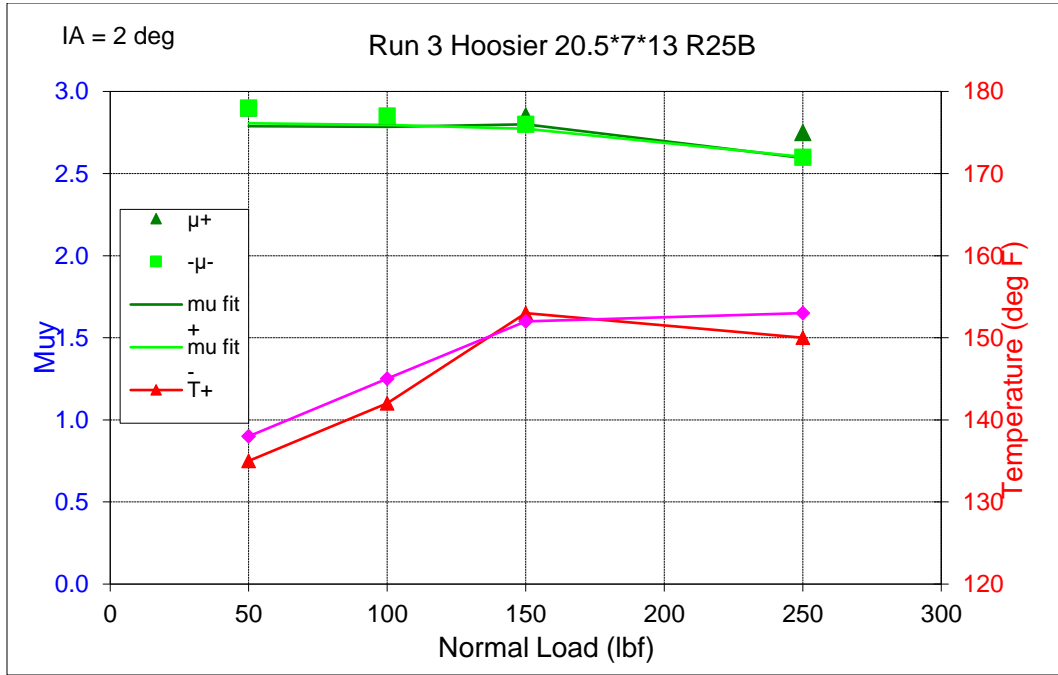


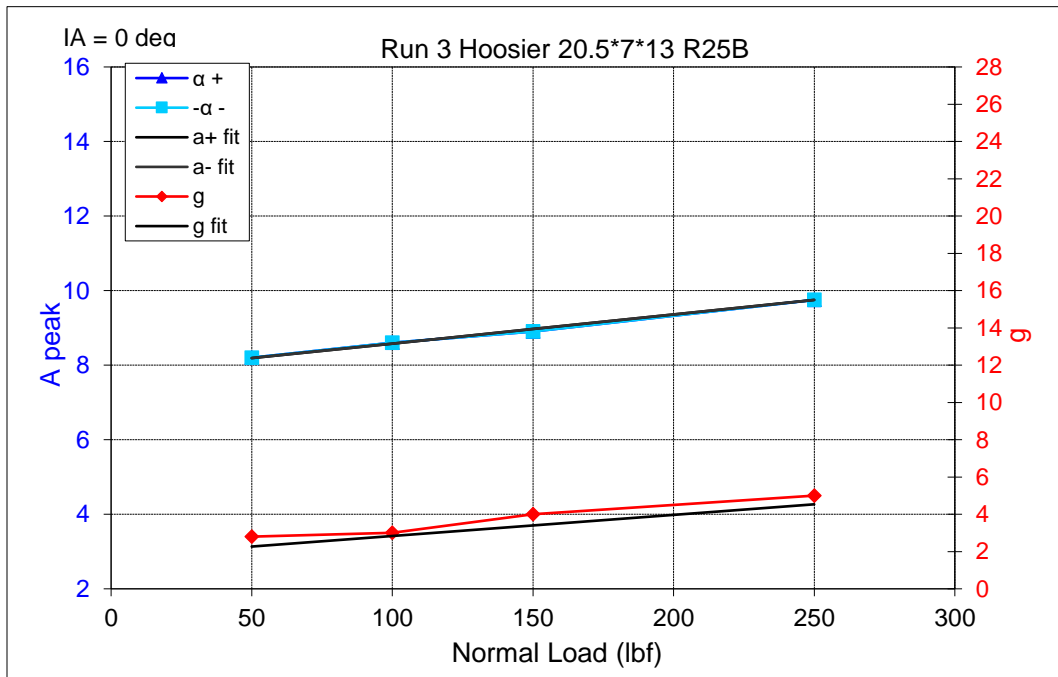
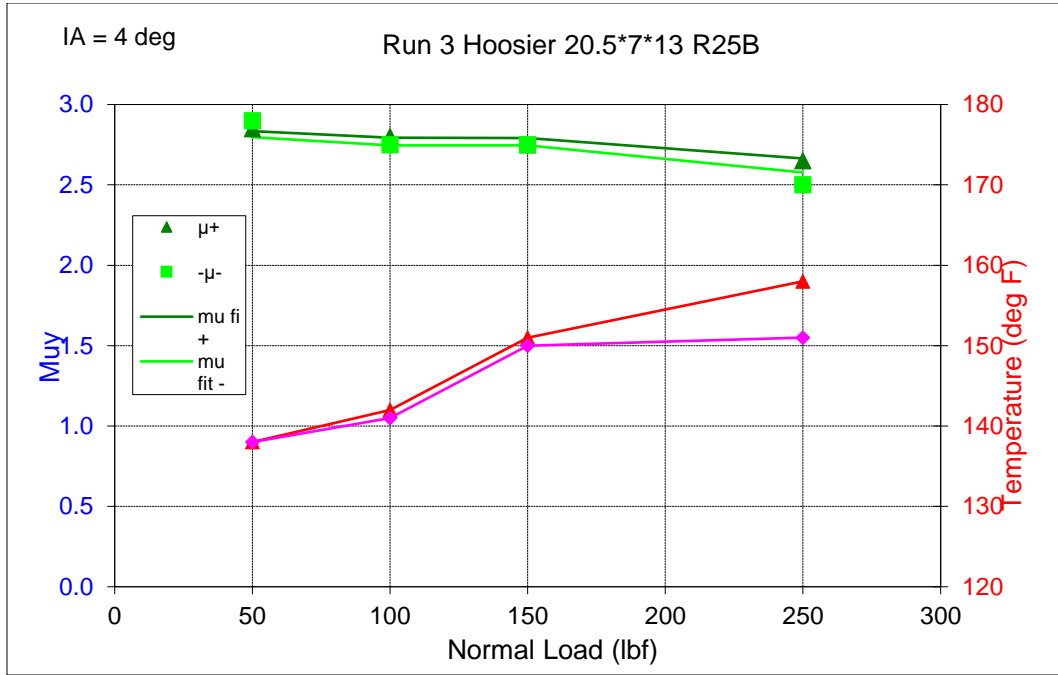


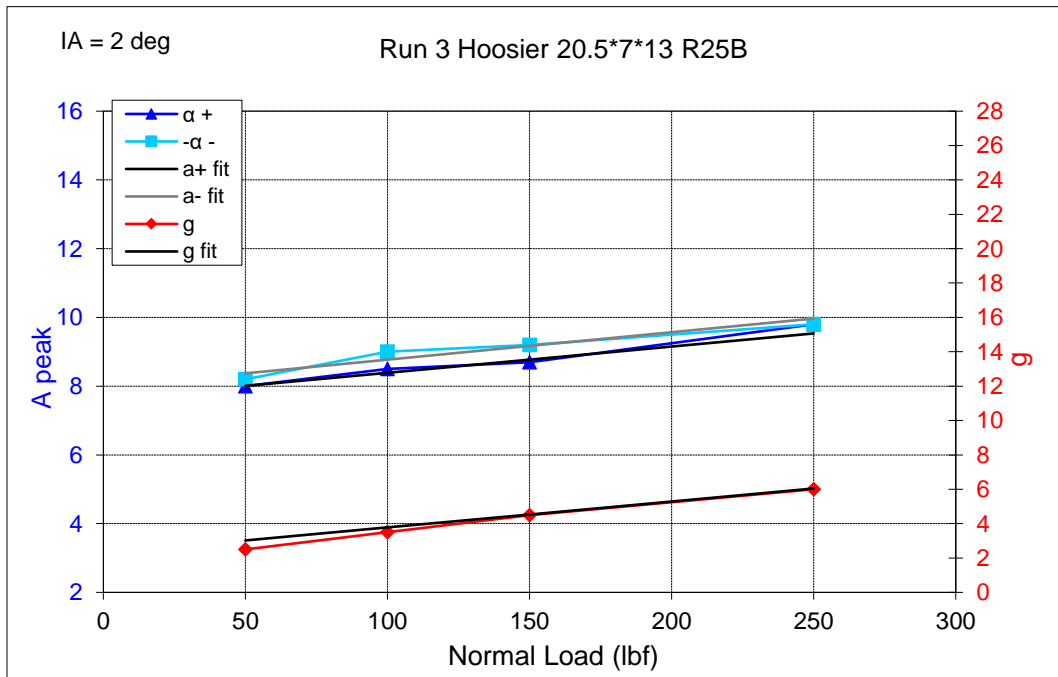
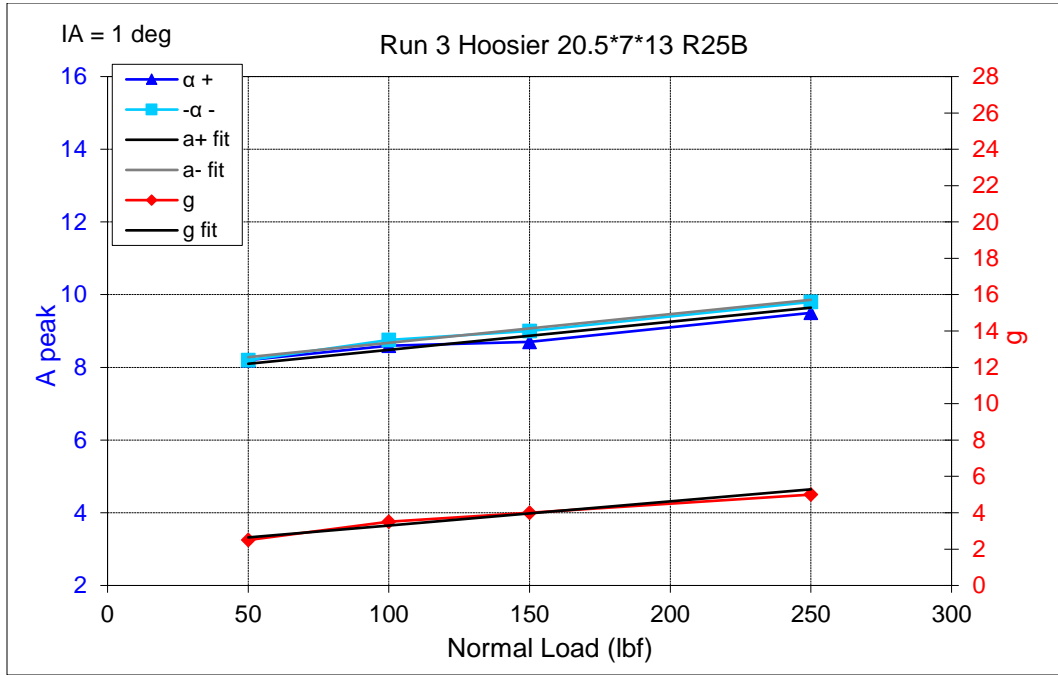


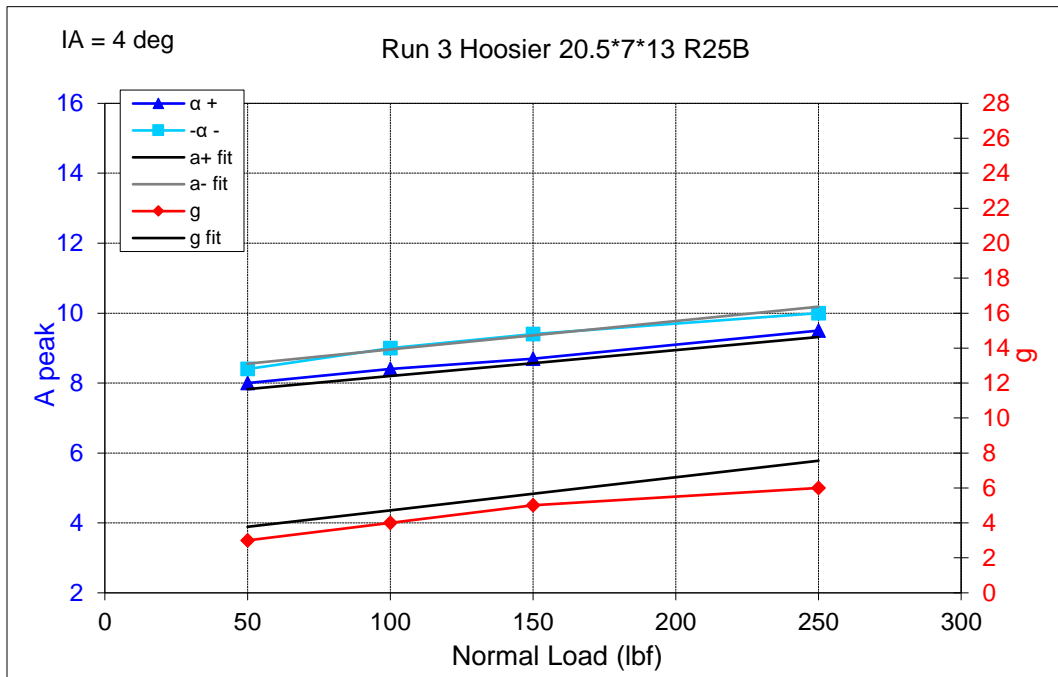
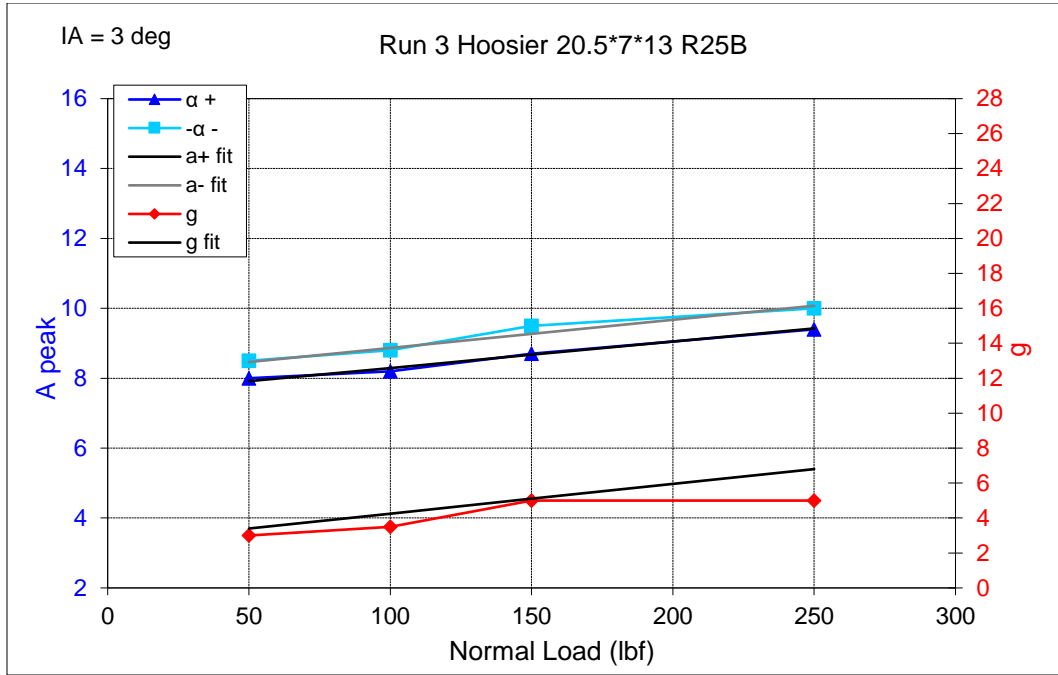


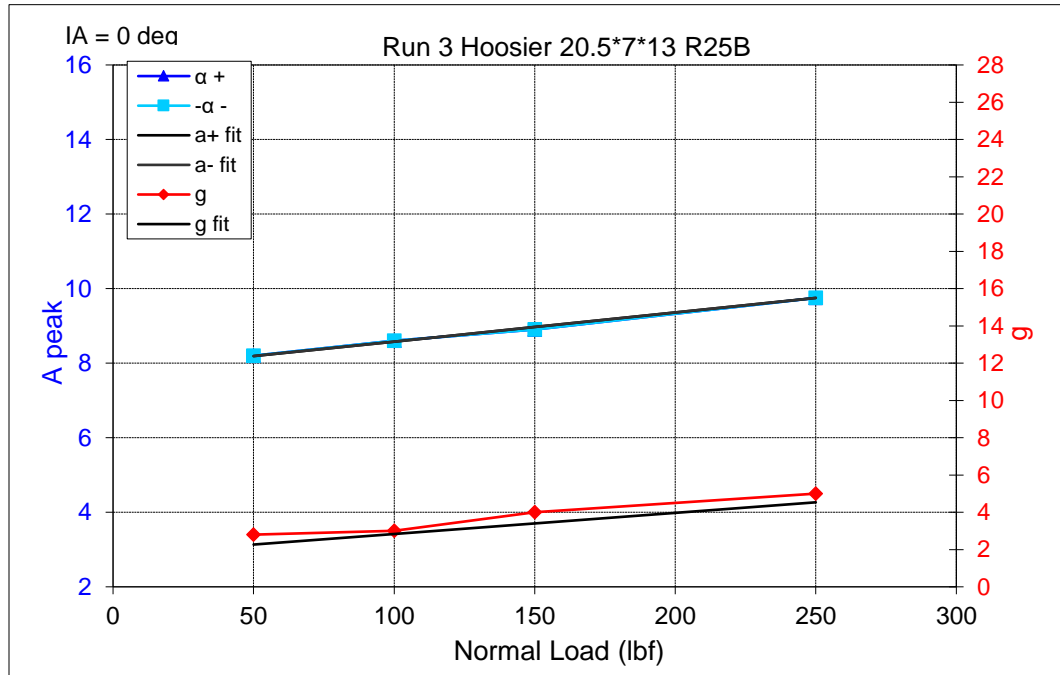
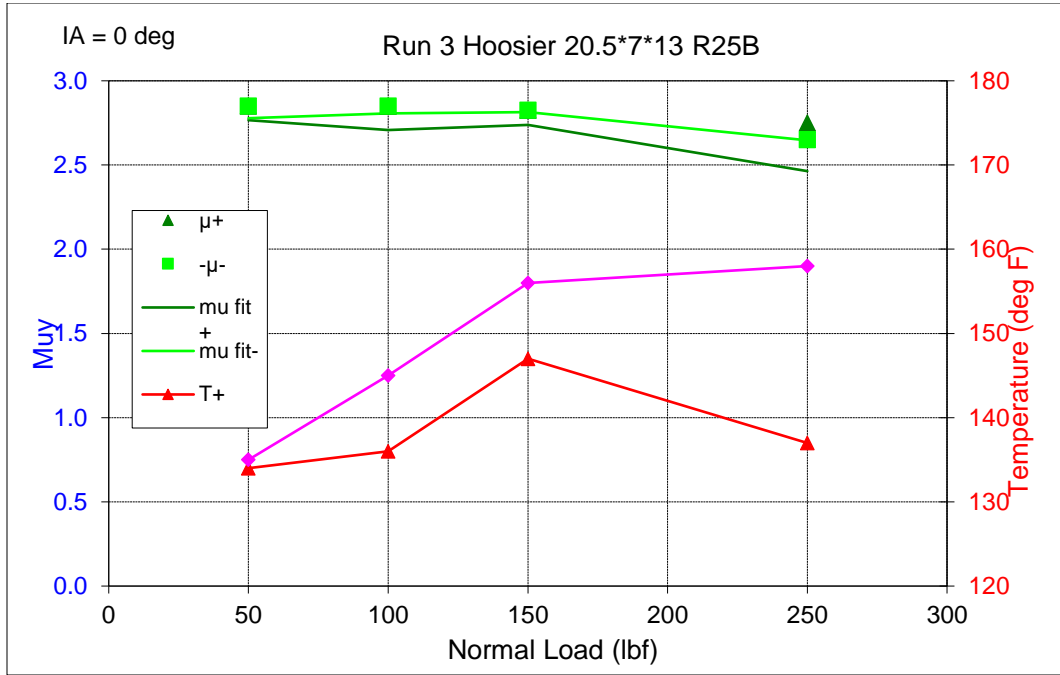


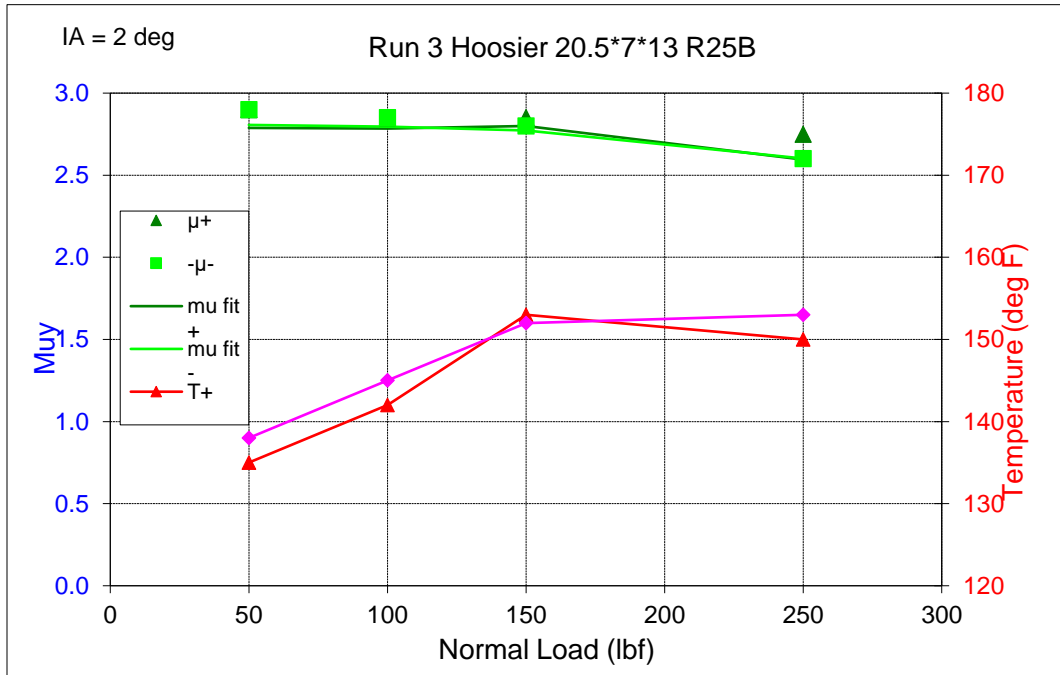


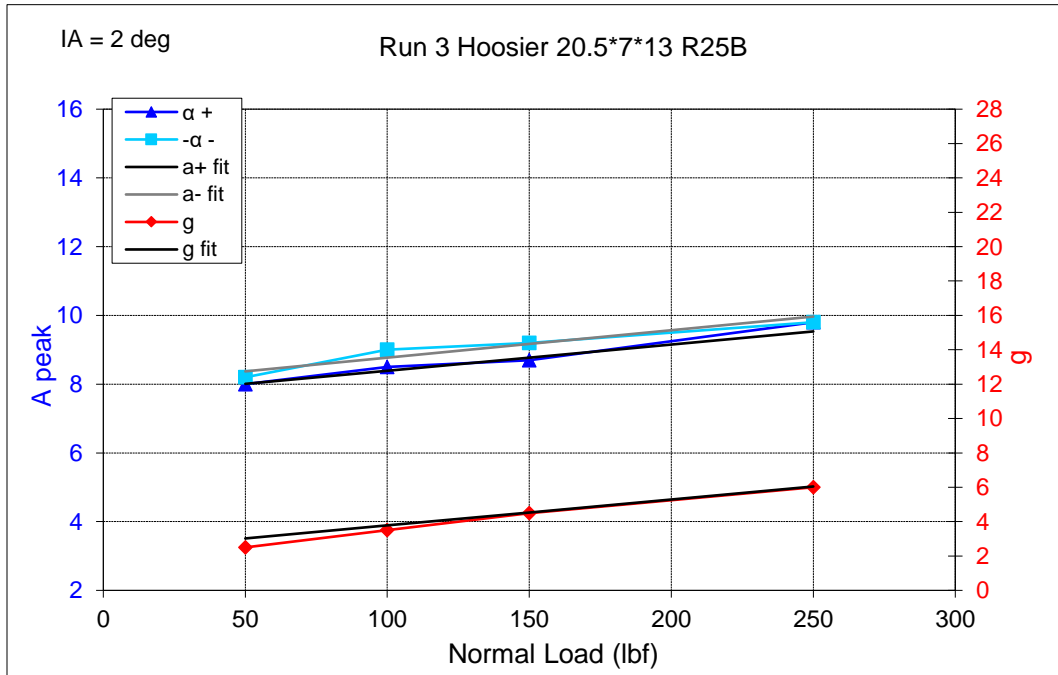


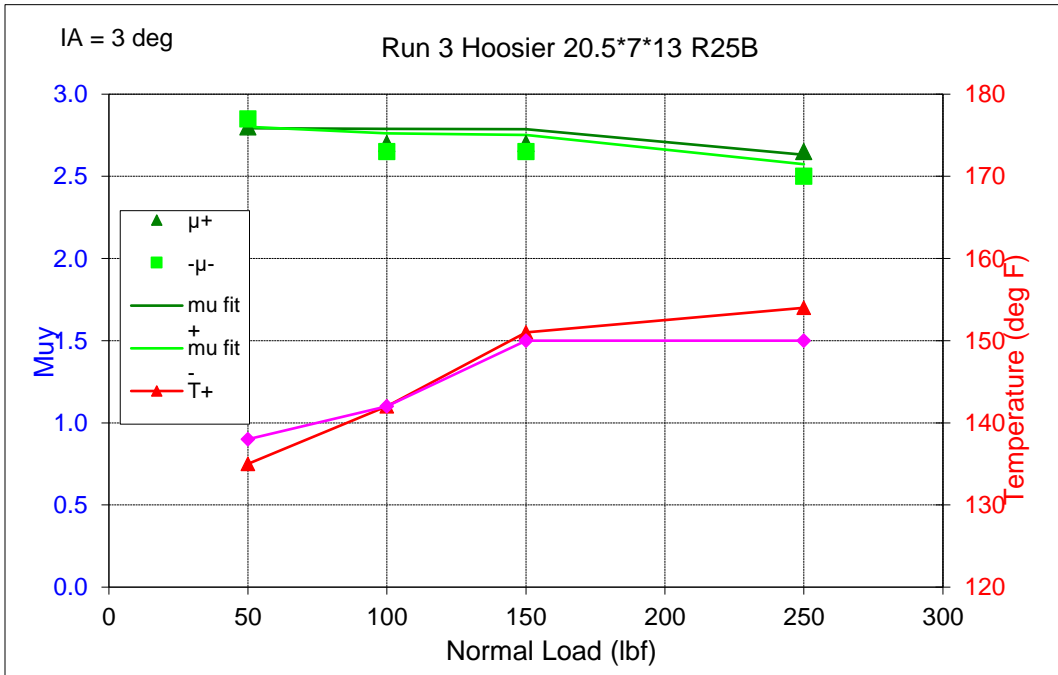
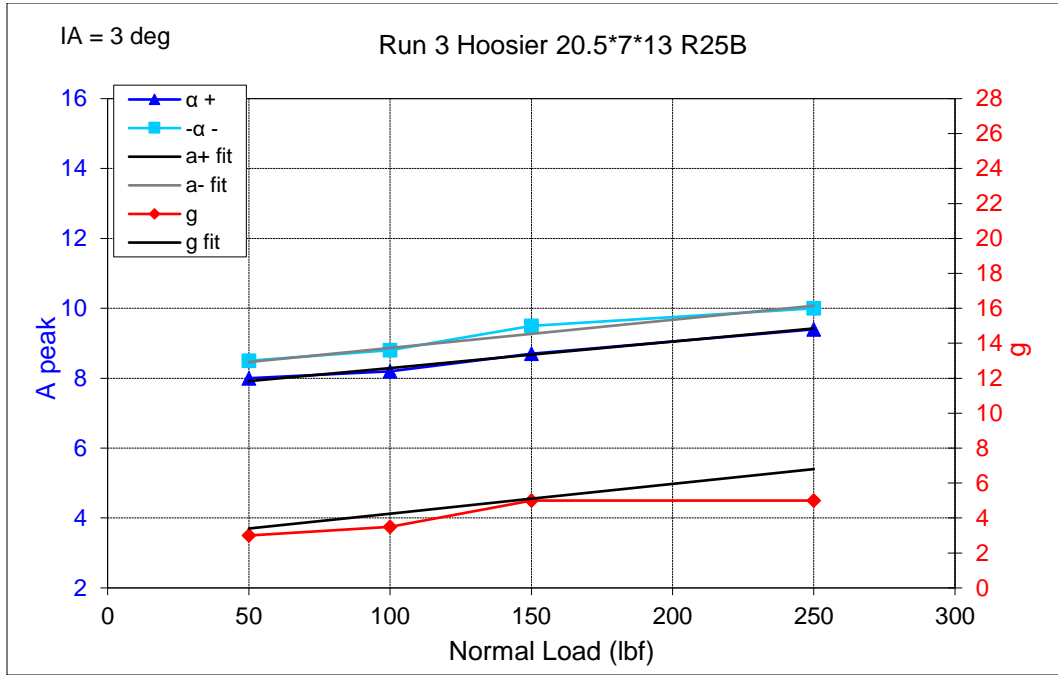


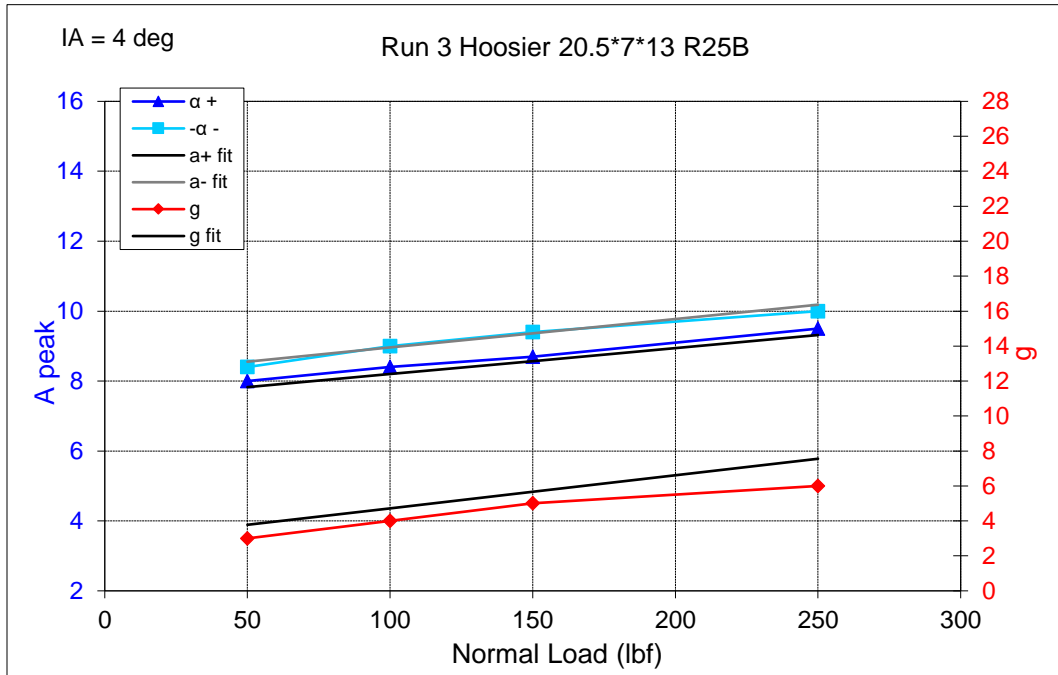


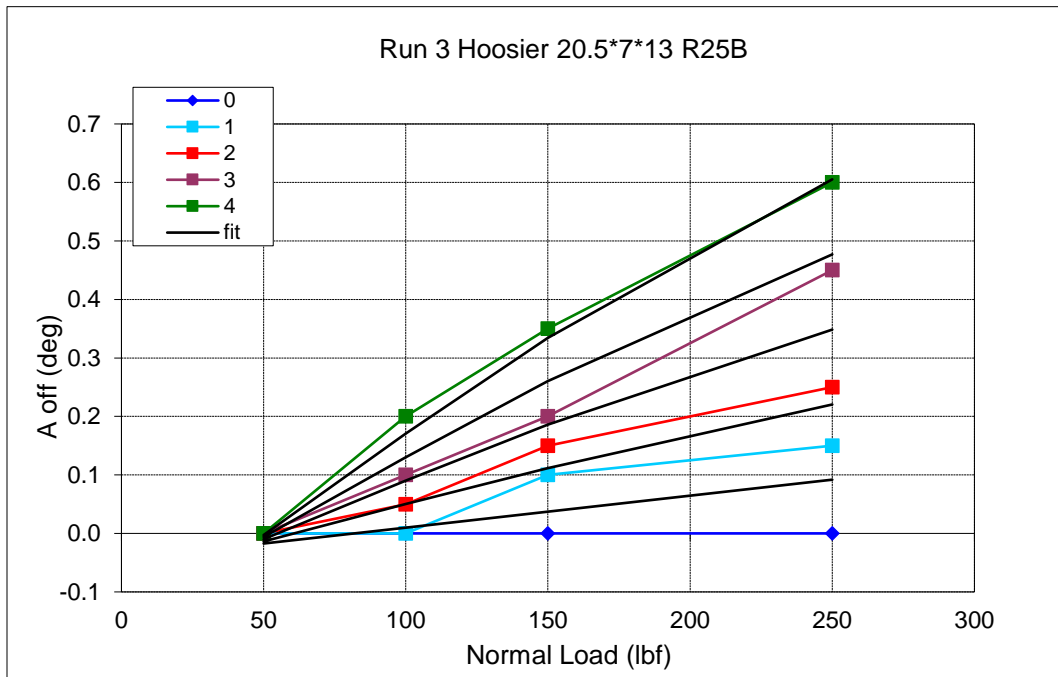
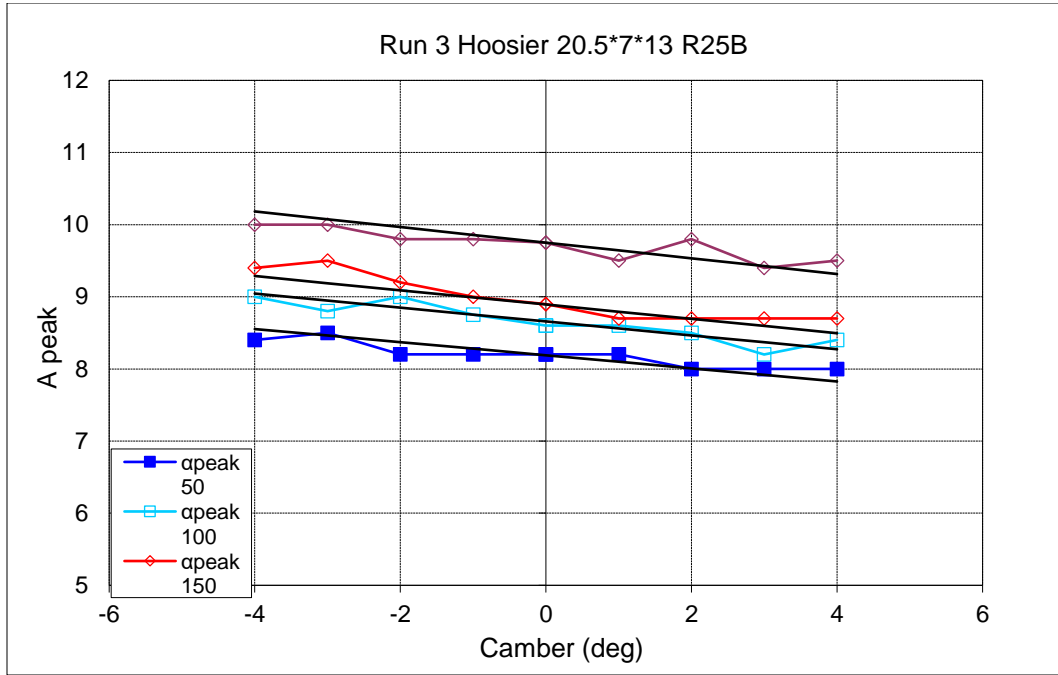




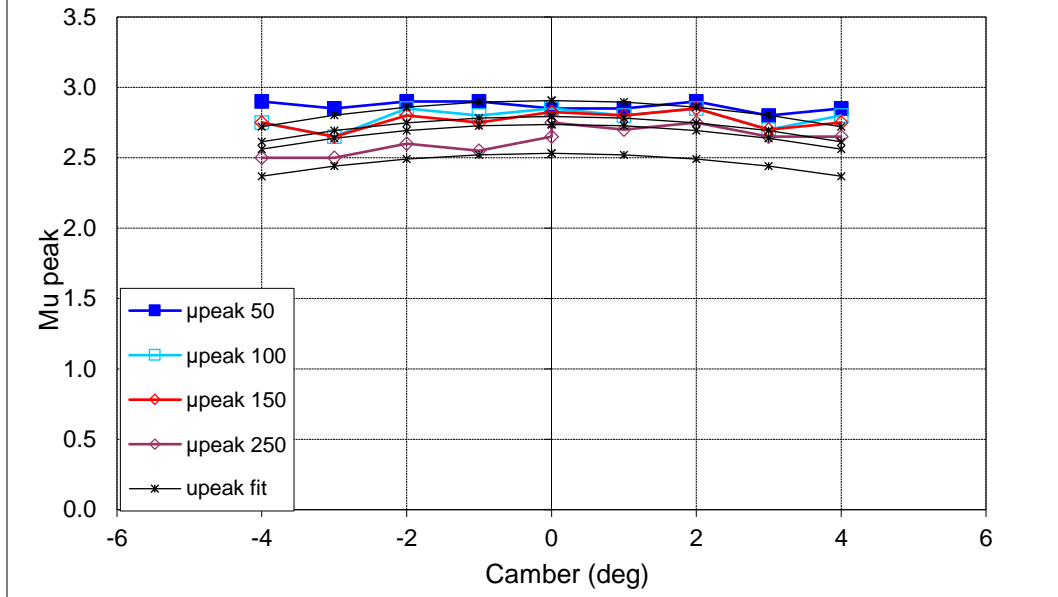








Run 3 Hoosier 20.5*7*13 R25B



References

- [1] W. F. Milliken and D. L. Milliken, "Race Car Vehicle Dynamics," *Race*, vol. 1. p. 1000, 1995.
- [2] R. Woods, "Normalization of the Pacejka Tire Model," *SAE Technical Paper*, no. 724. 2004.
- [3] M. Schmid, "Tire Modeling for Multibody Dynamics Applications," p. 62, 2011.
- [4] N. York and A. Engineering, "Extension of the Nondimensional Tire Theory To," no. December, 2006.
- [5] E. M. (University A. B. Kasprzak and D. (Calspan C. . Gentz, "The Formula SAE Tire Test Consortium — Tire Testing and Data Handling," *Soc. Automot. Eng.*, no. 724, p. 12, 2006.
- [6] N. J. Trevorrow, "Development of a Dynamic Force Model for Racing Slick Tyres," *Measurement*, no. Figure 1, pp. 1–17, 1995.